IJCESEN

ISSN : 2149-9144

International Journal of Computational and Experimental Science and ENgineering

Volume: 7 - Issue: 3 - 2021

ijcesen@gmail.com

Founder-Editor-in-Chief : Prof.Dr. İskender AKKURT

dergipark.org.tr/en/pub/ijcesen

Journal Info	
Web	dergipark.org.tr/en/pub/ijcesen
E-mail	ijcesen@gmail.com
ISSN	2149-9144
Frequency	March-July-November
Founded	2015
Journal Abbreviation	IJCESEN
Language	English-Turkish

Indexing/Abstracting Databases

ASOS indeks

INDEX COPERNICUS INTERNATIONAL

ISIFI International Services for Impact Factor and Indexing

GENERALIMPACTFACTOR
Universal Digital Object Information

Google Scholar

DRJI

ISI INTERNATIONAL Scientific Indexing

publons

Cosmos

SIA

J-Gate

WorldCat

ESJI Eurasian Scientific Journal Index
www.ESJIndex.org

JIF Global Society for Scientific Research JIFACTOR

CiteFactor Academic Scientific Journals

Academic Resource Index ResearchBib

Scientific Journal Impact Factor
TOGETHER WE REACH THE GOAL

Table of Contents

International Journal of Computational and Experimental Science and ENgineering (IJCESEN)
Vol. 7-No.3 (2021) pp. 110-113
http://dergipark.org.tr/en/pub/ijcesen

ISSN: 2149-9144

Research Article

Modeling of the Magnetic Field of Current Carrying Conductor with Finite Elements Method

Naim SYLA[1], Hajrudin HUSEJNI[2*], Gazmend NAFEZI[3] and Fisnik ALIAJ[4]

[1]University of Prishtina, FMNS/Department of Physics, 10000 Prishtina, Kosovo
naim.syla@uni-pr.edu **ORCID:** 0000-0003-0857-4685

[2]University of Prishtina, FMNS/Department of Physics, 10000 Prishtina, Kosovo
*** Corresponding Author** : hajrudin@yahoo.com **ORCID:** 0000-0003-4100-5564

[3]University of Prishtina, FMNS/Department of Physics, 10000 Prishtina, Kosovo
gazmend.nafezi@uni-pr.edu **ORCID:** 0000-0002-9259-7259

[4]University of Prishtina, FMNS/Department of Physics, 10000 Prishtina, Kosovo
fisnik.aliaj@uni-pr.edu **ORCID:** 0000-0002-9967-8334

Article Info:

DOI: 10.22399/ijcesen.820667
Received: 03 November 2020
Accepted: 04 August 2021

Keywords

Magnetic field,
Conductor,
Modeling,
Finite Element Method,
Ansoft Maxwell

Abstract:

In this paper, we have modeled and simulated the magnetic field of the conductor by using the finite element method, which is incorporated in Ansoft Maxwell software. Modeling and simulation are done for a conductor and two conductors located at a small distance between them. Our study is based on the method of finite elements and Biot-Savart law for calculating the magnetic field depending on the distance from the conductor. We have observed that the calculated values of the magnetic field are in good accordance with Biot-Savart law [1]. We have found that magnetic field normal to the main axis of the conductor falls linearly towards it, whereas outside the conductor magnetic field is inversely proportional to distance.

In the case of simultaneous calculation of the field inside and outside the conductor, a small margin has been found. This difference is as a result of the simultaneous calculation of magnetic field in two environments with different magnetic permeability.

Finally, we have computed the magnetic field at an equal point between two conductors when the currents have opposite and same direction, whereby a huge difference between the magnetic fields is found. We show that we can amplify or reduce the intensity of the magnetic field, based not only on the distance between the conductors but also on the basis of the directions of the currents flowing through these conductors.

1. Introduction

The magnetic field created by the current-carrying conductor can be calculated by Biot-Savart law. The magnetic field at a given point depends on several factors such as the length of the conductor, the intensity, the distance of the point from the conductor and the angle that the current element closes with the point where the magnetic field is required. On the other hand, in the case of two conductors, the magnetic field either can be amplified or weakened, depending on the distance between the two conductors and on the directions of currents flowing through these conductors. As a result, conductors either can attract or repel from each other. Magnetic fields are treated through Maxwell equations [2], which in most cases are difficult to be solved considering the complex nature of the problem (boundary conditions of integration). Therefore, approximate numerical methods should

be applied in their solution. One of these methods is the Finite Elements Method (FEM). Characteristic of this method is the division of the research area (integration) into small suitable elements. Then all the necessary steps that lead to the solution of a certain problem are followed. In our case, Ansoft Maxwell software is used to model the magnetic field. In order for a problem to be solved through Ansoft (Ansys) Maxwell, we have to go through three stages: pre-processing, solving and post-processing [3].

2. Modeling and Simulation

Modelling is the process of building the model, which must be compatible with the real system that has to be analyzed; while simulation is the process performed on the model, we have created using suitable software [3-11]. The advantage of modelling and simulation is the short time needed to solve any problem, low cost, testing of different situations, testing with different materials, etc. The most important steps for magnetic field modelling and analysis that we have followed are: defining the type of analysis, defining the type of element, constructing the (model) geometry, determining the properties of the material, applying boundary conditions and loads, defining the mesh, specifying of analysis for solutions as well as control (verification) of the results. Once the model is created, the automated Maxwell solution sequence takes over and fully controls the solution process without any interaction from the user.

We have dealt with three separate cases. In all three cases the dimensions of the conductor, in cylindrical shape, are the same. The conductor has a radius of 0.25mm and length of 5mm. The conductor/s in the direction of z component are traversed by steady current with magnitude of 20A, while as a material for those conductors we have used copper due to its very good conductivity.

When modelling the magnetic field of current-carrying conductor we not only should be careful in modelling correctly the geometry of the conductor, but also, we should be careful in the creation of region we wish to analyze magnetic field. If we want to determine the magnetic field inside the conductor, then the result is not affected by the size of the region, but on the other hand if we want to determine the magnetic field outside the conductor then the size of the region should be as large as possible, so as not to limit the convergence of (the lines of) magnetic field. In our case, we have given 300% padding in x and y directions, whereas 0% padding in z direction [3]. This is so because the magnetic field is normal to the z direction, figure 1.a. Regarding the mesh we have used an automatic adaptive mesh refinement technique, figure 1.b, while for the boundary condition we have selected default boundary

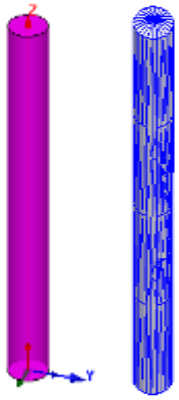

Figure1. *Selected model and mesh*

3. Results

In the following we will present three cases of magnetic field modelling: for a single conductor, and two parallel conductors where in one case the directions of currents flowing through conductors are parallel, while in the other case anti-parallel.

3.1 The case of a single conductor

After imposing boundary condition, Ansoft software automatically calculates the magnetic field of the conductor, figure 2. While the change of magnetic induction intensity from the center of the conductor to an arbitrary point outside the conductor it will be as in figure 3.

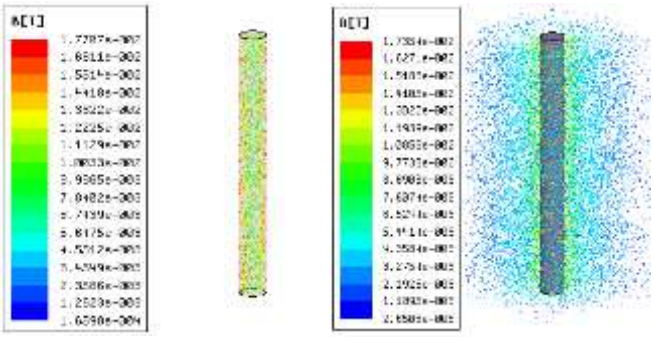

Figure 2. *Value and distribution of magnetic induction inside and outside the conductor*

3.2 The case of two conductors in which parallel currents flow

Same as for the conductor above the same parameters and material are used. Assume that these two conductors are located close to each other at a distance of 0.50mm. In the case of two conductors,

the magnetic fields created by these current-carrying conductors interact with each other. The resulting magnetic field depends not only on the distance, the intensity of the currents, but also on the direction of the currents.

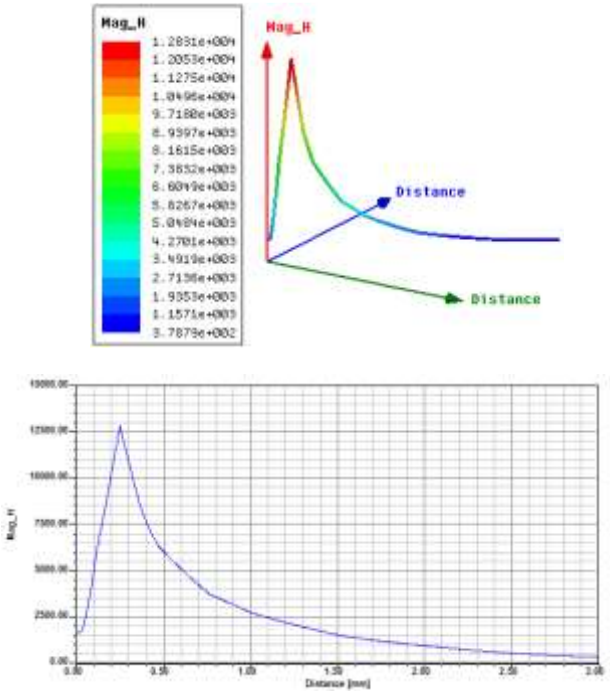

Figure 3. *Intensity of the magnetic field of the conductor depending on the distance*

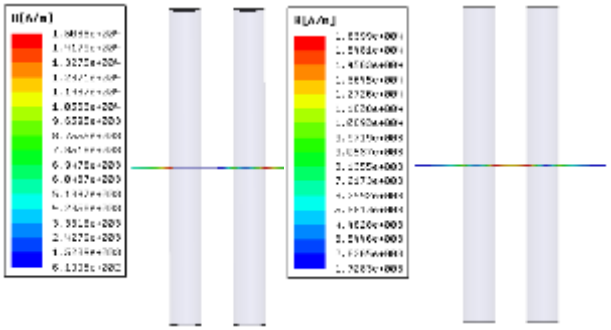

Figure 4. *Magnetic field of two conductors for the cases when their currents are: a. parallel respectively b. anti-parallel.*

In the figure below we have presented the resulting magnetic field in cases where currents have the same direction and opposite direction, figure 4. For this case the dependence of the magnetic induction on the distance changes as is shown in Figure 5. As a result of the interaction of magnetic fields at the distance of 1.50mm from the coordinate system, i.e. at the distance of 0.25mm between the conductors, we have a significant decrease of the magnetic field.

3.3 The case of two conductors through which anti-parallel currents flow

All physical parameters are also preserved in this case, except that the currents flowing through the conductors once have the same direction and the next time have the opposite direction. Compared to the previous case, we not only have a noticeable amplification of the magnetic field in the distance between the two conductors, but we also have amplification in a certain part of the surface of the conductors. The dependence of the magnetic induction intensity on the distance in the occasion when currents are anti-parallel is shown in figure 6.

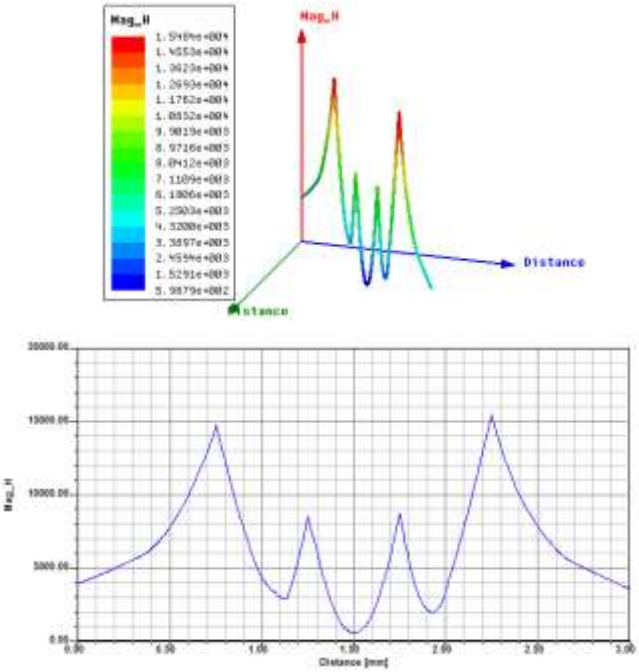

Figure 5.*The change of magnetic field intensity depending on the distance when currents have the same directions*

4. Conclusions

- Through modeling and simulation, we have the ability to visually represent the magnetic field of a current-carrying conductor and predict the results for even more complex cases.
- In the case of one conductor, we have found how the intensity of the magnetic field (H) changes from inside to outside of the conductor. The magnetic field inside the conductor changes linearly with the conductor radius $B = (\mu Ir)/(2\pi R^2)$, while outside the conductor the magnetic field follows the law of Biot-Savart $B = (\mu_0 I)/(2\pi r)$ so as field falls off as 1/r, figure 3.

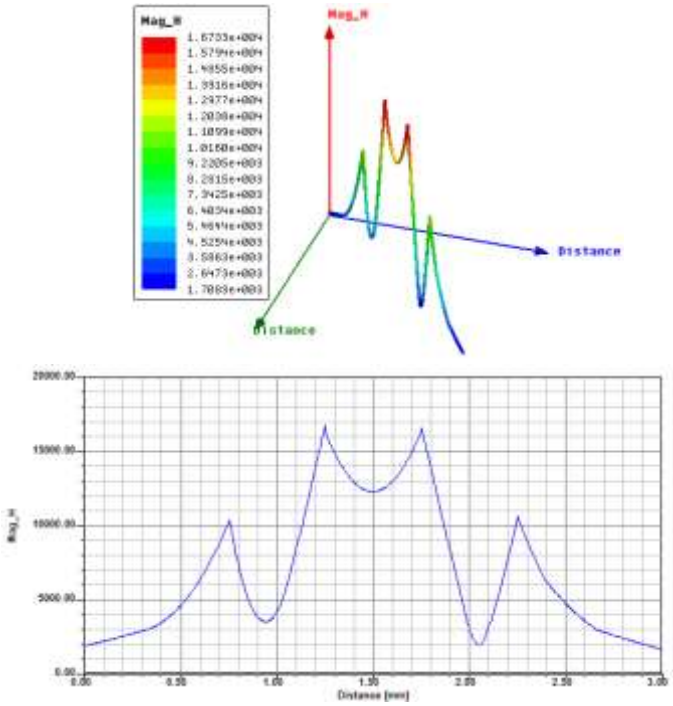

Figure 6. *The change of magnetic field intensity depending on the distance between two conductors when currents have opposite directions.*

- The magnetic field has minimum value near the main axis of the conductor, H = 1710 A / m. The intensity of the magnetic field decreases significantly going towards the center due to the fact that the magnetic fields formed by each particle cancel each other out, so as we have weakening of the field, figure 3.
- In the case of two conductors two situations arise: the amplification and the weakness of the magnetic field depending on the directions of the currents within the conductors.
- When currents have same direction, we notice that magnetic field between the conductors weakens. Exactly at the distance 0.25mm between the conductors we have the minimum value H = 598.78 A / m, while the magnetic field depending on the distance, changes as in figure 5
- While in the case when currents have opposite directions, we have a significant amplification of the magnetic field. Exactly in the middle of the distance between the conductors (i.e. d / 2 = 0.25mm), the magnetic field has the value H = 12301 A / m. This amplification occurs because the magnetic field lines of the two conductors, in the space between them, have the same direction, so they do not cancel each other out, figure 6. In this case, two maxima that belong to two separate parts of the surfaces of these conductors are clearly seen.

Author Statements:

- The authors declare that they have equal right on this paper.
- The authors declare that they have no known competing financial interests or personal relationships that could have appeared to influence the work reported in this paper
- The authors declare that they have nobody or no-company to acknowledge.

References

[1] Mário H Oliveira and José A Miranda, Biot-Savart-like law in electrostatics, European Journal of Physics 22(1), 2020 DOI:10.1088/0143-0807/22/1/304

[2] Daniel Maystre, Maxwell: A new vision of the world, Comptes Rendus Physique 15 (5), 2014, 387-392, DOI:/10.1016/j.crhy.2014.02.004

[3] C. H. Chen et al., Effect of surrounding air region size on finite element modeling for permanent magnetic solenoids, journal of Applied Physics 109(7),2011 DOI:10.1063/1.3540410

[4] Martín Martínez Villar, Finite element modelling of the magnetic field of guitar pickups with ANSYS 2003 DOI: 10.13140/RG.2.1.3765.5920

[5] Dagoberto s. severo et al., Modeling magnetohydrodynamics of aluminum electrolysis cells with ANSYS and cfx, light metals 2005 edited by halvor kvande tms (the minerals, metals & materials society), 2005

[6] A.A. Jadallah et al.Modeling and Simulation of a Photovoltaic Module in Different Operating Regimes, Acta Physica Polonica A, 128B, 461. 2015. DOI: 10.12693/APhysPolA. 128.B-461

[7] B. Nagy, B. Thermal Calculation of Ground Contact Structures: New Methods Based on Parametrized Transient Finite Element Thermal Modeling, Acta Physica Polonica A, 128.B-164,2015 DOI: 10.12693/APhysPolA. 128.B-164

[8] Y. Özcanli et al. Comparison of Mechanical Properties and Artificial Neural Networks Modeling of PP/PET Blends, Acta Physica Polonica A, 130, 444, 2016 DOI:10.12693/APhysPolA.130.444

[9] A. Özdemir, State-Space Modeling of an EPW in Discrete Time and an Observer Design for State Variable Estimation, Acta Physica Polonica A, 130, 228, 2016 DOI:10.12693/APhysPolA.130.228

[10] I. Cayiroglu, Wing Aerodynamic Optimization by Using Genetic Algoritm and Ansys, Acta Physica Polonica A, 132, 981, 2017 DOI: 10.12693/APhysPolA.132.981

[11] A. Beycioğlua, Usability of Fuzzy Logic Modeling for Prediction of Fresh Properties of Self-Compacting Concrete, Acta Physica Polonica A, 132,1140, 2017 DOI: 10.12693/APhysPolA.132.1140

International Journal of Computational and Experimental Science and ENgineering (IJCESEN)

Vol. 7-No.3 (2021) pp. 114-118
http://dergipark.org.tr/en/pub/ijcesen

ISSN: 2149-9144

Research Article

Examination of the Composition and Microorganisms in the Oral Microflora with to Immunological Parameters Identification of Saliva

Abdulrazaq Mohammad SABAH [1*], Ikonnikova NATALIYA [2]

[1] International Sakarov Enviromental Institute of Belarusian State University, 32200, Minsk
***Corresponding Author Email :** mohmmedaldraje4@gmail.com **ORCID:** 0000-0003-1737-2874

[2] International Sakarov Enviromental Institute of Belarusian State University, 32200, Minsk
Email: i.nataliya@gmail.com - **ORCID:** 0000-0002-1733-1832

Article Info:

DOI: 10.22399/ijcesen.1011764
Received : 18 October 2021
Accepted : 04 November 2021

Keywords

Mucosa
Micro flora
Oral cavity

Abstract:

The oral mucosa is a mucous membrane that connects the lips to the pharyngeal and gastrointestinal mucosa. Its particular properties enable it to function as a gatekeeper, regulating the impact of inhaled and ingested antigens, and the degrees of inflammation and immunological responses tolerated in a normal healthy mouth cavity. The objectives of this study are to: (1) quantification of the composition of the oral micro flora in individuals of 18-50 years old; (2) examination of the oral cavity microorganisms (culture-morphological and microscopic studies); and (3) determination the biochemical parameters (lysozyme concentration, active acidity level) of the oral fluid (saliva). Swabs from the oral cavity (within the cheeks) were used to inoculate agar media (MPA, Endo medium). Colonies (CFU) on the agar medium's surface were counted and converted to an area of the oral cavity (4 cm2). The oral fluid was collected in the morning, on an empty stomach, before brushing the teeth, into a sterile test tube with a tight-fitting cover. This was done by thoroughly cleaning the individual's mouth with a sterile 0.9% NaCl solution. We used indicator strips of paper with pH ranges of 5.4–7.8, 0.2 steps. Oral fluid centrifuged (2000 rpm for 20 min). The research revealed that those with periodontitis and caries had pH alterations in their saliva. The results showed that individuals with dental and periodontal issues had substantially lower levels of Lysozyme than healthy people. A severe decrease of nonspecific oral tissue resistance lowers oral fluid resistance to pathogens. Morever, Oral bacteria were all Amoxicillin resistant. Lactobacillus.

1. Introduction

The oral mucosa is defined as a mucous membrane that is continuous with the skin at the lips, and more importantly continuous with the pharyngeal mucosa and the gastrointestinal mucosa. While the oral mucosa shares many features with the skin and gastrointestinal mucosa it has many unique features that enable this sophisticated tissue to act as a gatekeeper controlling the effects of both inhaled and ingested antigens and the levels of inflammation and immune responses that are permitted in a normal healthy oral cavity. Most invaders access the body via external surfaces and the oral mucosa is exposed to a huge antigenic challenge in the form of ingested food and the microbes that make up the commensal oral flora [1 - 2].

It has been estimated that >1000 kg of nutrients will pass through the adult gut per year and more than 700 different species colonise the oral cavity. Microbes, necrotic cells and hypoxia initiate inflammatory responses which, depending on the duration and severity, may result in clinical or pathological manifestations. The distinction of these tissues is important in understanding the differential immune responses that are possible within the oral cavity [3, 4]. The major lymphoid organs are the tonsils and adenoids, making up Waldeyer's ring and there are numerous lymph nodes draining the head and neck that contribute to the immune function of the oral immune system. Mammals have evolved a sophisticated innate and adaptive immune system that integrates this network of tissues, cells and effect of molecules and protects the body from disease by recognition of potential pathogens or diseased tissues [5, 6].

Saliva is uniquely adapted to the functions it needs to perform in the oral cavity. It continually bathes the

hard and soft tissues to maintain the healthy tissues of the oral cavity, oropharynx, and larynx. Saliva is formed by three pairs of major salivary glands, namely parotid, submandibular, and sublingual, and hundreds of minor salivary glands, with some of the GCF being secreted from the gingival sulcus [7].

With the help of microorganisms, a person is able to perform functions that are not encoded by their own genome, for example, protection against invasive pathogens, extracting additional energy from food, synthesizing key molecules for the development of their own cells and tissues. Moreover, these functions of the microbiota are highly specialized and differ depending on the localization of microorganisms in the gastrointestinal tract and other loci of the human body. The main goal of the study is to the microflora of the human oral cavity, its participation in the formation of the body's immune system reactivity. However, the objectives of this study are to (1) characterize the qualitative and quantitative composition of the oral microflora from among the examined people aged 18-50 years; (2) identify the microorganisms of the oral cavity (culture-morphological and microscopic studies); and (3) determine the biochemical parameters (lysozyme concentration, active acidity level) of the oral fluid (saliva) [8].

2. Methodology

To accomplish the study's objectives, 65 people of various ages (ranging from 18 to 50 years old) were examined, including students, teachers, laboratory assistants, and employees of Belarusian State University's International Sakharov Environmental Institute, as well as patients of the Slutsk district hospital who provided written informed consent for the collection of biological material. The study examined 65 individuals ranging in age from 18 to 50 years, including students, teachers, laboratory assistants, and employees of Belarusian State University's International Sakharov Environmental Institute, as well as patients of the Slutsk district hospital who provided written informed consent for the collection of biological material. A questionnaire survey was administered to the respondents to ascertain their susceptibility to colds or chronic illnesses, their bad habits (smoking), their practice of regular oral hygiene, and their lack of practice. Two groups were created on the basis of age: group 1 consisted of 37 individuals aged 18-25 years and group 2 consisted of 28 individuals aged 43-50 years. According to the survey's findings, 15 individuals were found to have different oral cavity illnesses. The remaining respondents did not have any oral cavity illnesses, as presented in Table 1.

Table 1: *Group of people who took part in the study*

Category	**Group 1**	**Group 2**
Age	18 - 25 years (n=37)	43 – 50 years (n=28)
Diseases of the oral cavity	Present (n=15)	Absent (n=50)

The oral cavity (inside surface of the cheeks) was swabbed and inoculated onto agar media (MPA, Endo medium) using sterile cotton swabs. The quantitative count of microorganisms was accomplished by counting colonies (CFU) on the agar medium's surface and then converting to a specific unit of the oral cavity's area (4 cm^2).

Saliva was collected in the morning, on an empty stomach, before to brushing the teeth, into a sterile test tube with a tight-fitting lid to determine the various parameters of the oral fluid. After thoroughly washing the mouth cavity with a sterile 0.9 percent NaCl solution, a 3-5 ml sample of saliva was obtained from the individual.

pH was determined using indicator strips of paper with a pH range of 5.4–7.8, with a step of 0.2. Centrifuged the pre-collected oral fluid (2000 rpm for 20 min). The pH of the supernatant was determined by dropping it onto indicator paper and calculating the pH value using a standard scale. To determine the lysozyme content, saliva from patients was collected in 1 ml polyethylene tubes, diluted 1:1 with saline, and centrifuged at 1500 rpm for 10 minutes. We analysed the supernatant. The ability of serum to act on a culture of micrococci grown on slanting agar is one way for determining lysozyme. A daily culture suspension in saline is made in accordance with an optical standard (10 U). The test serum is diluted with physiological solution tenfold, twentyfold, fortyfold, and eightfold, respectively. Each test tube is filled with an equal volume of microbial suspension. The tubes are shaken and then placed in a thermostat set to 37 ° C for 3 hours. The reaction is considered in relation to the serum's degree of clarity. The lysozyme titter is the final dilution at which the microbiological suspension is completely lysed. However, the measurements are made in calibrated test tubes to which 1 ml of the studied lysozyme solution is added three times in parallel. 0.5 M phosphate buffer is used as a control. To quantify lysozyme in unknown concentration solutions, a calibration curve is developed using enzyme concentrations of 2, 4, 6, 8 g in the sample. Use a standard solution of 200 g / ml to dilute lysozyme. It is then used to make a stock solution of lysozyme at a concentration of 8 g / ml. 50 mg / 100 ml from dried lysozyme To construct the calibration curve, take ten tubes and arrange them as follows: (i) 1 and 2 - control without lysozyme (1 ml of water), (ii) 3 and 4 - 2 μg of lysozyme (0.25 ml of lysozyme + 0.75 ml of

water), (iii) 5 and 6 - 4 µg of lysozyme (0.5 ml of lysozyme + 0.5 ml of water), (iv) 7 and 8 - 6 µg L of isozyme (0.75 ml of lysozyme + 0.25 ml of water), and (v) 9 and 10 - 8 µg of lysozyme of 1 ml of the original solution of lysozyme). Following the creation of all lysozyme solutions, 6 ml of a suspension of micrococcus acetone powder is added to each test tube at a 30 second interval. Additionally, the hygienic state of the oral cavity was examined by inoculating the test material on the following nutrient media: meat-peptone agar (MPA), Endo's medium, Levin's medium, yolk-saline agar, Muller-medium, Hinton's and Czapek [9, 10].Inoculations should be incubated at 37 ° C for 18–24 hours. The inoculations were permitted to incubate for up to 5 days in the absence of growth on blood agar, thioglycolic medium, or sugar broth. For 72 hours, inoculations in Sabouraud's medium were incubated simultaneously at 37 ° C and room temperature. The mean values, standard deviation (M + SE), median and spread of values, as well as correlation analysis, were determined using statistical methods during data processing. The Student's t-test was used to determine the significance of differences between indicator groups. Significant differences were defined as those with a p 0.05 value. When statistical analysis of the data was performed, a software package of 10.0 STATISTICA was used.

3. Results and Discussions

The hydrogen index of oral fluid (saliva) from healthy persons evaluated (table 2) was 6.97 0.07, which is within the range of normal values. Saliva pH changes were seen in a sample of patients with periodontal disease and tooth decay. The pH of the persons evaluated in this group was 5.03 0.2. The results indicated a statistically significant reduction in pH value when compared to a healthy control group and the norm. Fluctuations in saliva's hydrogen index can result in a significant decrease in its mineralizing ability (acidification) or in its strengthening and the production of dental calculi. Acids created during microbial metabolism from carbohydrates that collect in the plaque due to the delayed flow of saliva through it can induce a drop in pH. Thus, chronic sugar consumption can lower the pH of dental plaque to 5.0, promoting the growth of acid-producing bacteria such as lactobacilli and S. mutans and predisposing to the formation of caries. Plaque pH decreases mostly as a result of sugar usage. According to the acquired findings, the concentration of lysozyme in the oral fluid of patients suffering from dental and periodontal illnesses is much lower than that of healthy individuals (Figure 1). The results indicated a severe deterioration of oral tissues' nonspecific resistance, which ultimately results in a deterioration of oral fluid's ability to resist the corrosive influence of pathogenic agents.

Table 2: *pH value of oral fluid*

Indicator	Group of relatively healthy people (n= 50)	Group of people with caries and periodontal diseases (n=15)	Normal pH value
pH	6,97± 0,07 *	5,03 ± 0,2 *	6,5–7,4

*Take note that * denotes differences with a p0,05 statistical significance.*

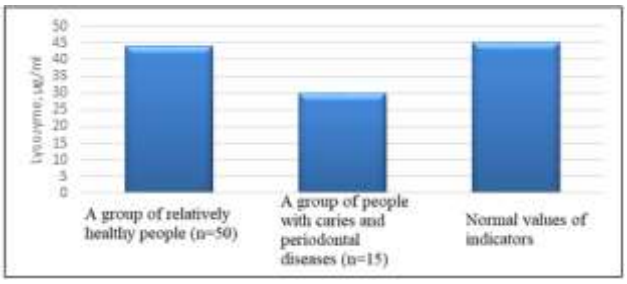

Figure 1*: Lysozyme concentration µg/ml in the examined individuals*

It is well established that lysozyme is an enzyme involved in the formation of lysosomal cell structures. It is a critical component of non-specific protection related with the monocyte-macrophage system's function. The oral microbiota of the comparative groups was dominated by staphylococci and streptococci. Additionally, enterobacteria, veillonella, bacteria, bacteroids, actinomycetes, and Neisseria were Identified (table 4 and 5). Streptococcus genus representatives were the most commonly planted - accounting for 57% of all microorganisms sown in this biotope. Representatives of the staphylococci genus occupied 22%, enterobacteria accounted for up to 15%, occupied around 4%, and Neisseria accounted for 2%. Figure 2 illustrates the formation of several bacterial cultures in the form of distinct microorganism

Figure 2 : *examples of growth parameters of microbial colonies of the main representatives of the oral microflora on nutrient media*

Table 3: *Stabilizing (resident) flora 1. Aerobes and facultative anaerobes*

Staphylococcus spp:					
S. mutans	39,8	2,3±0,28	18,1	of 5.3±1.01	at least 5-7
S. salivarius	46,2	of 1.7±0,12	12,4	4,4±0,84	at least 5-7
S. milleri	21,2	1,5±0,31	24,8	of 6.2±0.93	at least 5-7
S. sanguis	60,4	1,5±0,26	58,2	3,5±0,70	at least 5-7
Neisseria spp.	28,4	4,2±0,54	23,5	4,7±0,34	at least 5-7
Lactobacillus spp.	31,4	3,1±0,12	29,6	of 5.4±0.46	no more than 3-4
Enterococcus spp.	13,1	3,2±0,71	56,2	3,4±0,67	no more than 1-2
Corinebacterum spp.	38,4	of 2.6±0,94	39,1	of 5.4±0.36	3-4
2. Obligate anaerobes:					
Veilonella spp.	13.1	3.2±0.71	39.1	5.4±0.36	no more than 3-4
Fusobacteria	38.4	2.6±0.94	56.2	3.4±0.67	no more than 1-2
Non-permanent(transient) microbiota. Aerobes and facultative anaerobes:					
Gram-negative rods:					
S. aureus	0	Not determined	35.2	4.7±0.52	0
S. epidermidis, S. saprophyticus	10.4	1.5±0.24	44.4	4.7±0.42	not more than 1-2
Escherichia coli	2.8	1.7±0.16	16.2	3.3±0.65	not more than 1-2
Klebsiella	1.1	1.5±0.12	5.7	2.8±0.31	not more than 1-2
Obligate anaerobes: Clostridia:					
Clostridium tetani	0	Undetected	39.1	5.1±0.26	0
Clostridium spp. ramosum	0	Not determined	24.8	3.2±0.93	0

colonies. The majority of the saliva flora is made up of facultative streptococci and veillonella, which enter mostly through the back of the tongue. Streptococcus salivarius is constantly vegetating on the tongue, where it is washed away by saliva, which also contains large concentrations of the bacteria. Neisseries are continually present in the oral cavity (and frequently in saliva), accounting for 3-5 percent of the bacteria produced (Table 3). Quantitative indications of microbial seeding from the oral cavity showed a considerable rise in titers of the following microorganisms: Lactobacillus spp., Staphylococcus aureus, Staphylococcus sepidermidis, Staphylococcus saprophyticus, and Staphylococcus mutans (Table 6). It is observed two characteristics of oral microbiocenosis: decreased colonization by representatives of the normal microbiota and

Table 4: *Identification of qualitative and quantitative composition of carious-pathogenic oral microbiota*

Carious-pathogenic microbiota					
Microorganisms	detection Rate, %	Quantity in 1 ml		Standard parameters
		1 group 18-25 years (n =	2 group 43-50 years (n	
Klebsiella	15	10±5	40±9	0
Escherichia coli	2	7±3	60±5	±
Aerobacter	3	9±6	35±7	0
Pseudomonas	±	Not	9±3	0
Proteus	±	Not determined	16±6	0

Table 5: *Identification of the qualitative and quantitative composition of paradontopathogenic oral microbiota*

Paradontopathogenic microbiota				
Microorganisms	detection Rate, %	Quantity in 1 ml		Standard parameters
		1 group, 18-25 years, (n	2 group, 43-	
Porphyromonasgingiv	15	25±4	60±9	0
Escherichia coli	2	6±2	28±5	±
Aerobacter	3	14±3	35±7	0
Pseudomonas	±	Not determined	15±3	0
Proteus	±	Not determined	22±6	0

increased colonization by oral opportunistic microbiota with high adhesive qualities.The established method for determining the qualitative and quantitative composition of oral biocenoses expands the possibilities for early diagnosis, monitoring, and prognosis of the development of oral inflammatory illnesses.

4. Conclusions

The objectives of this study were to) quantify the composition of oral microflora in people aged 18-50; and examine oral cavity microorganisms (culture-morphological and microscopic studies); as well as assess oral fluid biochemical parameters (lysozyme concentration, active acidity level) (saliva). The study examined 65 individuals ranging in age from 18 to 50

Table 6 *: Quantitative composition of oral microflora in the examined individuals (M+m)*

	Number of microorganisms in 1 ml

Type of microflora	Standard indicators	1 group , 18-25 years, (n = 37)	group 2, 43-50 years, (n = 28)
Lactobacillus spp.	no more than 3-4	of 3.01±0,12	↑5,44±0,46
Staphylococcus aureus	no more than 3-4	of 2.54±0,08	↑ 6,35±0,68
Staphylococcus epidermidis, saprophyticus	more than 3-4	of 2.86±0,06	4,17±0,21
Staphylococcus salivarius	at least 5-7	of 7.98±0,06	5,19±0,28
Staphylococcus sanguis	no more than 5-7	of 7.01±0,71	4,27±0,89
Staphylococcus mutans	no more than 5-7	and 3.21±0,12	↑ 8,26±0,1
Staphylococcus haemolyticus	the absence of	0	to 2.47±0,34
Enterococusfaecium	no more than 1-2	of 1.01±0,05	2,26±0,8
Neisseria spp.	no more than 5-7	4.26±0.28	5.93±0.25
Actinomyces species	no more than 2-3	2.17±0.06	1.54±0.05

years, including students, teachers, laboratory assistants, and employees of Belarusian State University's International Sakharov Environmental Institute, as well as patients of the Slutsk district hospital who provided written informed consent for the collection of biological material. The results obtained from the analysis indicated that the A group of persons with periodontitis and caries had pH changes in their saliva. The pH of this group was 5.03 0. 2. The pH dropped significantly compared to the healthy group. The results revealed that the Lysozyme level in oral fluid is much lower in patients with dental and periodontal problems than in healthy persons. This suggests a severe loss of nonspecific oral tissue resistance, which necessarily reduces oral fluid resistance to pathogenic agents. Morover, The oral bacteria were all resistant to Amoxicillin. Carbenicillin-resistant Lactobacillus, Staphylococcus, Bifidobacterium, Escherichia, and Sarcina bacteria. Streptomycin, Doxycycline, and Tetracycline were all active.

Author Statements:

- The authors declare that they have equal right on this paper.
- The authors declare that they have no known competing financial interests or personal relationships that could have appeared to influence the work reported in this paper
- The authors declare that they have nobody or no-company to acknowledge.

References

[1] Ebersole, J. L., Schuster, J. L., Stevens, J., Dawson, D., Kryscio, R. J., Lin, Y., & Miller, C. S. (2013). Patterns of salivary analytes provide diagnostic capacity for distinguishing chronic adult periodontitis from health. *Journal of clinical immunology*, *33*(1), 271-279.

[2] Gursoy, U. K., Könönen, E., Pradhan-Palikhe, P., Tervahartiala, T., Pussinen, P. J., Suominen-Taipale, L., & Sorsa, T. (2010). Salivary MMP-8, TIMP-1, and ICTP as markers of advanced periodontitis. Journal of clinical periodontology, 37(6), 487-493.

[3] Özcan, E., Saygun, N. I., Serdar, M. A., & Kurt, N. (2015). Evaluation of the salivary levels of visfatin, chemerin, and progranulin in periodontal inflammation. Clinical oral investigations, 19(4), 921-928.

[4] Tabari, Z. A., Azadmehr, A., Nohekhan, A., Naddafpour, N., & Ghaedi, F. B. (2014). Salivary visfatin concentrations in patients with chronic periodontitis. Journal of periodontology, 85(8), 1081-1085.

[5] Kinney, J. S., Morelli, T., Braun, T., Ramseier, C. A., Herr, A. E., Sugai, J. V., & Giannobile, W. V. (2011). Saliva/pathogen biomarker signatures and periodontal disease progression. Journal of dental research, 90(6), 752-758..

[6] Teles, R. P., Likhari, V., Socransky, S. S., & Haffajee, A. D. (2009). Salivary cytokine levels in subjects with chronic periodontitis and in periodontally healthy individuals: a cross-sectional study. Journal of periodontal research, 44(3), 411-417., 1-13.

[7] Koh, D. S. Q., & Koh, G. C. H. (2007). The use of salivary biomarkers in occupational and environmental medicine. Occupational and environmental medicine, 64(3), 202-210.

[8] Gursoy, U. K., Könönen, E., Uitto, V. J., Pussinen, P. J., Hyvärinen, K., Suominen-Taipale, L., & Knuuttila, M. (2009). Salivary interleukin-1β concentration and the presence of multiple pathogens in periodontitis. Journal of clinical periodontology, 36(11), 922-927.

[9] Tobón-Arroyave, S. I., Jaramillo-González, P. E., & Isaza-Guzman, D. M. (2008). Correlation between salivary IL-1β levels and periodontal clinical status. Archives of oral biology, 53(4), 346-352.

[10] Mirrielees, J., Crofford, L. J., Lin, Y., Kryscio, R. J., Dawson III, D. R., Ebersole, J. L., & Miller, C. S. (2010). Rheumatoid arthritis and salivary biomarkers of periodontal disease. Journal of clinical periodontology, 37(12), 1068-1074.

International Journal of Computational and Experimental Science and ENgineering (IJCESEN)
Vol. 7-No.3 (2021) pp. 119-122
http://dergipark.org.tr/en/pub/ijcesen

ISSN: 2149-9144

Research Article

Modelling of Global Solar Radiation in Algeria Based on Geographical and all Climatic Parameters

Sabah FETAH[1]*, Mohamed SALMi[2]

[1] Department of Physics, Faculty of science. University of M'sila, 28000, Algeria
* **Corresponding Author** : **Email:** sabah.fetah@univ-msila.dz - **ORCID:** 0000-0001-8483-7016

[2] Department of Physics, Faculty of science. University of M'sila, 28000, Algeria
Email: mohamed.salmi@univ-msila.dz - **ORCID:** 0000-0002-4146-3592

Article Info:

DOI: 10.22399/ijcesen.1018844
Received : 01 October 2021
Accepted : 07 November 2021

Keywords :

Global solar radiation
Modelling
Statistical regression
Geographical parameters
Climatic parameters

Abstract:

The design of photovoltaic or solar systems and estimating their performance require knowledge of the intensity of solar radiation. The measurement of this parameter for some sites in Algeria is unfortunately not obvious. However, researchers are moving towards the modelling, estimation and prediction. To model the global solar radiation, we must take into account the geographical and climatic parameters such as sunshine duration, relative humidity, temperature, latitude site, etc. In this study, the modelling of daily global solar radiation on a horizontal plane according to the parameters mentioned above is based on the statistical linear regression technique. The daily data used in the development and validation of models are extracted from the database of O. N. M (National Office of Meteorology, Dar el Beida. Algeria) for 2001-2005. We test the proposed models on two sites such as Djelfa and Ain-Bessam. For each site, validity and performance of the model will be studied based on the number of parameters introduced in the analytical expressions and results are discussed in terms of statistical errors as: R, MBE and RMSE between the measured global solar radiation and global solar radiation estimated. It was found that air temperature and relative humidity are indeed important climatic parameters for the prediction of solar radiation.

1. Introduction

Solar energy is the most ancient source of energy; it is the basic element for almost all fossil and renewable types. Using solar energy to generate electrical energy for any specific site location necessitates an exact estimation of global solar radiation; a provision should be made to forecast solar energy which will convert to electrical energy to recover the load demand, that is, the amount of solar energy for that place ought to be known. Technology for measuring global solar radiation is costly and has instrumental hazards. The importance of the actual work lies on the fundamental need of quantification of the global solar radiation data in this site. The solar radiation reaching the earth's surface depends on the climatic condition of the specific site location [1-3]. Therefore, over the last decades, different models have been proposed to predict the amount of solar radiation using various parameters. Most analyses of the correlation between solar radiation and climatic parameters involve the use of relative sunshine duration [4-7]. However, air temperature and humidity should also be considered as an important climatic variable for solar radiation prediction because it is a reflection of both the duration and intensity of the solar radiation incident on a given location [8, 9], [10- 12].

2. Data

Measured global solar irradiation (G) and climatic parameters data, between 2001 and 2005, for two cities in Algeria: Ain-Bessem (Latitude 36.31°N, Longitude 3.67°E, Altitude 629 (m)) and Djelfa (Latitude 34.68°N, Longitude 3.25°E, Altitude 1126 (m)), were obtained from Algerian Meteorological Agency O.N.M, Dar el Beida.
Our aim is to develop a best model with a few climatic parameters to estimate the solar radiation data (G/G0) in future time domain. The estimations

were made by many combinations of data, by using a linear regression analysis. These data are chosen due to their correlation with the global solar radiation. In linear regression model, the dependent variable comprises the ratio of the global solar irradiation (G) to the available radiation at the top of the atmosphere (G0); and the independent variables comprise the different climatic parameters (mean daily maximum temperature, mean daily relative humidity, mean daily sea level pressure, mean daily vapor pressure, wind, precipitation and the ratio of hours of bright sunshine (S) to the day length (S0). The measured data between 2001 and 2004 have been used for calculating the coefficients of the model while those from 2005 are used for testing data. The testing data are not used in modeling. The values of the extraterrestrial radiation G0 and the day length S0 were calculated. The data was subjected to quality checks before being used in the analysis. It was ensured only complete data set was used. The values of G/Go and S/So are all less than one.

3. Discussions

The choice of a number of models is conducted by the fact that the single model does not give a good generalization for the sites under study. Accordingly, several models have been tested to choose the more suitable for each location. Statistical analysis of the results was performed using the correlation coefficient (R), the root mean square error (RMSE) and the mean bias error (MBE) criteria [12, 13].

Table 1. *Pearson's correlation coefficients*

	P	V	R	Tx	Tm	Tn	Um	S/S0	T/Tx	U/U x	(Tn/Tx)
Ain Bessem	0.644	0.307	-0.329	0.723	0 .66 1	0.546	-0.114	0.454	-0.068	-0.636	-0 .257
Djelfa	0.215	0.012	-0.272	0.605	0.460	0.343	-0.591	0.293	0.316	-0.534	0.199

The study of correlations among solar radiation and several climatic parameters has shown that (S/So) is not the best single parameter to be used for predicting solar radiation. For example, Table 1 shows Pearson's correlation coefficients for Ain-Bessem and Djelfa cities. It is seen that for Ain-Bessem, (G/Go) correlate best with (Tx), followed by Tm and S/So, respectively, while (Um) and (Tx) are best followed by Tm for Djelfa. Thus in both cases, the best single parameter for estimating (G/Go) is not (S/So). From Table 3, we can observe that the correlation coefficient for the studied models, listed presented in Table 2, is arranged between 72.30% and 91.00%. It is clearly shown that, the best performance is obtained by the models (7, 8, 9 and10) where the correlation coefficient R is arranged between 90.30% and 91.10%.

Table 2. *Models used for estimating (G/G0) for Ain-Bessem city.*

Models	Ain Bessem
1	G/G0 = 0.2597 + 0.103 (Tx)
2	G/G0 = 0.142 + 0.069 (Tx) -0.075 (Tm)
3	G/G0 = 0.1621 + 0.0352 (Tx) -0.0418 (Tn)
4	G/G0 = 0.152 + 0.046 (Tx) -0.021 (Tm) – 0.031(Tn)
5	G/G0 =0.4365 +0.0305 (Tx) -0.0312 (Tn) -0.3924(Tm/Tx)
6	G/G0 = 0.7152 +0.077 (Tx) – 0.0294 (Tn) – 0.4701 (Tm/Tx) -0.2372(Um/Ux)
7	G/G0 = 0.6740 +0.0238 (Tx)- 0.0266 (Tn) -0.3743 (Tm/Tx) -0.3503 (Um/Ux) + 0.0001(P)
8	G/G0 = 0. 6855 +0.0219 (Tx) – 0.0244 (Tn) -0. 3357 (Tm/Tx) - 0. 4033 (Um/Ux) + 0002(P) -0.0051 (Vx)
9	G/G0 = 0.6731 + 0.0216 (Tx) – 0.0242 (Tn) – 0.3326 (Tm/Tx) - 0.3851 (Um/Ux) + 0.0002 (P) – 0.0042 (Vx) -0.0034 (R)
10	G/G0 =0.5707+ 0.0004 (P) - 0.0046 (Vx) - 0.0028 (R) + 0.0257 (Tx) - 0.0202 (Tn) - 0.0116 (Tm) - 0.2817(Tm/Tx)- 0.2905(Um/Ux) - 0.0026 (Um)

However, the best correlation in test is obtained for the model 7, and this model need in his input only (T, U) parameters and P that are always available, and they can be measure easily. The obtained R is 95.20%, which is higher than other models. The RMSE is 0.032799 and the MBE is -0.034701. Figure1 shows a comparison between measured and estimated daily global solar radiation by using model 7. In addition, we have developed others models for Djelfa city, where the relative humidity is always combined with temperature. Therefore, we develop these models in order to show the influence of each parameter for estimating daily global solar radiation. Table 4 resumes the different models used for estimating (G/G0) for Djelfa city. Therefore, in the case, when we use as input only the relative humidity and temperature, the best correlation coefficient is decreases to 79.10% (model 11).

Table 3. *Statistical analysis of the results. The correlation coefficient (R), the root mean square error (RMSE) and the mean bias error (MBE)*

Model	R	TEST Ain Bessem (2005)		
		R	RMSE	MBE
1	0.7230	0.3625209827	0.01852814	0.225915
3	0.8880	0.2111230077	0.00739882	0.002873
5	0.8930	0.938316204	0.04267256	-0.173248
6	0.8960	0.9084633204	0.09311018	-1.245345
7	0.9030	0.9519602352	0.03279829	-0.034701
8	0.9070	0.9399992203	0.02980376	-0.042758
9	0.9040	0.9379488948	0.02951324	-0.048033
10	0.9110	0.9399489003	0.02980376	-0.042758

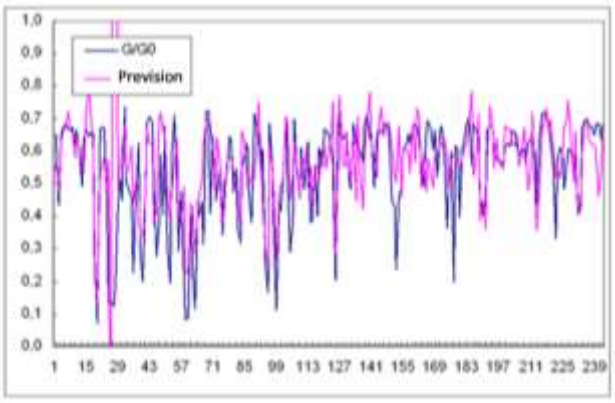

Figure1. *comparison between measured and estimated daily global solar radiation by using model 7 (Ain-Bessem).*

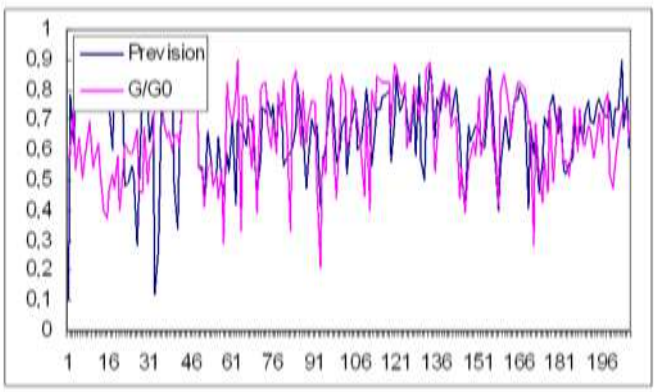

Figure 2. *comparison between measured and estimated daily global solar radiation by using model 11 (Djelfa).*

Table 4. *Models used for estimating for Djelfa city*

Model	R	Djelfa
1	0.591	G/G0 = 0.8670 - 0.0037 (Um)
2	0.691	G/G0 = 1.0761 - 0.0062(Um) - 0.4876(Tn/(Tx))2
3	0.711	G/G0 = 1.1558 - 0.0057(Um) - 0.5361(Tn/(Tx))^2 - 0.0058(Vx)
4	0.719	G/G0 = 0.9215 - 0.0044(Um) - 0.6990(Tn/(Tx))2 - 0.0050(Vx) + 0.0060(Tx)
5	0.729	G/G0 = 0.8608 - 0.0036(Um) - 0.6986(Tn/(Tx))2 - 0.0043(Vx) + 0.0070(Tx) - 0.0090(R)
6	0.756	G/G0 = 0.8542 - 0.0038(Um) - 0.6833(Tn/(Tx))^2 - 0.0055(Vx) + 0.0096(Tx) - 0.0091(R) - 0.0002(Tx^2 (Um/Ux)^2)
7	0.766	G/G0 = 0.7009 - 0.0029(Um) - 0.6843(Tn/(Tx))2 - 0.0056(Vx) - 0.0051(Tx) - 0.0094(R) - 0.0011(Tx2(Um/Ux)2) + 0.0367(Tx(S/S0))
8	0.777	G/G0 = 1.3177 - 0.0031(Um) - 0.7299(Tn/(Tx))^2 - 0.0048(Vx) - 0.0465(Tx) - 0.0099(R) - 0.0019(Tx^2 (Um/Ux)^2) + 0.1077(Tx)(S/S0) - 0.9871(S/S0)
9	0.794	G/G0 = 1.9491 - 0.0032(Um) - 0.7658(Tn/(Tx))^2 - 0.0026(Vx) - 0.0400(Tx) - 0.0102(R) - 0.0018(Tx^2 (Um/Ux)^2) + 0.0983(Tx(S/S0)) - 2.3323(S/S0) + 1.1687(Um/Ux)^2
10	0.802	G/G0 = -2.3357 - 0.0040(Um) - 0.7222(Tn/(Tx))^2 - 0.0019(Vx) - 0.0506(Tx) - 0.0087(R) - 0.0020(Tx\(Um/Ux)^2) + 0.1139(Tx(S/S0)) - 2.6457(S/S0) + 1.2358(Um/Ux)^2 + 0.0051(P)
11	0.791	G/G0 = -3.089 - 0.004 (Um) + 0.049 (Tm)+ 0.085 ((Tn/Tx)^2) 0.004 (P) - 0.003 (Vx) - 0.010 (R) + 0.812 (Tm/Tx) +0.059 (Um/Ux) -0.001 (Tx(Um/Ux)^2) - 0.126 (Tn/Tx) - 0.015 (Tx(Um/Ux)) -0.015 (Tn) + 0.049 (Tx)

Also, when we mixed air temperature, relative humidity and the ratio S/S0 the correlation coefficient is decreases only to 80.20% (model 10). Therefore, the model combined (T and U) can be used in the case when we have not the sunshine duration. Figure 2 shows a comparison between measured and estimated daily global solar radiation by using model 11. It is clear that air temperature and relative humidity are indeed important climatic parameters for the prediction of solar radiation.

4. Conclusions

Using different combinations of different variables to analyse available data for two different stations in Algeria, it is clearly demonstrated that air temperature and humidity are an important climatic parameters which should be sufficient in solar radiation modelling in Algeria. The use of only temperature and relative humidity for solar radiation prediction is important because there are many stations in Algeria with sufficient data for T and U (which are relatively easier to measure).

Author Statements:

- The authors declare that they have equal right on this paper.
- The authors declare that they have no known competing financial interests or personal relationships that could have appeared to influence the work reported in this paper
- The author would like to thank the Algerian Meteorological Agency for providing data for achieving the present work.

References

[1] J. A. Prescott, “Evaporation from a water surface in relation to solar radiation”. Trans. R. Soc. Sci. Austria 46, (1940) 114–118

[2] S. M Robaa, “Validation of the existing models for estimating global solar radiation over Egypt”. Energ. Convers. Mgmt. 50, (2009)184–193.

[3] K.Skeiker, “Correlation of global solar radiation with common geographical and meteorological parameters for Damascus province, Syria”. Energy Convers. Mgmt. 47,(2006)331–345.

[4] J.Almorox, C.Hontoria, “Global solar estimation using sunshine duration in Spain”. Energ. Convers. Mgmt. 45 , (2004)1529–1535.

[5] D. B.Ampratwum, and A. S. S. Dorvlo, “Estimation of solar radiation from the number of sunshine hours” App. Energ. 63(1999),161–167.

[6] R.Kumar and L. R.Umanand, “Estimation of global radiation using clearness index model for sizing photovoltaic system”. Renew. Energ. 30, (2005)2221–2233.

[7] E-M. Mossad, “Sunshine and global solar radiation estimation at different sites in Egypt”. J. Atmos. and Sol-Terr. Phy. 67, (2005)1331–1342.

[8] B. G.Akinoglu and A.Ecevit, “Construction of a quadratic model using modified Angström coefficients to estimate global solar radiation”. Sol. Energy 45,(1990)85–92.

[9] A. Al-Mohamed, “Global, direct and diffuse solar radiation in Syria”. Appl. Energ. 79,(2004)191–200.

[10] A.A.El-Sebaii and A.A.Trabea, "Estimation of global solar radiation on horizontal surfaces over Egypt". Egypt. J. Solids 28(2005)163–175.
[11] N. A Elagib and M. G Mansell. "New approaches for estimating global solar radiation across Sudan". Energ. Convers. Mgmt. 41(2000)419–434.
[12] O.Galip, H. Arif and G.Asir, "Statistical analysis of solar radiation data". Energ. Source. 25(2003),1089–1097.
[13] J.Almorox, M.Benito, and C.Hontoria, "Estimation of monthly Angström-Prescott equation coefficients from measured daily data in Toledo", Spain. Renew. Energ. 30,(2005) 931–936.

International Journal of Computational and Experimental Science and ENgineering (IJCESEN)

Vol. 7-No.3 (2021) pp. 123-127
http://dergipark.org.tr/en/pub/ijcesen

ISSN: 2149-9144

Research Article

Immunological Parameters Examination of the Oral Fluid in Normal and Pathological Conditions: Sensitivity Analysis of Microorganisms in Modern Therapeutic practice in vitro

Abdulrazaq Mohammad SABAH [1], Ikonnikova NATALIYA [2]

[1] International Sakarov Enviromental Institute of Belarusian State University, Minsk, Belarus
***Corresponding Author Email :** mohmmedaldraje4@gmail.com **ORCID:** 0000-0003-1737-2874

[2] International Sakarov Enviromental Institute of Belarusian State University,Minsk, Belarus
Email: i.nataliya@gmail.com - **ORCID:** 0000-0002-1733-1832

Article Info:

DOI: 10.22399/ijcesen.1011762
Received : 18 October 2021
Accepted : 07 November 2021

Keywords

Mucosal Immune
Oral fluid
Immunological

Abstract:

Inflammation of the mucosal immune system is a common occurrence (saliva). The masticatory process and salivary enzymes destroy antigenic material that enters the mouth cavity, yet it can still activate immunological responses. Many soluble components are secreted by epithelial cells or incorporated into oral cavity fluids. Defensins, histatins, lysozyme, and lactoferrin all have antibacterial action. They appear to work synergistically with secretory IgA. The objectives of this study is to examine the immunological parameters (concentration of total IgA and secretory IgA) of the oral fluid of the examined individuals in normal and pathological conditions; and to identify the sensitivity/resistance of microorganisms-the main representatives of the oral microflora to antimicrobial drugs widely used in modern therapeutic practice (antibiotics) in vitro. To measure secretory IgA in oral fluid, we used a solid-phase immunoassay and a ZAO Vector Best sIgA ELISA BEST strip. The "secretory IgA-ELISA" reagent collection is designed to quantify secretory IgA in body fluids using enzyme-linked immunosorbent assay. The enzyme-linked immunosorbent assay measures secretory IgA. The t-test was used to assess the significance of differences across indicator groups. Results indicated that amount of total IgA in oral fluid is significantly lower in people with dental and periodontal problems than in people who are healthy. This indicates a decrease in oral cavity resistance and an increase in carious/periodontal processes. Caries and/or periodontal disease have been linked to lgA deficiency. The results showed that staphylococci and streptococci dominated the oral cavity microbiota in the comparison groups. In addition to this, Neisseria and Veillonella were found. Streptococci accounted for 57 percent of all microorganisms planted in this biotope. Enterobacteria accounted for up to 15%, whereas Neisseria accounted for about 4% and 2%. The decrease in sIgA levels in periodontitis patients' saliva indicates a lack of local mucous membrane protection, increasing the risk of caries and periodontitis. The lower sIgA levels in the mouth make tooth tissue more susceptible to caries-causing microbe adherence than in healthy people.

1. Introduction

The mucosal immune system is permeable to external stimuli and is constantly bathed in fluid (saliva). Although antigenic material that enters the oral cavity is largely degraded by the masticatory process and salivary enzymes, it has the potential to elicit immunological responses. And early research into the development of vaccines against tooth cavities demonstrated that Strep. mutans induced IgA antibodies not only in saliva, but also in tears. This established the notion of a single mucosal immune system, in which the stimulation of immune responses on one mucosal surface resulted in a widespread immunological response in other mucosal tissues [1, 2]. Inflammation is a protective response that aims to clear the body of invading germs that cause tissue harm, as well as to deal with the resulting necrosis. Cytokines such as interleukin-1 (IL-1), interleukin-6 (IL-6), and tumor necrosis

factor (TNF) drive and regulate the inflammatory process. Inflamed tissues draw phagocytic cells such as neutrophils and macrophages (as well as mast cells and eosinophils) to eliminate invading pathogens. Leucocytes can migrate quickly to infection or tissue injury locations, whereas plasma proteins can diffuse into tissues [3, 4].

Numerous soluble factors are released by epithelial cells or incorporated into the fluids that surround the oral cavity. These factors perform a number of roles, including antibacterial activity for defensins, histatins, lysozyme, and lactoferrin. Certain of these compounds have been shown to interact synergistically with secretory IgA [5, 6].

Symbiosis between the human body and its microbial ecological system is the norm and form of life. It is generated during the processes of evolutionary (phylogenesis) and individual (ontogenesis) development. Microorganisms inhabit the human body in numbers tens to hundreds of times greater than the host's own cells [7 -9]. In essence, man (along with higher animals) has evolved into a superorganizational symbiotic system. Along with the macroorganism, the latter consists of a collection of numerous microbiocenoses with a specific composition that inhabit a particular biotope (niche) within the host body. The microbiome is a collection of human microorganisms that cohabit normally and pathologically with it, taking part in physiological and pathophysiological processes, as well as drug and hormone metabolism [10, 11].

It may be concluded that one of the most promising fields of medical research is the investigation of a group of genes involved in the creation of microbiota in diverse localizations, including the gastrointestinal tract, skin, and mucous membranes of the sexual organs. Thus, this study aims to determine immunological parameters (total IgA and secretory IgA concentrations) in the oral fluid of examined individuals under normal and pathological conditions. to determine the sensitivity/resistance of microorganisms—the primary representatives of the oral microflora—to antimicrobial drugs commonly used in modern therapeutic practice (antibiotics) in vitro.

2. Methodology

To carry out the study's objectives, 65 people of various ages (ranging from 18 to 50 years old) were examined, including students, teachers, laboratory assistants, employees of Belarusian State University's International Sakharov Environmental Institute, and patients of the Slutsk district hospital who gave written informed consent to the collection of biological material. A questionnaire survey was undertaken among those polled in order to identify people who had a susceptibility to colds or chronic diseases, poor habits (smoking), and whether or not they practiced regular dental hygiene. Group 1 consisted of 37 persons between the ages of 18 and 25, whereas group 2 consisted of 28 people between the ages of 43 and 50. The existence of various oral disorders was discovered in 15 participants, according to the results of the survey. The remaining respondents did not have any oral illnesses (Table 1).

Table 1. *Group of people who took part in the study*

Group number	Group 1	Group 2
Age	18 - 25 years (n=37)	43 – 50 years (n=28)
Diseases of the oral cavity	Present (n=15)	Absent (n=50)

The oral cavity (inside surface of the cheeks) was swabbed and inoculated onto agar media (MPA, Endo medium) using sterile cotton swabs. The quantitative count of microorganisms was accomplished by counting colonies (CFU) on the agar medium's surface and then converting to a specific unit of the oral cavity's area (4 cm^2).

We employed a solid-phase immunoassay and a sIgA ELISA BEST strip acquired from ZAO Vector Best to quantify secretory IgA in oral fluid. Photometric measurements at a wavelength of 450 nm were used to obtain the analysis results. Blood serum is used as the test material. 100L of material is required for analysis.

The "secretory IgA-ELISA" collection of reagents is intended for the quantitative determination of secretory IgA in bodily fluids using the enzyme-linked immunosorbent assay method. Secretory IgA is quantified using a "sandwich" form of the enzyme-linked immunosorbent test. On the inner surface of the plate wells, mouse monoclonal antibodies specific for secretory human IgA are immobilized. When the test sample is introduced to the wells of the plate, the secretory IgA in the test sample binds to antibodies on the solid phase. The resultant complex is identified using a horseradish peroxidase-conjugated mouse monoclonal antibody to the alpha chain of IgA. As a result, a plastic-encased "sandwich" containing peroxidase is formed. The fluids in the wells are stained following incubation with a tetramethylbenzidine (TMB) substrate solution. The color intensity is related to the secretory IgA concentration in the test sample. The calibration graph was used to determine the sIgA concentration in the samples.

To begin, a single colony was extracted from a Petri plate using a toothpick or a bacteriological loop and

transferred to a test tube (eppendorf). The test tubes were then filled halfway with acetonitrile and 70% formic acid solution, mixed, and the substance was applied in a volume of 1L to the wells of a metal target (chip). Each sample was loaded with 1 l of a MALDI-ToF matrix (-cyano-hydroxycinnamic acid in a 50/25 acetonitrile/ trichloroacetic acid, TPA) solution. After crystallization of the samples, the target was placed in the mass analyzer's chamber with the samples. To calibrate the instrument, E. coli strain CCUG 10797 cells were employed. To obtain a single mass spectrum, 100 laser pulses with a frequency of 60 Hz were employed; the registration range was 1000-20000 m / z; only positive ions were recorded; and the whole spectrum of each sample was assembled using 100 single shots. Each well of the chip was sampled for a spectrum, which was the sum of six individual spectra (600 laser pulses). The following properties of the mass spectrum were considered while examining the results: the number of peaks, their strength, and the total value of the noise component. For further examination, the resulting spectrums of each strain were exported to the S.A.R.A.M.I.S. TM database. Individual mass spectra in the "Identification" mode were compared to the S.A.R.A.M.I.S. TM database, supplemented by the obtained reference spectra, to determine the species or genus of the examined culture. Correct species identification was achieved with a score of 75%. Positive identification at the genus level is defined as a score of 1.7, while positive identification at the species level is defined as a score of 2.0 or higher.

Statistical methods were used to determine the mean, standard deviation (M + SE), median, and spread of values, as well as correlation analysis, during data processing. The significance of differences between indicator groups was determined using the Student's t-test. We classified significant differences as those with a p 0.05 value. When performing statistical analysis on the data, a software application was employed by STATISTICA 10.0.

3. Results and Discussions

The values of immunity indicators (IgA, lysozyme, and SIgA) in the oral cavity of participants are shown in Table 2 where * indicates a $p < 0,05$ statistical significance of differences. Individuals with oral illnesses demonstrated a statistically significant decrease in secretory IgA levels when compared to healthy and normal individuals (Figure 1). In dental caries, secretory immunoglobulin A (sIgA) in mixed saliva is a critical indication of local oral immunity. A critical aspect of the role of secretory IgA in the oral cavity's microbial ecology, and particularly in the pathology of the oral cavity, is the effect of these immunoglobulins on the local microflora. The decreased sIgA content in saliva of patients with caries and periodontal illnesses indicates a weakening of the mucous membranes' local defenses, increasing the chance of a carious process and deterioration of periodontal health.

Table 2. *The immunity indicators (IgA, lysozyme, and SIgA) in the oral cavity of participants.*

Indicator	Group of relatively healthy people (n= 50)	Group of people with caries and periodontal diseases (n=15)	Normal values
of IgA indicators, g/L	1,053 ± 0,002*	0,741 ±0,002*	1,20 ± 0,65
Lysozyme, µg/ml	44,0 ±1,3*	30,0 ±1,12*	40,0 – 50,0
SIgA, g/L	1.80 ± 0.33*	0.28 ± 0.05*	0.7 to 4

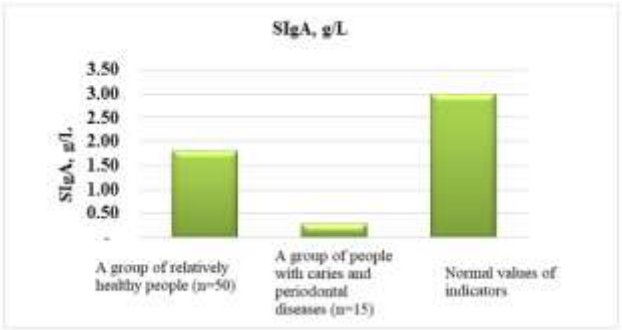

Figure 1*: secretory SIgA, g/L content in the examined individuals*

According to the findings obtained, the amount of total IgA in oral fluid is much lower in patients with dental and periodontal problems than in healthy individuals (figure 2). This reflects a decrease in the mouth cavity's specific resistance and the activation of carious/periodontal processes.

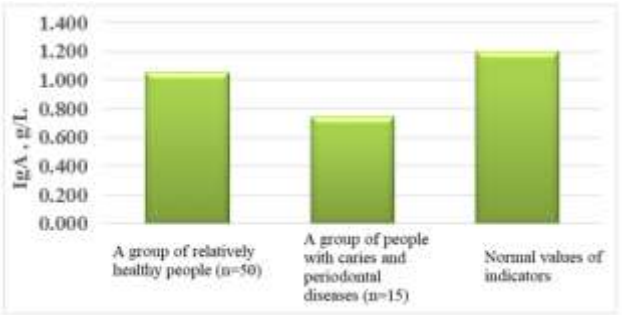

Figure 2: *total IgA, g/L Level in the surveyed individuals*

Individuals with lgA deficiency have been observed to be more prone to tooth decay and/or periodontal disease. Bacteria deglycosylate IgA, which regulates bacteria's adherence to dentin and mucosa, resulting in immunoglobulin proteolysis and a loss in antibacterial defense.

Despite large growth inhibition zones surrounding the anti-biotic disks, all bacteria shown resistance to amoxicillin. Carbenicillin resistance was observed in bacteria belonging to the genera Lactobacillus, Staphylococcus, Bifidobacterium, Escherichia, and Sarcina.

Streptomycin, Doxycycline, and Tetracycline were all susceptible to all microorganisms (Figure 2). According to the boundary data table for the diameter of growth retardation zones (Table 2), all of the bacteria examined are amoxicillin resistant. Lactobacillus, Staphylococcus, Bifidobacterium, Escherichia, and Sarcina are carbenicillin resistant. That is, these microbes have developed resistance mechanisms to these antibiotics.

Table 2. *Diameter of the zones of growth retardation of microorganisms under the influence of various antibiotics (mm)*

Microorganism	micrograms				
	Streptomycin, 30	Carbenicillin, 100	Doxycycline, 30	Amoxicillin20	Tetracycline, 30
Lactic acid bacteria (mixture 1)	30,0±0,40	23,0±0,10	26,0±0,62	8,0±0,20	28,0±0,20
Lactic acid bacteria (mixture 2)	35,0±0,21	14,0±0,09	20,0±0,41	10,0±0,40	17,0±0,50
Genus Bifidobacterium	35,0±0,30	10,0±0,20	24,0±0,32	12,0±0,50	29,0±0,30
Genus Lactobacillus	30,0±0,12	5,0±0,08	28,0±0,40	7,0±0,10	30,0±0,20
Genus Staphylococcus	40,0±0,51	5,0±0,20	37,0±0,07	4,0±0,07	30,0±0,41
Genus Streptococcus	30,0±0,22	15,0±0,08	35,0±0,43	5,0±0,09	35,0±0,40
Genus Escherichia	40,0±0,42	6,0±0,40	32,0 ±0,32	5,0±0,08	28,0±0,24
Genus Sarcina	30,0±0,23	6,0±0,20	26,0±0,52	5,0±0,20	30,0±0,40
Genus Bacillus	40,0±0,31	28,0±0,50	30,0±0,41	13,0±0,3	35,0±0,51
Genus Proteus	38,0±0,20	36,0±0,50	28,0±0,81	14,0±0,40	27,0±0,45
Genus Bacteroides	39,0±0,19	34,0±0,42	25,0±0,10	10,0±0,12	26,0±0,30

Amoxicillin is a semi-synthetic broad-spectrum penicillin antibiotic. Carbenicillin is a semisynthetic penicillin antibiotic with a broad spectrum of activity. It acts as a bactericide by inhibiting the bacterial cell wall production.

Beta-lactam antibiotics (also known as beta-lactams) are a class of antibiotics that share a beta-lactam ring in their structure. Penicillins, cephalosporins, carbapenems, and monobactams are all beta-lactam antibiotics. The identical chemical structure of all beta-lactams results in the same mechanism of action (inhibition of bacterial cell wall formation), as well as cross-allergy in some patients.

Penicillins, cephalosporins, and monobactams are all susceptible to hydrolysis by special enzymes called beta-lactamases, which are produced by a variety of bacteria. Carbapenems exhibit much greater resistance to beta-lactamases than other antibiotics.

Given their excellent clinical performance and minimal toxicity, beta-lactam antibiotics are the cornerstone of antimicrobial chemotherapy at the moment, occupying a prominent position in the treatment of the majority of illnesses.

Beta-lactamases are found in a wide variety of Gram-negative bacteria and are also produced by a number of Gram-positive bacteria (staphylococci). There are around 200 different types of enzymes recognized to date. Recently, it was discovered that up to 90% of resistant bacterial strains obtained in clinical settings are capable of generating beta-lactamases, which confers resistance.

Beta-lactam antibiotics' efficiency may be reduced as a result of the evolution of resistance, the most common mechanism of which is the creation of beta-lactamases by bacteria.

The development of new beta-lactam antibiotics and their implementation into practice for the treatment of infectious diseases caused by strains resistant to known antibiotics has resulted in an increasingly small time interval between the use of a new medicine and the emergence of resistance to it. Figure 3. Illustrates the sensitivity/resistance of the major representatives of the oral microbiota to antibiotics administered at various concentrations to the discs.

Figure 3*: Examples of the sensitivity/resistance of the main representatives of the oral microflora to antibiotic preparations applied to the discs in a certain concentration*

Antibiotic resistance prevention methods that are most successful should be directed at microbial populations in general. Antibiotic resistance has spread globally in recent years as a result of the selection pressure exerted by antibiotics used in medical treatment.

4. Conclusions

The objectives of this study were to examine the immunological parameters (total IgA and secretory IgA concentrations) in the oral fluid of examined

individuals under normal and pathological conditions; and to determine the sensitivity/resistance of microorganisms—the primary representatives of the oral microflora—to antimicrobial drugs widely used in modern therapeutic practice (antibiotics) in vitro. To accomplish the study's aims, 65 individuals ranging in age from 18 to 50 years were evaluated. Microorganisms were quantified quantitatively by counting colonies (CFU) on the agar medium's surface and then translating to a particular unit of the oral cavity's area (4 cm2). The analytical findings were obtained using photometric measurements at a wavelength of 450 nm. The test material is blood serum. For analysis, 100L of material is required.

The results of this study revealed that the amount of total IgA in oral fluid is considerably lower in persons with dental and periodontal disorders than in healthy individuals. This reflects a reduction in the oral cavity's particular resistance and the activation of carious / periodontal processes. Individuals with lgA deficiency have been reported to have an increased risk of developing caries and/or periodontal disease.

However, the results indicated that the oral cavity microbiota in the comparative groups was dominated by staphylococci and streptococci. There were discovered Enterobacteria, Veillonella, bacteroides, actinomycetes, and Neisseria. Streptococci representatives were the most often seeded – accounting for 57% of all microorganisms sown in this biotope. Staphylococcus representatives accounted for 22%, enterobacteria accounted for up to 15%, and Neisseria accounted for around 4% and 2%, respectively. There was a decrease in the colonization of the cavity by members of the normal microflora Neisseria lactamica, Clostridium sphenoides, and Clostridium ramosum, as well as an increase in the frequency of opportunistic microorganisms Enterococcus faecium and Streptococcus parvulus in the representatives of the older group 2.

Finally, the results indicated that a drop in sIgA levels in periodontal disease patients' saliva suggests a loss of local mucous membrane protection, therefore increasing the risk of caries and periodontal disease development. The decreased sIgA level in the oral cavity generates circumstances in which tooth tissue is more vulnerable to caries-causing microbe adhesion than in healthy individuals.

Author Statements:

- The authors declare that they have equal right on this paper.
- The authors declare that they have no known competing financial interests or personal relationships that could have appeared to influence the work reported in this paper
- The authors declare that they have nobody or no-company to acknowledge.

References

[1] Mestecky, J., McGhee, J. R., Michalek, S. M., Arnold, R. R., Crago, S. S., & Babb, J. L. (1978). Concept of the local and common mucosal immune response. In Secretory immunity and infection (pp. 185-192). Springer, Boston, MA.

[2] Mestecky, J. I. R. I., McGhee, J. R., Arnold, R. R., Michalek, S. M., Prince, S. J., & Babb, J. L. (1978). Selective induction of an immune response in human external secretions by ingestion of bacterial antigen. The Journal of clinical investigation, 61(3), 731-737.

[3] Aps, J. K., & Martens, L. C. (2005). The physiology of saliva and transfer of drugs into saliva. Forensic science international, 150(2-3), 119-131.

[4] Chiappin, S., Antonelli, G., Gatti, R., & Elio, F. (2007). Saliva specimen: a new laboratory tool for diagnostic and basic investigation. Clinica chimica acta, 383(1-2), 30-40.

[5] Wu, Z., Lee, S., Abrams, W., Weissman, D., & Malamud, D. (2006). The N-terminal SRCR-SID domain of gp-340 interacts with HIV type 1 gp120 sequences and inhibits viral infection. AIDS Research & Human Retroviruses, 22(6), 508-515.

[6] Stoddard, E., Cannon, G., Ni, H., Karikó, K., Capodici, J., Malamud, D., & Weissman, D. (2007). gp340 expressed on human genital epithelia binds HIV-1 envelope protein and facilitates viral transmission. The Journal of Immunology, 179(5), 3126-3132.

[7] Mandel, I. D. (1990). The diagnostic uses of saliva. Journal of Oral Pathology & Medicine, 19(3), 119-125.

[8] Streckfus, C. F., & Bigler, L. R. (2002). Saliva as a diagnostic fluid. Oral diseases, 8(2), 69-76.

[9] Nagler, R. M., Salameh, F., Reznick, A. Z., Livshits, V., & Nahir, A. M. (2003). Salivary gland involvement in rheumatoid arthritis and its relationship to induced oxidative stress. Rheumatology, 42(10), 1234-1241.

[10] Humphrey, S. P., & Williamson, R. T. (2001). A review of saliva: normal composition, flow, and function. The Journal of prosthetic dentistry, 85(2), 162-169.

[11] Saloom, H. F., & Carpenter, G. H. (2018). Saliva and Gingival Crevicular Fluid: Contributions to Mucosal Defense. In Oral Mucosa in Health and Disease (pp. 91-103). Springer, Cham.

International Journal of Computational and Experimental Science and ENgineering (IJCESEN)

Vol. 7-No.3 (2021) pp. 128-132
http://dergipark.org.tr/en/pub/ijcesen

ISSN: 2149-9144

Research Article

Estimating the Concentrations of Natural Isotopes of ^{238}U, ^{232}Th, ^{40}K & Radiation Dose Rates for Wasit Province-Iraq by Gr-460 system

Ahmed Abdulhasan ZARKOOSHI[1,2*], Kamal Hussein LATIF[2], Fadhil HAWI[3]

[1]Süleyman Demirel University, Science and Arts Faculty, Physics Department, 32200, Isparta-Turkey
* **Corresponding Author** : **Email:** ahmedeliraqi77@yahoo.com - **ORCID:** 0000-0001-6715-1709

[2]Iraqi Radioactive Sources Regulatory Authority- Baghdad – Iraq
Email: kamalhlatif@yahoo.com - **ORCID:** 0000-0001-6715-1709

[3]Iraqi Radioactive Sources Regulatory Authority- Baghdad – Iraq
Email: fadhil_mizban@yahoo.com - **ORCID:** 0000-0001-6715-1709

Article Info:

DOI: 10.22399/ijcesen.891935
Received : 06 March 2021
Accepted : 24 November 2021

Keywords

GR-460 system
Radiation doses rates
Concentration of natural isotopes
Wasit Province

Abstract:

This paper includes the measurement of the concentrations of natural radioactive isotopes of ^{238}U, ^{232}Th, ^{40}K, and radiation dose rates for selected areas of Wasit province .GR-460 system has been used for the radiological survey operations, it is a portable system, installed inside a minibus and inside the system there is a Sodium Iodide Detector (NaI), that has the ability to measure the concentrations of natural radioactive isotopes in (ppm) unit and measure the radiation dose rates in µR/h unit. The measurement results showed the absence of any significant increase in the ^{238}U ^{232}Th and ^{40}K concentrations where the average concentration of isotopes ^{238}U, ^{232}Th and ^{40}K were (3.22, 7.93 and 1.18) ppm respectively, it is authorized and acceptable. The values of radiation dose rates ranged between 5- 7.08 µR/h , and all these values are within the natural radiation background. Eleven radioactive sources type ^{226}Ra have been detected beside destroyed industrial facility because of the war 2003 they had been used in the lightning arresters technology in the last regime. These sources treated and placed in armored containers and taken to the Iraqi main store (Iraqi Organization of Atomic Energy Site), the radiation dose measurements ranged between 72- 48 µR/h, which is higher than the natural radiation background.

1. Introduction

Natural radioactivity is referred to that any source of radiation which non- made by a human, the main source of this type of radiation is cosmic rays and sources generated from the ground origin of radionuclides such as a uranium series ^{238}U and thorium series ^{232}Th and potassium ^{40}K that are found in the crust of the earth since the creation. But when the level of radiation exposure exceeds its natural limit that will be killing of human cells and possibly cause cancer diseases, especially the sources which have been produced by human [1][2]

There are many artificial radioactive sources were been made by a human, and can be used in different fields and application, such as medical section to diagnose and treat cancer disease, industrial applications, for example, Europium ^{152}Eu and Radium ^{226}Ra that used in lightning arresters technology, source of Cesium ^{137}Cs used in moisture and density measurements, and iridium source 192Ir used in industrial radiography and etc. [3][4].

There are many studies that have been done to determine the natural concentrations of radioisotope, whether by using high purity germanium detector (HPGe) or-Gamma-ray spectroscopy system NaI(Tl)[5],[6],[7], all of them, are installed inside a specific laboratory. GR-460 is a portable, modern and unique system, it is a

sodium iodide detector (NaI) with two crystal each one 256 Lang size becomes a total volume of 512 Lang cube, instilled inside the minibus, it has the ability to measure the radiation dose rate in units μR/h and the possibility to identify the type of radioactive source through displaying its spectrum. Also, it has the ability to determine the ratio of the concentrations of natural radioactive materials uranium ^{238}U, thorium ^{232}Th and potassium ^{40}K in the soil in ppm unite. The system produced by Exploranum Company (USA) as shown in Figures.1. During the war of 2003 and what resulted after this war, looting and destruction of many military and industrial facilities, especially those that used radioactive sources for a specific technique, and subsequently loss of these sources, which resulted in the negative impact on people's lives because of the long term of radiation exposure and generates cancer disease that increased in Iraq more than before 2003 according to the recent studies [8],[9],[10].

In this study, the GR-460 system and portable devices have been used to conduct the operation of the radiological survey for the Wasit province to search for missing radioactive sources and estimate the natural concentration of ^{238}U , ^{232}Th and ^{40}K.

2. Materials and Methods

Six sites have been selected for radiological surveys and these sites are the districts which affiliated to the province of Wasit (Center of Kut, AL-Hai, Al-Numania, Alazizia, Sowira and Badrah). The priorities of radiological survey it was for the areas which exposed of rocket fire by USA army during 2003 war, and scrap materials sites which possibly contain of radioactive sources. This information has been obtained from the directorate of environment and Wasit governorate council.
The areas have been divided into squares depending on the nature and size of the area based on the international atomic energy agency (IAEA) instructions[11][12]. The vehicle of the system were walked in slow speed proximately ranged between 50-40 km / h in order to analyze the measurements precisely, when observing any high level of radiation exposure, the vehicle will be stopped and then used portable devices to determine the place where the system observed high radiation activity. The background radiation of the province was estimated to be 5.7 μR/h.

3. Results and Discussions

Radiological survey has been done to the elected sties in Wasit province by GR460 system and by

Figure 1. *Two different images of GR-460 system.*

portable devices to measure the concentrations of natural radioactive isotopes ^{238}U, ^{232}Th, ^{40}K respectively in unit ppm, and the radiation dose rates in unit μR/h the results of the measurements are shown in the Figures2. Figure 3. Figure 4. and figure 5. Respectively.

The results of radiation measurements were conducted of the elected sites, showed absence of any significant increase in the concentrations of radioactive isotopes from natural limits, where the concentration values in (ppm) unit of the isotope ^{238}U ranged from (2.87-4.1), the values of isotope ^{232}Th ranged from (5.77-7.93) and the values of isotope ^{40}K ranged from (0.37-1.18) respectively and table1. Shown the maximum value for each isotope and its equivalent values to the specific radioactivity in Bq/kg unit as shown in the following equations [13],[14].

$$U\ ppm = 12.45\ U\ Bq/kg \quad (1)$$

$$Th\ ppm = 4.6\ Th\ Bq/kg \quad (2)$$

$$K\ ppm = 313\ K\ Bq/kg \quad (3)$$

All these values are acceptable and agreement with the global values of the average

Table1. *The maximum values of concentration of the radioisotopes in ppm unit and Bg/kg unit*

Isotopes	Concentration in (ppm) unit	Concentration in (Bq/Kg) unit
^{238}U	3.22	40.08
^{232}Th	7.93	36.47
^{40}K	1.18	369.34

radioactivity concentration of ^{238}U, ^{232}Th, and ^{40}K, are (40, 40 and 580) Bq/kg respectively, it is also agreement with the previous studies [15],[16],[17].

The average of radiation dose rates for all the areas ranged between 5- 7.08 µR/h where it is in the normal limits, as shown in Fig 5. it is in agreement with globally limits [18], [19].

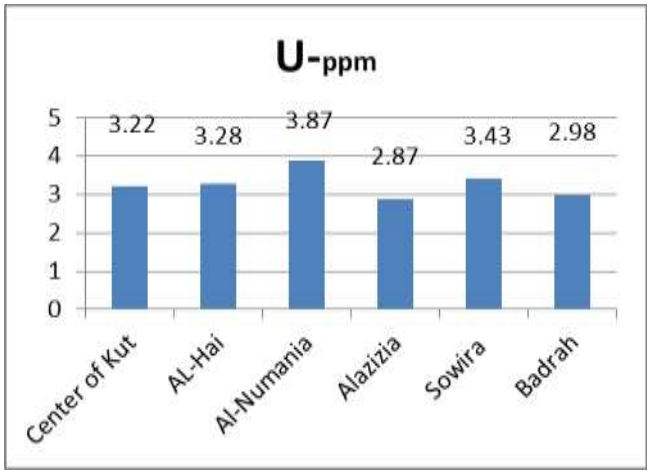

Figure 2. *The rates of concentrations of Uranium isotope ^{238}U in ppm unit.*

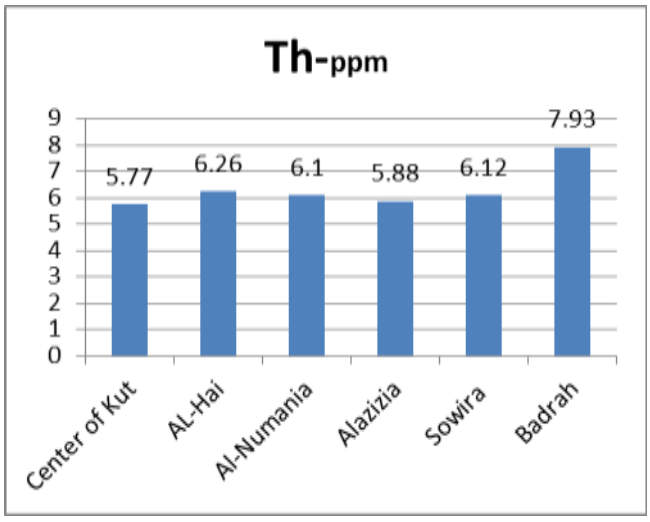

Figure 3.*The rates of concentrations of Thorium isotope ^{232}Th in ppm unit.*

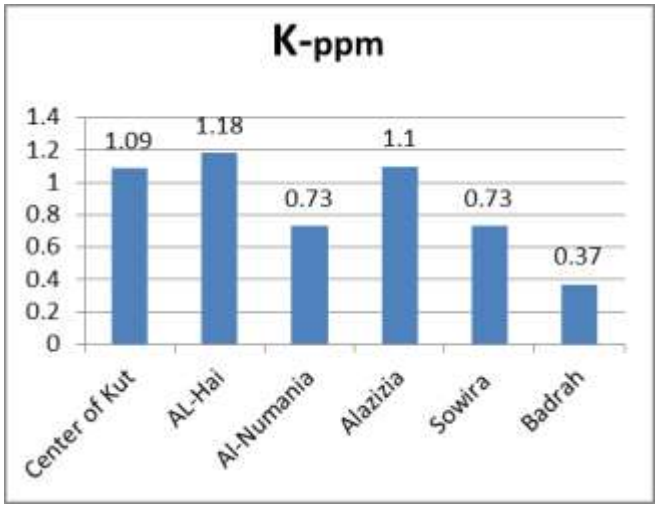

Figure 4. *The rates of concentrations of potassium isotope ^{40}K in ppm unit*

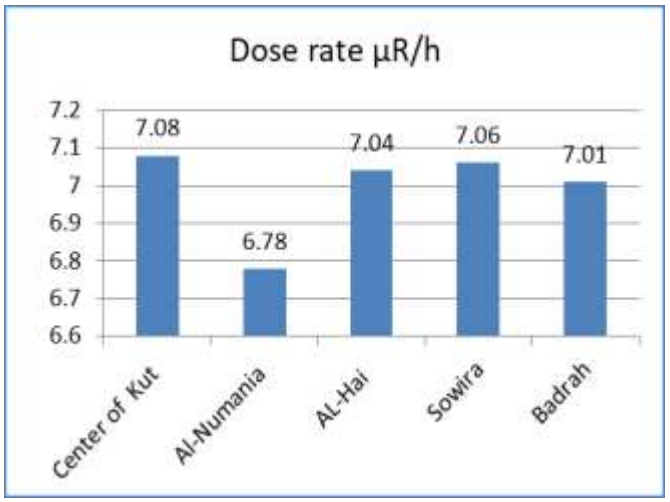

Figure 5*.Radiation dose rates for the elected areas in µR/h unit*

Abnormal radioactivity has been observed beside old destroyed industrial facilities near of Kut city, eleven radioactive sources type Radium ^{226}Ra have been detected, that separated at three locations because of the war 2003 and they were been used in the lightning arresters technology in the last regime[20]. These sources treated and placed in armored containers and have been transported to the national store in the (Iraqi Atomic Energy Organization site) according to the IAEA standards [21]. The radiation dose rate ranged between 48- 76.52µR/h, which is higher than the natural background radiation as shown in Figures 6.

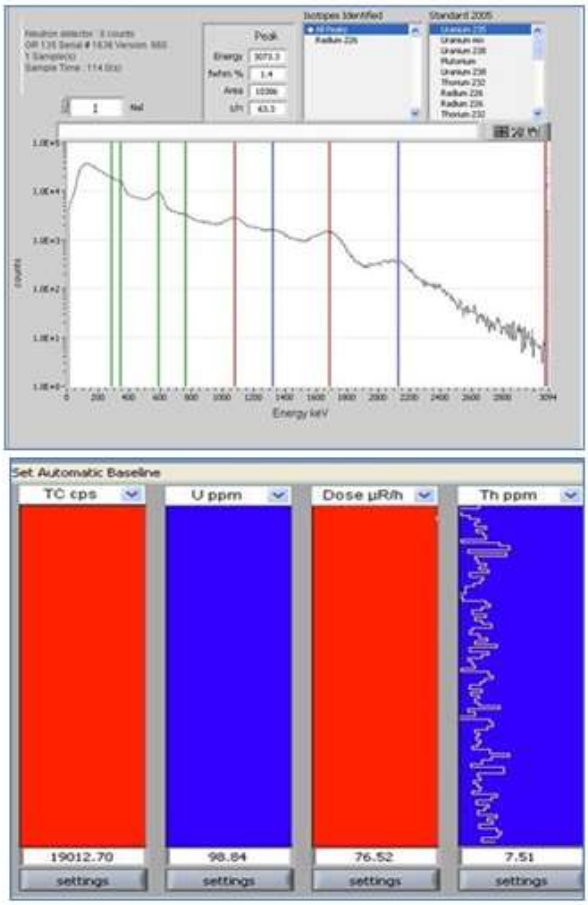

Figure 6.*Spectrum of radioactive source ^{226}Ra (in upper). Radiation dose rate of GR-460 system when observed high radiation exposure (in lower)*

4. Conclusions

According to the results of radiological survey measurements of Wasit province by GR-460 system, the concentration of thorium and uranium isotopes are within natural concentration and globally accepted, and agreement with previous studies. The average of radiation doses for all the regions were been selected, is not exceeded from the natural background, except eleven radioactive sources type ^{226}Ra have been found during radiological survey operation, they were used in the lightning arrester application before 2003 ware, and treated carefully according to IAEA standards, and transformed to the national store of Iraq.
These results have been sent to the Iraqi Ministry of Health and Environment to take place its procedures through estimating the number of individuals infected by cancer disease whether by the high level of radiation exposure or because of biological problems.

Author Statements:

- The authors declare that they have equal right on this paper.
- The authors declare that they have no known competing financial interests or personal relationships that could have appeared to influence the work reported in this paper
- The authors declare that they have nobody or no-company to acknowledge.
- The authors certified that they have participated sufficiently in this work to take public responsibility for the content, including participation in the concept, design, analysis, writing and revision of the manuscript. Furthermore this article has not been published in other publication before

References

[1] International Agency Energy Atomic (IAEA), Natural occurring radioactive material (NORMV), proceeding of the fifth international symposium on naturally occurring radioactive material, Spain, 1-549, (2007).
[2] O. Brıgido Flores, A. Montalvan Estrada, R. Rosa Suarez, J. Tomas Zerquera, A. Hernandez Perez, Natural radionuclide content in building materials and gamma dose rate in dwellings in Cuba, Journal of Environmental Radioactivity, 99(1), 1834–1837, (2008).
[3] International Agency Energy Atomic (IAEA), Sealed radioactive sources, Information, resources, and advice for key groups about preventing the loss of control over sealed radioactive sources, Vienna, Austria, 1- 40, (2013).
[4] International Agency Energy Atomic (IAEA), Nuclear Security Seies No.11-Security of Radioactive Sources Implementation Guide , Veina, Austria, 1-77, (2009).
[5] Ali A. Ridha , Mahdi M. Mutter and Manar D. Salim, Natural radioactivity of U-238, Th-232 and K-40 in surface soil of Baghdad, Nahrain and AL-Mustansiritah University in IRAQ, Jurnal Sains Nuclear Malaysia, 27(2), 7-15, (2015).
[6] El seed Hashim Gad and AL-Bashir Mohammed Hashim, Assessment of Natural Radioactivity Concentration and Dose in Surface Soil Samples from Atbara, European Academic Research, 2(7), 1-8, (2016).
[7] Termizi Ramli A., Wahab M.A., Hussein A., Khalik, Environmental 238U and 232Th concentration measurements in an area of high level natural background radiation at Palong,

Journal of Environmental Radioactivity, Johor, Malaysia, 287–304, (2005).

[8]AL-Janabi Ali Abdul Hussein, Zhoor H Naseer and Thuha A. Hamody, Epidemiological Study of Cancers inIraq-Karbala from 2008 to 2015, International Journal of Medical Research & Health Sciences, 79-86, (2017).

[9] Al yaseri Isam, Performance of Wastewater Treatment Plants in Iraq: Life Cycle Assessment Approach, Journal of Environmental Science Toxicology and Food Technology, 29-36, (2016).

[10] Ramy A. Ibrahim, The Environmental Crisis of the 2003 Iraq War: A Moral Obligation or a Mandatory Measure Under International Treaties, City University of New York Law Review, 1-12, (2015).

[11] International Agency Energy Atomic (IAEA), Generic procedures for assessment and response during a radiological emergency, Vienna, Austria, 1-193, (2000).

[12] International Agency Energy Atomic (IAEA), Manual for First Responders to a Radiological Emergency, Vienna, Austria, 1-94, (2006).

[13] Alsaif, Abdulkarem Salem, Radioecological Aspect of Hail Region Behavior of Some Radionuclide in Soil , MSc thesis, College of Science , King Saud University,1- 81, (2000).

[14] Environmental Protection Agency, Radiological Laboratory Sample Analysis Guide for Incident Response – Radionuclides in Soil, National Air and Radiation Environmental Laboratory, USA, 1-141, (2012).

[15] International Agency Energy Atomic (IAEA), Radiation Protection and Safety of Radiation Sources International Basic Safety Standards part 3, Vienna, Austria, 1-303, (2011).

[16] UNSCEAR. (Exposure from natural sources of radiation: Report to the general assembly/United Nations scientific committee on the effects of atomic radiation, 48- the Session (New York: United Nations), (1993).

[17] S. Fares, Measurements of natural radioactivity level in black sand and Sediment samples of the Temsah Lake beach in Suez Canal region in Egypt, Journal of Radiation Research and Applied Sciences, 194-203,(2017).

[18] United nations, Sources and effects of ionizing radiation, New York, vol (1), 1- 659, (2000).

[19] International Agency Energy Atomic (IAEA), Radiation Biology a Handbook for Teachers and Students, Vienna, Austria, 1-166, (2010).

[20] International Agency Energy Atomic (IAEA), Identification of Radioactive Sources and Devices, nuclear security series, Vienna, Austria, 1-154, (2007).

[21] International Agency Energy Atomic (IAEA), Regulations for the Safe Transport of Radioactive Material, Specific Safety Requirements, Vienna, Austria, 1- 190, (2018).

International Journal of Computational and Experimental Science and ENgineering (IJCESEN)

Vol. 7-No.3 (2021) pp. 133-136
http://dergipark.org.tr/en/pub/ijcesen

ISSN: 2149-9144

Research Article

Design and Manufacture of a Centrifugal Water Pump with a Circular Casing

Francis INEGBEDION[1]*, Chidiebele Nnadike OKONKWO[2], Joseph Okechukwu NDIFE[3]

[1]Department of Production Engineering, University of Benin, Benin City, Nigeria.
* **Corresponding Author** : **Email:** francis.inegbedion@uniben.edu - **ORCID:** 0000-0002-2142-8079

[2]Department of Production Engineering, University of Benin, Benin City, Nigeria.
Email: ogenessmayoro@gmail.com - **ORCID:** 0000-0002-9543-04542

[3]Department of Production Engineering, University of Benin, Benin City, Nigeria.
Email: ndifendife2@gmail.com - **ORCID:** 0000-0001-9222-99693

Article Info:

DOI: 10.22399/ijcesen.907292
Received : 31 March 2021
Accepted : 24 November 2021
Keywords

Circular casing
Local content
Pump

Abstract:

A Centrifugal water pump is a machine that imparts mechanical energy to a fluid flowing through it, this allows the fluid to move from one point to another. This paper reports the design, manufacture and testing of a centrifugal water pump having a circular casing. A single stage, end suction centrifugal pump designed and manufactured, using locally sourced materials. This pump finds application in homes, agriculture and industries. It consists of an impeller, shaft, suction, delivery pipes and an electric motor. Experiments performed with this pump shows that it can deliver 0.0045m3 of water per second with a pressure head of 34.7m. A 2.5kW electric motor running at a speed of 2900rpm was used to drive the pump.

1. Introduction

Pumping is the addition of energy to a fluid to move it from one point to another [1]. A pump is a machine that imparts mechanical energy from some external source to a fluid flowing through it, to move it from one point to another [2]. The development of pumps has enabled man to transport and move liquids from one point to another. The centrifugal pump is the type widely used for general services (home, agriculture, industries etc.) because of its simplicity, low cost, high volumetric discharge, uniform flow, quiet operation, adaptability of use with electric motor, turbine or internal combustion engines and low maintenance expense [3].

A centrifugal pump is a machine consisting of a set of rotating vanes enclosed within a housing or casing. The vanes impart energy to a fluid through centrifugal force, which causes the fluid to move. A centrifugal pomp has two main parts: a rotating element, including an impeller and a shaft, and a stationary element, made up of a casing, stuffing box and bearings. Centrifugal pump usage finds application in machine tools, automobile and aeronautic industries [2]. Most of the centrifugal pumps in Nigeria today are of the volute type casing. It is the aim of this paper to design and manufacture a centrifugal pump having a circular casing using locally available materials. A simple design with a circular casing enclosing an impeller was designed. The impeller and casing material were made from cast iron. The entire unit is a mono block pump i.e. it is a direct coupling of the motor to the impeller.

The development of the centrifugal pump dates back to about 3,000 B.C., where the Mesopotamians used buckets alone to water their crops in the Nile River valley. This later gave way to the waterwheel around 500 B.C. French inventor Dewis Papin invented the centrifugal pump in the late 1600s. His impeller had straight vanes, whereas that developed by the British inventor John G. Appold, in 1851 had the curved vanes still preferred today.

Pumps finds application in automobiles and in the refinery, loading and unloading of tankers, direct handling of boiler feed water, water treatment chemicals, condensate, cooling water etc. The development of pumps has enhanced the level of man civilization, economic, conducive environment and has led to the technological development of modern industries. There is the need to develop,

design and construct pumps using locally available materials [4].

The significant considerations in the selection of materials for construction of the centrifugal pump included, local availability, low cost, easy handling during fabrication, lightness of weight for easy handling during use, weather ability and long service life (ability to withstand environmental and operating conditions) and non-toxic effects [5].

2. Methodology

2.1 Nomenclature

Mmm
Q = Capacity (m3/s)
H = Head (m)
N = Rotational Speed (rpm)
Ns = Shape Number (m/s)
Nusf = Useful Power (kW)
ρ = Density (kg/m3)
Nmp = Motor Power (kW)
η = Efficiency
D1 = Impeller eye diameter (mm)
D2 = Impeller outer diameter (mm)
D3 = Casing inside diameter (mm)
D4 = Casing outer diameter (mm)
b1 = Impeller eye width (mm)
b2 = Impeller outer width (mm)
b3 = Casing width (mm)
Tc = Casing thickness (mm)
Ø = Speed Ratio
U2 = Impeller rim velocity (m/s)
U1 = Impeller inner velocity (m/s)
ηh = Hydraulic Efficiency
Vn = True Whirl velocity component (m/s)
Z = Number of blades
V∞ = Ideal whirl velocity component (m/s)
Kn = Factor ranging from 3 – 5
ψ = Flow ratio
Y2 = Velocity of flow (m/s)
Y1 = Inlet flow velocity (m/s)
γ = Outlet blade angle (deg)
β = Inlet blade angle (deg)

2.2 Design of the Centrifugal Pump

The design data required for the design of the centrifugal pump are as follows:

Flow rate, Q 0.0045m^3/s
Head, H =34.7m
Pump Speed, N = 2900rpm
Gravitational acceleration, g = 9.81m/s^2
Density of water, ρ = 1000kg/m^3

K_s = 3.65
$\emptyset$ = 0.97
$\delta = 0.07$
D = 35.5
P = 50m of water
X = 4.5
Y = 1.6
Z = 6
dt = 2.5

$$N_s = K_s N\left(\frac{\sqrt{Q}}{H^{\frac{3}{4}}}\right) = 47.06 m/s \quad (1)$$

$$N_{usf} = \frac{Q\rho gH}{1000} = 1.962 kW \quad (2)$$

$$N_{mp} = 2.5 kW \quad (3)$$

$$\eta = \frac{N_{usf}}{N_{mp}} = 0.7848 \quad (4)$$

2.3 Impeller Design

$$U_2 = \emptyset\sqrt{2gH} = 27.174 \text{m/s} \quad (5)$$

$$D_2 = \frac{60U_2}{\pi N} = 0.178959m = 178.959mm \quad (6)$$

$$D_1 = 0.3D_2 = 53.688mm \quad (7)$$

$$U_1 = \frac{\pi D_1 N}{60} 8.152 m/s \quad (8)$$

$$b_1 = \frac{1.5D_1}{4} = 0.020133m = 20.133mm \quad (9)$$

$$b_2 = \frac{b_1 D_1}{D_2} = 0.006034m = 6.034mm \quad (10)$$

2.4 Impeller Blade Angles

This paragraph deals only with blades suited for two dimensional flows, they are described as cylindrical because they form part of surfaces. The routine calculation proceeds thus:

$$\eta_h = 1 - \{K_h(1-\eta)\} = 0.8924 \quad (11)$$

$$V_n = \frac{gH}{\eta_h U_2} = 0.1681 m/s \quad (12)$$

$$V_\infty = V_n\{1 + (K_n/Z)\} = 0.2522 m/s \quad (13)$$

$$Y_2 = \psi\sqrt{2gH} = 7.844 m/s \quad (14)$$

$$\gamma = \tan^{-1}\left(\frac{Y_2}{U_2 - V_\infty}\right) = 16.244^0 \quad (15)$$

$$Y_1 = Y_2\left(\frac{D_2 b_2}{D_1 b_1}\right) 7.836 m/s \quad (16)$$

$$\beta = \tan^{-1}\frac{Y_1}{U_1} = 43.87^0 \quad (17)$$

Check for exact number of blades, Z

$$Z = 6.5\left(\frac{m+1}{m-1}\right) sin\left(\frac{\beta+\gamma}{2}\right) = 6\ blades \quad (18)$$

$$m = \frac{D_2}{D_1} = 3.3333 \quad (19)$$

2.5 Casing Design

$$D_3 = D_2(\delta + 1) = 191.486 mm \quad (20)$$

$$b_3 = 1.25 b_1 = 25.17 mm \quad (21)$$

$$T_c = \left((XYDP) / 200 dt \right) + 2 = 4.56 mm \quad (22)$$

From tables;
10m of water = 1kg/mm^2 and 50m of water = 50 x 0.1= 5kg/mm^2

$$D_4 = 2T_c + D_3 = 201.486 mm \quad (23)$$

3. Results

3.1 Testing of the Centrifugal Pump

During the testing of the centrifugal pump the Head, Capacity and Efficiency of the pump were measured directly while the pump was in operation. The pump tested in the Department of Production Engineering workshop, University of Benin, Benin City, Nigeria was done by empting water filled in measured containers. The time taken to empty each measured quantity was noted against the Head of water pumped. Water rose to a height of 34.7m and the discharge recorded was 16,200 litres/hour i.e. 4.5 litres/sec.

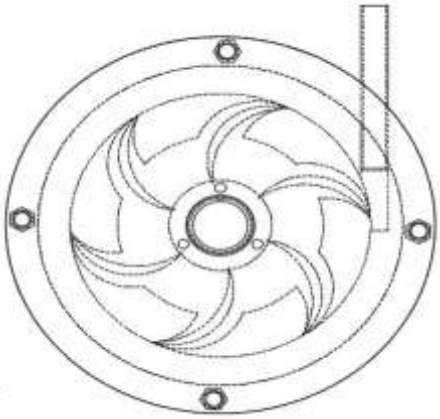

Figure 1: *Drawing of the impeller in the circular casing*

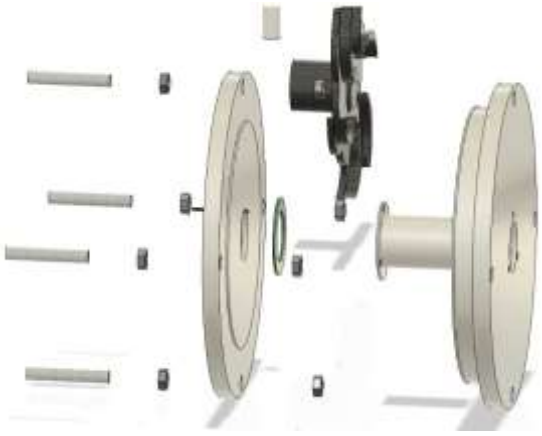

Figure 2: *Assembly drawing of the impeller and the circular casing*

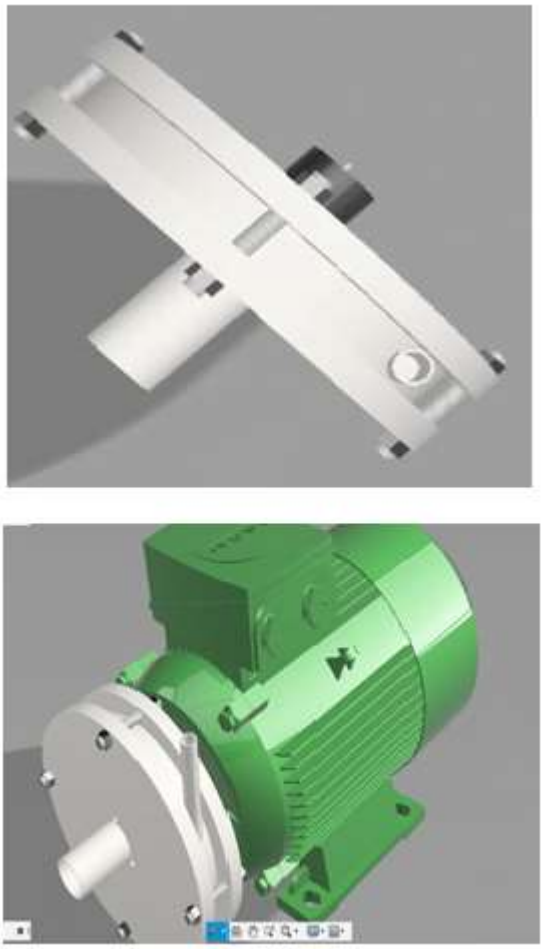

Figure 3. *The assembled centrifugal pump with a circular casing*

4. Discussions

The centrifugal water pump with a circular casing was designed to deliver 5 litres of water per second at a height of 40m. Therefore, the achieved performance of 90% efficiency is satisfactory and acceptable for a centrifugal pump that falls within this category of specific speed.

5. Conclusions

In the work we have shown that from the simple principle of operation of a centrifugal pump – a motor rotating an impeller in a round casing – water can be raised to an appreciable height. This is evident from the test results obtained. A Head of 34.7m and a volume flow rate of 16,200 litres / hour prove very satisfactory. This pump was manufactured using locally sourced materials and fabricated in the Department of Production Engineering workshop. This work will no doubt enhance the technological base of the nation and create jobs if harnessed.

Author Statements:

- The authors declare that they have equal right on this paper.
- The authors declare that they have no known competing financial interests or personal relationships that could have appeared to influence the work reported in this paper
- The authors declare that they have nobody or no-company to acknowledge.

References

[1] Karassik Igor J. and Carter Ray (1960). Centrifugal Pumps Selection, Operation and Maintenance. McGraw – Hill Book Company.

[2] Anderson, H. H. (1957). Centrifugal Pumps. The trade and Technical Press Ltd, England

[3] Okokowa L. E. (2003). A project on the Design and Construction of a 2-Stage Centrifugal Pump, submitted to the Department of Mechanical Engineering, Ambrose Ali University, Ekpoma.

[4]Ozora P.A., Ojoborb S.N., (2012). Design, Construction And Measured Performance Of A Single-Stage Centrifugal Pump Demonstration Unit Nigerian Journal Of Technology Vol. 31, No. 3

[5]Douglas, J.F., Gasiorek, J.M. and Swaffield, J.A. (2001). Fluid Mechanics. 4th edition, Pearson Education.

International Journal of Computational and Experimental Science and ENgineering (IJCESEN)
Vol. 7-No.3(2021) pp. 137-142
http://dergipark.org.tr/en/pub/ijcesen

ISSN: 2149-9144

Research Article

Health Services Vocational School Students' Opinions About Smartphone Usage and The Relationship Between Internet Addiction

Arslan SAY[1*], Demet ÇAKIR[2]

[1]Sabuncuoğlu Şerefeddin Vocational School of Health Services, Amasya University, Amasya, Turkey
* **Corresponding Author** : **Email:** arslan.say@amasya.edu.tr **ORCID:** 0000-0002-1695-5624

[2]Sabuncuoğlu Şerefeddin Vocational School of Health Services, Amasya University, Amasya, Turkey
Email: demet.cakir@amasya.edu.tr **ORCID**: 0000-0003-4794-516X

Article Info:

DOI: 10.22399/ijcesen.987432
Received: 26 August 2021
Accepted: 26 November 2021

Keywords

Smartphone
Internet addiction
Student

Abstract:

In this research, it was aimed to determine the students' smartphone and internet addiction levels and related factors. The universe of the research consists of 825 students studying at the Vocational School of Health Services of a university in the 2015-2016 academic year. Of the 825 students, 668 students who agreed to participate in the research constituted the sample of the study. The data of this research were collected with Internet and Smartphone Usage Information Form, Internet Addiction Scale (IAS), and Smartphone Addiction Scale-Short Form (SASF). The average age of the students is 20.2±1.12, and 44.3% (n=298) of them mostly connect to the internet from home. The mean scores obtained from the scales were 38.41±16.26 in IAS and 28.09±11.93 in SASF. A significant difference was determined between IAS and gender, monthly expenditure, daily and weekly internet use, and purpose of using the internet ($p<0.05$). A significant difference was determined between SASF and age, daily and weekly internet use, and purpose of using the internet ($p<0.05$). A moderately significant positive correlation was found between the IAS and the mean SASF score ($r=0.515$, $p=0.000$). The level of internet addiction was found to be high in 20-year-old males, staying at home, and students with a monthly expenditure of 650 TL or more. Smartphone addiction was found to be high in 20-year-old women, those living with their relatives, and students whose monthly expenditure was between 250-449 TL. According to the average score obtained from the Internet addiction scale, it was determined that the students participating in the study were addicted without symptoms. In addition, according to the correlation analysis, as internet addiction increases, smartphone addiction also increases. It is thought that students' internet and smartphone use may affect their social interactions and prevent students from using emotional and cognitive processes effectively.

1. Introduction

Since The iPhone was introduced to market by Steve Jobs in 2007, smartphones have been gained power with a rapid development. This rapid development has influenced to a large number of smartphone users worldwide. Recent statistics indicate that approximately two billion people in the world use smartphones to communicate, browse the Internet or simply play video games [1].

Nomophobia, which is considered the phobia of the 21st century [2], means for NO Mobile Phone PHOBIA and in clinical psychology defined as an irrational fear such as inability to reach a mobile phone or not being able to communicate with a mobile device [2]. Individuals exhibiting nomophobic behaviours worry when they forget to take their mobile phones with them, battery is out of charge or be in no network coverage area. This anxiety state negatively affects the concentration of the individual to perform daily activities [3].

Although nomophobia is not included in the field of clinical psychology, worldwide studies have been conducted on the prevalence of nomophobia among individuals. According to the results of a study conducted by SecurEnvoy (2012), which evaluated the nomophobia status of working people in their business life's, the number of mobile phone users exhibiting nomophobic behaviours increased in the last four years. As stated by this research, 66% of smartphone and mobile phone users expressed that they were worried and afraid at the thought of losing their phones [4].

The use of the Internet on a global scale started to become widespread in the 1990s and has deeply affected our lives. The rapid spread of smartphones after 2010 has made the use of the internet even more common. The widespread use of the Internet has increased its use, especially among students. According to the research, it has been determined that students who are internet literate and good at use of internet perform better academically [5]. However, it is known that internet have some negative effects. As a result of not being able to control excessive internet use, it has been observed that internet addiction occurs by causing severe problems with the environment in daily life. The effect of this such addiction can be compared to alcoholism or compulsive gambling [6].

With the continuous increase in internet and smart phone use, it is thought that this new technology affects the habits, behaviours and emotions of individuals, and it is necessary to examine the relationship between internet and smart phone use, especially the prevalence of nomophobia in the younger generation. Besides, it has become important to evaluate the relationship between university students' smartphone use and internet addiction.

2. Materials and Methods

2.1 Type of the Study

The research was conducted in a cross-sectional descriptive type in order to determine the opinions of student at vocational school of health services on smart phone use and internet addiction.

22. Location of the Study Conducted

The universe of the research consists of students studying at the Vocational School of Health Services (VSHS) of a university in the spring semester of the 2015-2016 academic year. There are 825 students enrolled in VSHS in the spring semester of the 2015-2016 academic year. By using the simple random sampling technique to determine the sample, 668 students who agreed to participate in the research were reached. The data were collected between 01-31 March 2016. After the purpose of the research was explained to the students in the classroom and their informed consent was obtained, questionnaire forms were applied to those who agreed to participate in the study. Personal Information Form, Internet and Smartphone Usage Information Form, Internet Addiction Scale and Smartphone Addiction Scale-Short Form were used as data collection tools.

2.3 Data Collection Tools

Personal Information Form: This form, which was developed by the researchers in accordance with the literature [7,8], consists of a total of 4 questions including the informative characteristics of the students (gender, age, residence during the study period, monthly expenditure amount).

Internet and Smartphone Usage Information Form: This form, which was developed by the researchers in accordance with the literature [9,10], consisted of a total of 4 questions including the internet and smart phone usage characteristics of the students (where the use of internet started, daily and weekly internet usage time, internet usage reason).

Internet Addiction Scale (IAS): The scale was developed by Young in 1996 [11], The Turkish validity and reliability of whom was performed by Bayraktar in 2001. The scale is a 6-point Likert-type scale consisting of 20 questions. It was counted "never" as 0 points, "rarely" as 1 point, "occasionally" as 2 points," often" as 3 points, "very often" as 4 points and" always" as 5 points. There is no reverse scored item in the scale. The highest score that can be obtained from the scale is 100 and the lowest score is 0. By summing up the scores obtained as a result of the survey, users who score 50 points or less are classified as "No Symptom", 50-79 points as "Limited Symptom", and 80 points and above as "Pathological Internet User". The high scores obtained from the scale indicate that internet addiction is high. The scale has a single factor, and the Cronbach Alpha reliability coefficient was calculated as 0.89 in the study in which Turkish validity and reliability were conducted [7]. In this study, the Cronbach's Alpha value of the scale was found to be 0.89.

Smartphone Addiction Scale (SAS)-Short Form: The Scale which developed by Kwon and his friends [13] and whom of Turkish validity and reliability was performed by Noyan and his friends [15]. The scale has a 6-point Likert type structure consisting of 10 questions. It was taken "strongly disagree" as 1 point, "disagree" as 2 points, "partially disagree" 3 points, "partially agree" as 4 points, "agree" as 5 points, "strongly agree" as 6 points. The highest score that can be obtained from the scale is 60 and the lowest score is 10. An

increase in the scores obtained from the scale indicates addiction risk increase. The scale has one factor and has no sub-dimensions. The Cronbach's Alpha coefficient of internal consistency and concurrent validity of the original form was 0.91. In this study, the Cronbach's Alpha value of the scale was found to be 0.87.

2.4 Statistical Analysis

Statistical evaluation of the data was done with SPSS 22.0 for Windows in computer environment. In the analysis of data, in addition to descriptive statistical criteria (mean, standard deviation, minimum and maximum values and percentiles), Chi-Square, OneWay Anova and t tests were used to compare the scale score with the variables. The homogeneous distribution of the variables was analysed by Kolmogrov Smirnov. Tamhane T2 test was used in the post hoc analysis of groups with 3 and more than 3 variables. When the variables were not homogeneously distributed, Mann Whitney U test was used and otherwise the t test was used. Statistical significance was accepted as $p<0.05$.

2.5 Ethical Aspect of the Research

Application permission was obtained from the VSHS Directorate of the university where the study was conducted, and written informed consent was taken from the students participating in the study. The study was conducted in accordance with the Principles of the Declaration of Helsinki.

3. Results

While 76.8% (n=517) of the students within the scope of the research were women, 23.2% (n=156) were men. Moreover, the average age of the students is 20.2±1.12, and students of 23.2% (n=156) are 20-year-old. 45.2% (n=304) of the participants stated that they resided with their families, and 27.9% (n=188) of them stated that their monthly expenditure at education season was between 450-649 TL. In the comparison of the socio-demographic characteristics of the students participating in the research with the total score they got from the SAS and IAS, it was determined that there was a significant difference between gender & monthly expenditure amount and ISI, and between age variable and SAS ($p<0.05$). It was seen that there is no significant difference between the other variables and the scales ($p>0.05$). According to the post hoc analysis, the significance between the IAS and the amount of monthly expenditure existed in students whose monthly expenditures are between 50-249 TL and 650 TL and above; The significance between SAS and the age variable was found to be between 20 years old and 23 years old and over students (Table 1).

Table 1: *Comparison of Students' Total Scores of Internet Addiction (IAS) and Smartphone Addiction (SAS) Scales and Sociodemographic Characteristics (n=668)*

		n	%	IAS		SAS	
				X±SS	p	X±SS	p
Gender	Female	517	76,8	37.67±16.08	***-2.127*/0.034***	**28.41±12.17**	1.537*/0.199
	Male	156	23,2	**40.82±16.67**		27.01±11.05	
Age	18	104	15.5	39.27±13.48	1.182**/0.317	29.93±12.47	***3.347**/0.005***
	19	154	22.9	37.77±15.56		28.40±11.86	
	20	156	23.2	**40.33±15.79**		**30.01±11.89**[a]	
	21	97	14.4	37.89±14.77		26.12±10.77	
	22	43	6.4	39.65±17.79		28.05±11.44	
	23 and above	119	17.7	35.89±20.04		25.16±12.06[a]	
Residence During The Study Period	Home alone	22	3.3	35.45±17.62	1.397**/0.223	29.77±17.12	1.627**/0.151
	Home with friends	72	10.7	**42.31±16.98**		28.63±10.16	
	With family	304	45.2	38.25±17.65		27.50±12.06	
	With relatives	30	4.5	41.37±16.84		**32.83±15.68**	
	Dormitory	207	30.8	37.24±13.19		28.39±11.05	
	Hostel/hotel	38	5.6	38.00±16.75		25.42±11.21	
Monthly Expenditure Amount	50-249 TL	169	25.1	36.76±15.86[a]	3.512**/0.015	27.95±11.69	1,227**/0.299
	250-449 TL	188	27.9	37.51±15.23		**29.23±11.30**	
	450-649 TL	154	22.9	37.57±15.12		26.75±12.67	
	650 TL ve üzeri	162	24.1	**41.96±18.36**[a]		28.18±12.12	

*Indenpendent Sample T Test was used

**One Way Anova Test is used

***a: There is a difference between the groups with the same letter with the scale grand total

At Table 2, in which the internet usage information is evaluated, it was determined that 44.3% (n=298) of the students are connected to the internet at home, 35.2% (n=237) use the internet for more than 241 minutes daily, 70.9% (n=477) use internet regularly everyday of week, 50.7% (n=341) use the internet to follow the events. In the comparison of the total scores obtained from the IAS and SAS of the students participating in the research and their internet usage characteristics, it was determined that there was a significant difference between the total score averages of the IAS and SAS scales for daily and weekly internet and internet use ($p<0.05$). It is seen that there is no significant difference between the other variables and the scales ($p>0.05$). According to the post hoc analysis, the significance between IAS and daily internet use exists in those who use the internet less than 30 minutes a day and those who use the internet between 121-240 minutes and less than 30 minutes and more than 241 minutes; In SAS, on the other hand, it was found that this significance exist in those who used less than 30 minutes and more than 241 minutes (Table 2).

Table 2: *Evaluation of Students' Total Scores of Internet Addiction (IAS) and Smartphone Addiction (SAS) Scales and Internet Usage Knowledge (n=668)*

		n	%	IAS		SAS	
				X±SS	p	X±SS	p
Internet connection location	Home	298	44.3	38.20±17.05		27.28±11.35	
	School	24	3.6	38.79±16.41		**32.46±17.75**	
	Internet cafe	9	1.3	35.53±18.42		21.22±13.12	
	Library	6	0.9	37.83±22.29	0,182*/0.982	24.17±11.75	1.663*/0.127
	Mobile phone	187	27.8	39.18±16.53		28.45±11.80	
	Acquaintance's place	12	1.8	**40.09±25.28**		27.00±14.91	
	Dormitory	137	20.4	37.82±12.75		29.31±11.59	
Daily internet usage	less than 30 min.	47	7.0	28.78±16.03^{ab}		22.66±10.94^{a}	
	31-120 min.	219	32.5	32.32±14.01	**30.408*/0.000**	24.39±9.65	**18.618*/0.000**
	121-240 min.	170	25.3	40.72±15.88^{a}		29.85±12.24	
	Above 241 min.	237	35.2	**44.24±15.82^{b}**		31.32±12.53^{a}	
Weekly internet usage	1 day a week	29	4.3	29.07±12.64ab		22.17±9.98^{ab}	
	2-3 days a week	67	10.0	33.75±12.63c		25.61±10.41^{c}	
	4-5 days a week	100	14.9	38.36±18.80a	**5.919/0.001**	26.77±11.54^{a}	**4.909*/0.002**
	Every day of the week regular	477	70.9	**39.62±16.07^{bc}**		29.07±12.16^{bc}	
Purpose of using the internet	Following events	341	50.7	36.76±14.84^{a}		27.73±11.53^{a}	
	E-mail/instant	115	17.1	40.77±16.86		28.57±12.18	
	messaging	14	2.1	**46.21±18.05**	**3.474/0.004**	27.86±14.12	
	Playing online games	86	12.8	42.29±14.27^{a}		33.22±12.82^{a}	**5.500*/0.000**
	Surfing on internet	10	1.5	44.40±21.05		29.90±8.93	
	Online shopping	107	15.9	36.40±19.53		24.45±10.83	
	Doing homework						

*One Way Anova Test is used

**a-c: There is a difference between the groups with the same letter with the scale grand total

According to the correlation analysis performed with the double-tailed hypothesis method to determine the relationship between IAS and SAS, it was determined that there was a moderate, positive and significant relationship between the scales ($r=0.515$; $p=0.000$). ($p<0,05$) (Table 3) (Graphic 1). It was determined that as internet addiction of students increased, smart phone addiction increased, and as smart phone addiction increased, internet addiction increased.

The data obtained in this study, which was conducted to determine the factors related to smartphone and internet addiction level in students, were discussed in line with the literature. In the study, it was determined that as the internet addiction level of the students increased, the smart phone addiction increased. When the studies on internet and smartphone addiction are evaluated, studies on different groups of university students are encountered. It is thought that this study will contribute to the knowledge in the literature.

4. Conclusions

Table 3: *Correlation and Graph of Internet Addiction Scale (IAS) and Smartphone Addiction Scale (SAS)*

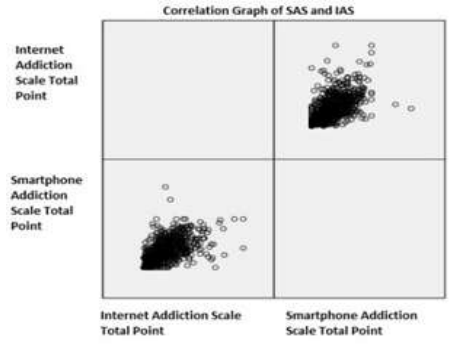

		IAS	SAS
IAS	r	1	0.515
	p		0.000
SAS	r		1
	p		

The average score of the students from the Internet Addiction Scale (IAS) was determined as 38.41±16.26. With this score, the students participating in the research are classified in the "asymptomatic" group. In a study conducted by Sharma & Sharma (2018) on university students, this point was determined as 31.99±18.20. This difference is thought to be caused by cultural and socioeconomic factors. Considering the mean scores obtained from the IAS according to the gender of the participants, it was determined as 37.67±16.08 for women and 40.82±16.67 for men. A similar result to our study was obtained in the study of Anlayışlı&Bulut Serin [12], and it was found 37.00±22.87 in women and 40.97±18.82 in men.

The average score of the students from the Smartphone Addiction Scale (SAS) was determined as 28.09±11.93. With this score, it was concluded that the students participating in the study showed moderate smartphone addiction. When the distribution of the mean scores obtained from the SAS according to the genders was analysed, it was determined as 28.41±12.17 for women and 27.01±11.05 for men. A similar result to our study was found by Keskin and Friends [9], the mean score of the scale was 29.2±11.2; 31.6±11.3 in females and 26.9±10.8 in males, and it was determined a significant difference between the groups ($p<0.05$). Considering at the literature, there are differences in smartphone addiction scale scores according to gender. In general, women's smartphone addiction scale scores are higher than men, and this difference is not significant statistically [13,9].

Although the use of smartphones makes life easier, it can also cause problems such as the length of use and because of these negative effects on daily life. Due to the direct proportionate between smart phone use and internet use, in our study, it was determined that there was a significant difference between students' daily internet use and smart phone addiction ($p<0.05$).

It was determined that there was a moderate, positive and significant ($r=0.515$; $p<0.05$) relationship between internet addiction and smartphone addiction scales. In another study conducted by Tohumcu and friends [14], a high-level, positive and significant relationship was determined between IAS and SAS ($r=0.72$; $p<0.01$). Existing such kind of relationship between smartphone addiction and internet addiction is considered as a normal situation. The continuous use of the two tools together and the high level of correlation as a result of the analysis for the two variables indicate this situation.

As a result, it was found that students' smart phone addiction scale and internet addiction scale mean scores were similar to previous studies. It has been determined that smartphone addiction is related to age, daily and weekly internet usage, and purpose of internet usage. It was determined that the students were in the "asymptomatic" group according to the average score obtained from internet addiction scale, and there was a significant difference between gender, monthly expenditure, daily and weekly internet usage and purpose of internet usage. According to these results, it can be said that there is a connection between smart phone usage and internet usage.

Author Statements:

- The authors declare that they have equal right on this paper.
- The authors declare that they have no known competing financial interests or personal relationships that could have appeared to influence the work reported in this paper
- The authors declare that they have nobody or no-company to acknowledge.

References

[1]. Duke, E., Montag, C. Internet addiction. "smartphone addiction and beyond: Initial insights on an emerging research topic and its relationship

to internet addiction. 2017. Chapter 21, p:359, Switzerland, https://doi.org/10.1007/978-3-319-46276-9.

[2]. YILDIRIM, Caglar; CORREIA, Ana-Paula. Exploring the dimensions of nomophobia: Development and validation of a self-reported questionnaire. Computers in Human Behavior, 2015, 49: 130-137.

[3]. GEZGIN, Deniz Mertkan; CAKIR, Ozlem; YILDIRIM, Soner. The relationship between levels of nomophobia prevalence and internet addiction among high school students: The factors influencing Nomophobia. International Journal of Research in Education and Science, 2018, 4.1: 215-225.

[4]. SecurEnvoy. (2012, February 16). 66% of the population suffer from Nomophobia the fear of being without their phone. Retrieved March 10, 2016, from https://www.securenvoy.com/blog/2012/02/16/66-of-thepopulation-suffer-from-nomophobia-the-fear-of-being-without-their-phone/

[5]. SIRAJ, Harlina Halizah, et al. Internet usage and academic performance: a study in a Malaysian public university. International Medical Journal, 2015, 22.2: 83-86.

[6]. SEKI, Tomokazu, et al. Relationship between internet addiction and depression among Japanese university students. Journal of affective disorders, 2019, 256: 668-672. https://doi.org/10.1016/j.jad.2019.06.055

[7]. BAYRAKTAR, F. İnternet kullanımının ergen gelişimindeki rolü (Yüksek lisans tezi, Ege Üniversitesi Sosyal Bilimler Enstitüsü, İzmir). 2001.

[8]. ADNAN, Müge; GEZGIN, Deniz Mertkan. Modern çağın yeni fobisi: Üniversite öğrencileri arasında nomofobi prevalansı. 2016.

[9]. KESKIN, Tahir, et al. ÜNİVERSİTE ÖĞRENCİLERİNDE AKILLI TELEFON KULLANIMI VE BAŞ AĞRISI İLİŞKİSİ. Adıyaman Üniversitesi Sağlık Bilimleri Dergisi, 2018, 4.2: 864-873. https://doi.org/10.30569/adiyamansaglik.428223

[10]. Sharma, A., Sharma, R. Internet addiction and psychological well-being among college students: a cross-sectional study from central india. J Family Med Prim Care. Jan-Feb 2018, 7.1:147-151. DOI: 10.4103/JFMPC.JFMPC_189_17

[11]. YOUNG, K. S. Internet addiction: The emergence of a new clinical disorder. Cyberpsycholoy & Behavior, 1, 237-244. 1998.

[12]. ANLAYIŞLI, Cemre; SERIN, Nergüz Bulut. Lise öğrencilerinde internet bağımlılığı ve depresyonun cinsiyet, akademik başarı ve internete giriş süreleri açısından incelenmesi. Folklor/edebiyat, 2019, 25.97: 730-743. https://doi.org/10.22559/folklor.977

[13]. KWON, Min, et al. The smartphone addiction scale: development and validation of a short version for adolescents. PloS one, 2013, 8.12: e83558. https://doi.org/10.1371/journal.pone.0083558

[14]. TOHUMCU, Mehmet Utku, et al. AKILLI TELEFON BAĞIMLILIĞI VE İNTERNET BAĞIMLILIĞI İLE BENLİK SAYGISI VE YALNIZLIK ARASINDAKİ İLİŞKİNİN İNCELENMESİ. Trakya University Journal of Social Science, 2019, 21.2. DOI: 10.26468/trakyasobed.545391

[15]. NOYAN, Cemal Onur, et al. Akıllı Telefon Bağımlılığı Ölçeğinin Kısa Formunun üniversite öğrencilerindeTürkçe geçerlilik ve güvenilirlik çalışması. Anatolian Journal of Psychiatry/Anadolu Psikiyatri Dergisi, 2015, 16. DOI: 10.5455/apd.176101

International Journal of Computational and Experimental Science and ENgineering (IJCESEN)

Vol. 7-No.3 (2021) pp. 143-145
http://dergipark.org.tr/en/pub/ijcesen

ISSN: 2149-9144

Research Article

Fast Neutrons Shielding Properties for Fe_2O_3 added Composite

Roya B. MALIDARRE[1,*], Iskender AKKURT[2], Kadir GUNOGLU[3], Hakan AKYILDIRIM[4]

[1]Payame Noor University, Tehran-Iran
* **Corresponding Author** : **Email:** roya_boodaghi@yahoo.com - **ORCID:** 0000-0003-4505-7900

[2]Süleyman Demirel University, Science and Arts Faculty, Physics Department, Isparta-Turkey
Email: iskenderakkurt@sdu.edu.tr - **ORCID:** 0000-0002-5247-7850

[3]Isparta Applied Science University, Science and Arts Faculty, Physics Department, Isparta-Turkey
Email: kadirgunoglu@isparta.edu.tr - **ORCID:** 0000-0002-9008-9162

[4]Süleyman Demirel University, Science and Arts Faculty, Physics Department, Isparta-Turkey
Email: hakanakyildirim@sdu.edu.tr - **ORCID:** 0000-0001-5723-958X

Article Info:

DOI: 10.22399/ijcesen.1012039
Received : 20 October 2021
Accepted : 28 November 2021

Keywords

Neutron attenuation
Composite
Radiation shielding

Abstract:

Neutron has been one of the most interesting particle since its discovery. Being an uncharged particle it is more difficult to shield in comparison with the other radiation types. This may be due to the differences of its interaction with matter. The main interaction processes of neutron with a matter may be via (n,p) reaction and thus hydrogenous materials are generally preferred to shield neutron. In this study neutron shielding properties for HAP composites have been investigated. This is done using Phy-X/PSD software.

1. Introduction

All alive are exposed to many types of radiation sourced due to natural or man-made. Especially in the 20th century when neutron is discovered and radiation started to be used in a variety of different fields, the radiation protection science developed. This was required due to the radiation hazardous effect to human cell. In order to be protected from radiation of X-rays, gamma rays and neutrons, there are three basic methods of time, distance and shielding. Beside first two methods the shielding is most important. Although lead and lead based materials are conventional materials for radiation shielding different types of materials have been studied as alternative [1-21].

As the neutron shielding is more difficult than others it is important to know neutron interaction with the matter. Being electrically neutral particle, neutron interacts only weakly with matter into which it can penetrate deeply. On the other hand gamma-rays interact dominantly with the electron shell of the atom, the neutron does on the level of the nucleus. This makes neutron quite sensitive to light atoms such as hydrogen, oxygen, etc. Those atoms have much higher interaction probability with neutrons than with gamma-rays. For neutron shielding the universal law of attenuation of radiation passing through matter (Beer-Lambert law) is valid. The neutron interaction mechanisms with a material may vary with the energy of incoming neutron and also the physical properties of the target nuclei. The total microscopic cross section (σ_t) of neutrons of any energy expresses the probability of the interaction with the medium and it is given as in equation 1.

$$\sigma_t = \sigma_s + \sigma_a \qquad (1)$$

where σ_s is the both inelastic and elastic scattering while σ_a includes nuclear fusion, nuclear spallation and capture of neutrons.

The fast (or fission energy) neutron attenuation is called the fast neutron effective removal cross section (FNRCS) plays an important role to express for neutron shielding properties. As it serves well for situations when there is not sufficient hydrogen in the material, it is worth calculating the removal cross sections of different materials. The removal cross section is defined as the probability of a first

collision which removes that neutron from its uncollided fast group [22] and it is obtained using equation 2.

$$\Sigma_R = \Sigma_i \rho_i (\frac{\Sigma_R}{\rho})_i \qquad (2)$$

where $\rho_i = \rho w_i$ is the partial density, (w_i is the weight fraction of element i) and ρ is the total density of the material. Weight fraction is the ratio of the molar weight of related element to the molar weight of the material [23-27].

In this study, the fast neutron removal cross section (FNRCS) and attenuation length (mfp) of four different type HAP composite have been calculated and the effect of Fe_2O_3 rate on this parameter were also investigated.

2. Materials and Methods

The fast neutron removal cross section (FNRCS) and attenuation length (mfp) properties of four different composite materials have been investigated. As a material Hydroxyapatite (HAP) composite is used and Fe_2O_3 is doped in different rate. The chemical formulation of composite is expressed as (*100-x*)HAP+*x*Fe_2O_3 where x= 0, 2.5, 5, and 7.5 (wt%), using Phy-X/PSD code. The Phy-X/PSD is a free online platform where radiation shielding parameters of any materials can be obtained [28].

3. Results and Discussions

The neutron attenuation properties of four different types of composites have been obtained in term of fast neutron removal cross section (FNRCS) and attenuation length (mfp). The obtained results are shown as a function of density of composite Fig. 1. It is seen from this figure that the FNRCS increased with the increasing density of composite. This could be the results of increasing Fe_2O_3 rate in the composite. This is shown in Fig. 2 where it can be clearly seen that Fe_2O_3 rate is important for neutron shielding capability of this composite. This can also be seen in Fig. 3 where attenuation length is displayed as a function of density. It is clearly seen from this figure that the mfp decreased linearly with the increasing density which means that the high density composite may stop neutron in short distance.

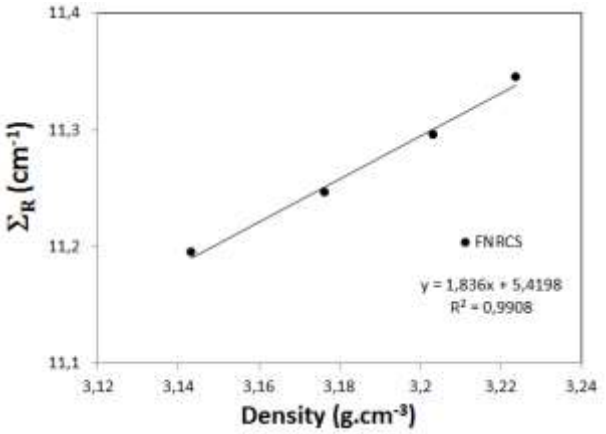

Figure 1. *Neutron removal cross section as a function of composite density*

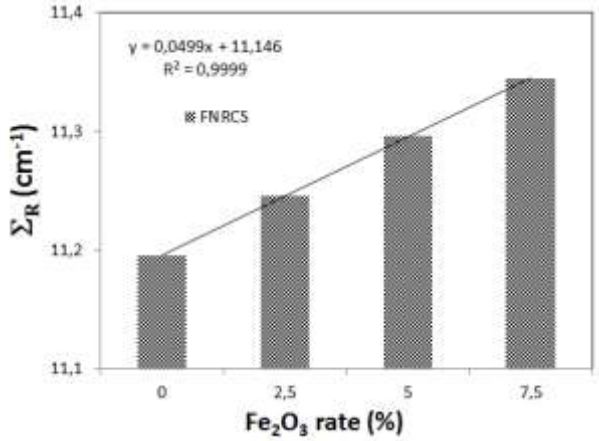

Figure 2. *Neutron removal cross section as a function of Fe_2O_3 rate in composite*

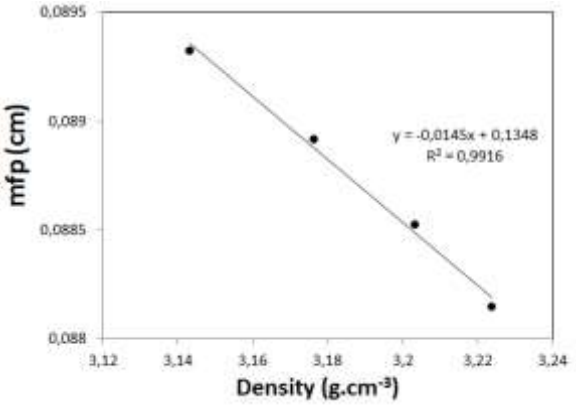

Figure 3. *Attenuation length as a function of composite density*

Author Statements:

- The authors declare that they have equal right on this paper.
- The authors declare that they have no known competing financial interests or personal relationships that could have appeared to influence the work reported in this paper
- The authors declare that they have nobody or no-company to acknowledge.

References

[1] Iskender Akkurt, "Effective atomic and electron numbers of some steels at different energies" Annals of Nuclear. Energy. 36,11-12 pp.1702-1705. 2009. DOI:10.1016/j.anucene.2009.09.005

[2]Aljawhara H. Almuqrin, M.I. Sayyed, Ashok Kumar, B.O. El-bashir, I. Akkurt. Optical, mechanical properties and gamma ray shielding behavior of TeO2-Bi2O3-PbO-MgO-B2O3 glasses using FLUKA simulation code . Optical Materials 113 (2021) 110900 https://doi.org/10.1016/j.optmat.2021.110900

[3] Al-Obaidi S., H. Akyıldırım, K. Gunoglu, I. Akkurt . 2020 Acta Physica Polonica A **137**. 551 DOI: 10.12693/APhysPolA.137.551

[4] Roya Boodaghi Malidarrea, Feride Kulali, Aysun Inal, Ali Oz. 2020. Emerging Materials Research. **9:**1334-1340. https://doi.org/10.1680/jemmr.20.00202

[5] A.M.El-Khayatt, İ.Akkurt 2013. Annals of Nuclear Energy.**60:**8-14. https://doi.org/10.1016/j.anucene.2013.04.021

[6]Yasser Saad Rammah, Ashok Kumar, Karem Abdel-Azeem Mahmoud, Raouf El-Mallawany, Fouad Ismail El-Agawany, Gulfem Susoy, Huseyin Ozan Tekin. 2020. Emerging materials research **9-3:**1000-1008. https://doi.org/10.1680/jemmr.20.00150

[7]O. Günay, M. Sarihan, O. Yarar, İ. Akkurt, M. Demir. 2020. Acta Physica Polonica A **137:**569 DOI: 10.12693/APhysPolA.137.569

[8] M.Y. Hanfi, M.I. Sayyed, E. Lacommeet al., 2020 Nuclear Engineering and Technology, https://doi.org/10.1016/j.net.2020.12.012

[9]Çelen, Y.Y., Akkurt, İ. & Kayıran, H.F. Gamma ray shielding parameters of barium tetra titanate (BaTi4O9) ceramic. J Mater Sci: Mater Electron (2021). https://doi.org/10.1007/s10854-021-06376-6

[10]I. Akkurt, R.B. Malidarre, I. Kartal, K. Gunoglu, Polymer Composites 2021,1.https://doi.org/10.1002/pc.26185

[11] Huseyin Ozan Tekin, Baris CAVLI, Elif Ebru ALTUNSOY, Tugba MANICI, Ceren OZTURK, Hakki Muammer KARAKAS "An Investigation on Radiation Protection and Shielding Properties of 16 Slice Computed Tomography (CT) Facilities "International Journal of Computational and Experimental Science and Engineering 4-2(2018)37 – 40. https://doi.org/10.22399/ijcesen.408231

[12]Feride Kulali. 2020 Emerging Materials Research. **9:**1341-1347. https://doi.org/10.1680/jemmr.20.00307

[13] Iskender AKKURT, Huseyin Ozan TEKIN 2020.Emerging Materials Research **9:** https://doi.org/10.1680/jemmr.20.00209

[14]Fouad Ismail El-Agawany, Karem Abdel-Azeem Mahmoud, Hakan Akyildirim, El-Sayed Yousef, Huseyin Ozan Tekin, Yasser Saad Rammah. Physical, neutron, and gamma-rays shielding parameters for Na2O–SiO2–PbO glasses. Emerging Materials Research 10-2(2021), pp. 227–237 https://doi.org/10.1680/jemmr.20.00297

[15]Şen Baykal, D , Tekin, H , Çakırlı Mutlu, R . (2021). An Investigation on Radiation Shielding Properties of Borosilicate Glass Systems . International Journal of Computational and Experimental Science and Engineering , 7 (2) , 99-108 . DOI: 10.22399/ijcesen.960151

[16]H.O. Tekin, Shams A.M. Issa, K.A. Mahmoud, F.I. El-Agawany,Y.S. Rammah, G. Susoy, M.S. Al-Buriahi, Mohamed M. Abuzaid, I. Akkurt. Nuclear radiation shielding competences of Barium (Ba) reinforced borosilicate glasses.. Emerging Materials Research 9-4(2020)1131-1144 https://doi.org/10.1680/jemmr.20.00185

[17]Yonca Yahşi Çelen. Gamma Ray Shielding Parameters of Some Phantom Fabrication Materials for Medical Dosimetry. Emerging Materials Research 10-3(2021). https://doi.org/10.1680/jemmr.21.00043

[18] Boodaghi Malidarre, R., Akkurt, I. 2021. J Mater Sci: Mater Electron https://doi.org/10.1007/s10854-021-05776-y

[19] Yonca Yahsi Çelen, Iskender Akkurt, Yusuf Ceylan, Hasan Atçeken. 2021. Application of experiment and simulation to estimate radiation shielding capacity of various rocks. Arab. J. GeoSci. 14:1471 https://doi.org/10.1007/s12517-021-08000-7

[20]Yonca Yahşi Çelen, Atilla Evcin. 2020. Emerging Materials Research **9:** https://doi.org/10.1680/jemmr.20.00098

[21] Boodaghi Malidarre, R., Akkurt, I. Monte Carlo simulation study on TeO2–Bi2O–PbO–MgO–B2O3 glass for neutron-gamma 252Cf source. J Mater Sci: Mater Electron (2021). https://doi.org/10.1007/s10854-021-05776-y

[22]Blizard, E.P., Abbott, L.S. 1962. Reactor Handbook, vol. III, Part B, Shielding, John Wiley and Sons, Inc.

[23]Chilton, A.B., Shultis, J.K., Faw, R.E. 1984. Principles of Radiation Shielding, Prentice-Hall, Englewood Cliffs.

[24]Woods, J. 1982. Computational Methods in Reactor Shielding, Pergamon Press Inc., New York.

[25]Schmidt, F.A.R. 1969. Analytical Radiation Shielding Calculations for Concrete – Formulas and Parameters, Nuclear Engineering and Design, 10, 308-324.

[26]Kaplan, M. F. 1989. Concrete Radiation Shielding. Longman Scientific and Technology, Longman Group UK Limited, Essex, London.

[27]Hakan AKYILDIRIM "Calculation of Fast Neutron Shielding Parameters for Some Essential Carbohydrates"Erzincan University Journal of Science and Technology 2019, 12(2), 1141-1148 2019, 12(2), 1141-1148 DOI: 10.18185/erzifbed.587514

[28]Erdem Şakar, Özgür Fırat Özpolat, Bünyamin Alım, M.I. Sayyed, Murat Kurudirek.2020. Radiation Physics and Chemistry **166** :108496 https://doi.org/10.1016/j.radphyschem.2019.108496

International Journal of Computational and Experimental Science and ENgineering (IJCESEN)
Vol. 7-No.3 (2021) pp. 146-155
http://dergipark.org.tr/en/pub/ijcesen

ISSN: 2149-9144

Research Article

Effect of Rosuvastatin on Fasting and Postprandial Lipid Profile in Hypertriglyceridemia Patients

Abdulkadir ÇAKMAK*

Assistant Prof., Amasya University Sabuncuoğlu Şerefeddin Education and Research Hospital, Department of Cardiology

* **Corresponding Author -Email:** abdulkadir.cakmak@amasya.edu.tr **ORCID:** 0000-0001-7427-3368

Article Info:

DOI: 10.22399/ijcesen.827419
Received : 17 November 2020
Accepted : 28 November 2021

Keywords

Coronary heart disease
Hypertriglyceridemia
Rosuvastatin
Triglycerides

Abstract:

Coronary heart disease (CHD) is a main cause of mortality due to cardiovascular diseases. Hypertriglyceridemia (HTG) is a multifactorial condition implicated in the pathogenesis of CHD. Serum triglyceride (TG) levels were routinely obtained under fasting conditions; however, recent evidences implicate that postprandial triglyceride levels may be more important for CHD risk. Aim of this study was to investigate the effect of rosuvastatin on fasting and postprandial TG levels in the patients with borderline-high TG levels. 51 patients (18-75 years old; 26 female) with LDL-c between 100 and 160 mg/dL and triglyceride levels between 150 and 300 mg/dL were included in this study. Basal fasting and postprandial lipid profile and hsCRP levels of the patients were obtained and patients were requested to take 10 mg/day rosuvastatin for one month. At the end of one month, the measurements were repeated. Rosuvastatin significantly decreased both fasting and postprandial TG levels compared to basal levels ($p<0.001$). The decrease in the postprandial TG levels after rosuvastatin treatment were significantly higher than the decrease in fasting TG levels ($p<0.001$). No differences between genders were observed with regards to decrease in the fasting and postprandial TG levels. In patients with metabolic syndrome, rosuvastatin treatment decreased fasting and postprandial TG levels after one month, however, the change was not different from the patients without metabolic syndrome. In conclusion, the decrease in postprandial TG levels after rosuvastatin treatment that was shown may be clinically important in prevention of CHD in HTG patients.

1. Introduction

Cardiovascular diseases (CVDs) are the major cause of death worldwide and coronary heart disease (CHD) is indicated to be a main cause of the death due to CVDs [1]. Despite of the gradual decrease in the CHD-related deaths, almost 30 % of mortality older than Hypertriglyceridemia (HTG) is a multifactorial condition that is the consequence of interaction between both genetic and environmental factors and develops due to increased very low-density lipoprotein (VLDL) cholesterol (LDL-c) and chylomicron levels, as well as their remnants [2,3]. HTG has a strong association with the low levels of high-density lipoprotein (HDL) cholesterol (HDL-c) and high levels of LDL-c that are the risk of coronary heart disease (CHD) and has been suggested to have a relation with premature CHD [4,5]. Multifactorial analyses weakened association between HTG and CHD [6,7] as the triglyceride (TG) levels are affected by various factors such as obesity, severe alcohol consumption, diabetes mellitus (DM), insulin resistance, hypertension and smoking [8], however, various studies indicated HTG as an independent risk factor for CVD [9].

Increased TG levels are defined by the National Cholesterol Education Program (NCEP) Adult Treatment Panel III (ATP III) as fasting TG levels are higher than 150 mg/dL in adults and levels spanning 150-199 mg/dL is defined as borderline-high TG levels, while TG levels equal or higher than 500 mg/dL is indicated as very high TG levels [10]. On the other hand, a following guidelines published by Endocrine Society focused on the connection between the pancreatitis risk in the

subjects with severely high TG levels and classified the TG levels higher than 2,000 mg/dL as very severe HTG resulting in pancreatitis [11, 12]. Both guidelines are prepared to help clinicians for the evaluation of the risk of both CVD and pancreatitis and to improve the treatment options [13].

Routine serum TG measurement has been conducted under fasting conditions to acquire more stable TG concentration measurement and calculate the LDL levels [14], however, recent suggestions are that the fasting is not required for the routine TG profile screening [15] and lipid measurements under fasting and postprandial conditions depends on the scenario that is questioned [16]. Fasting and postprandial TG levels may vary depending on the content and time of last meal [17] and postprandial HGT is associated with the CHD risk that is related to increased levels of chylomicron, as well as LDL-c and VLDL-c, have atherogenic activity as they potentiate the platelet activity and coagulation cascade [18]. In addition, evidences suggest that increased postprandial TG levels has been indicated to be a risk factor for CHD by several studies [19-21].

Statins that were firstly identified in 1976 [22] inhibits a rate limiting enzyme, hydroxymethyl glutaryl coenzyme A reductase (HMG-CoA), in cholesterol biosynthesis [23] exert their antiatherosclerosis activities by reducing the LDL-c [24] and decreasing thrombin formation [25]. Rosuvastatin exerts its beneficial cardiovascular activities by not only competitively inhibiting the HMG-CoA and improving the cholesterol profile but also acting as antioxidant, antithrombotic and anti-inflammatory [26]. Previous studies showed that 20 mg/day [27] rosuvastatin treatment led to 62 % decrease in the cardiovascular events in the patients with normal LDL-c levels and high levels of high-sensitivity C-reactive protein (hsCRP) and decreased fasting TG levels by 17 % [27]. Several studies also showed that statins lowered the fasting and postprandial plasma TG and apolipoprotein (apo)B-48 levels [28-33]. An 8-week treatment with 5 mg rosuvastatin was found to decrease fasting LDL-c, total cholesterol and TG levels significantly [34]. Therefore, in this study, we aimed to determine the effect of rosuvastatin on fasting and postprandial TG levels in the patients with TG levels between 150 and 300 mg/dL and LDL-c levels between 100 and 160 mg/dL

2. Patients and Methods

Patients admitted to and evaluated at Cardiology Department at Başkent University Faculty of Medicine between March 2009 and February 2010 were included in this study. Inclusion criteria of were determined being between 18 and 75 years old, having LDL-c levels between 100 and 160 mg/dL, indication of statin use according to the NCEP ATPIII [30], and having TG levels between 150 and 300 mg/dL, while the exclusion criteria were being younger than 18 and older than 75 years old, having medical history of DM, chronic liver disease, chronic kidney disease and chronic renal failure, connective tissue disease, gastrointestinal malabsorption disorders, enteropathies, acute myocardial infarction (MI), unstable angina pectoris, acute/chronic pancreatitis, hyperthyroidism and hypothyroidism, having TG levels below 150 mg/dL and above 300 mg/dL and LDL-c levels below 100 mg/dL and above 160 mg/dL. This study was approved by Başkent University Clinical Research Ethics Committee on 03/02/2009 (Approval no: B.30.2. BŞK.0.05.05.01/95).

A group of 51 patients who were evaluated in the cardiology department of our hospital, met the inclusion criteria and gave their consent were included in this study. Blood pressure, height, weight, CHD risk factors, alcohol consumption pattern of the patients, as well as the medications that they used, were recorded. Patients with body mass index (BMI) higher than 30 kg/m2 were classified as obese. Presence of three factors of that a waist circumference exceeding 102 cm in males and 88 cm in females, TG levels higher than 150 mg/dL, HDL-c below 40 mg/dL in males and 50 mg/dL in females, blood pressure equal or above 130/85 (systole/diastole) and blood glucose levels equal or higher than 100 mg/dL were considered as the diagnosis of metabolic syndrome in the patients. The activity level (sports, exercise) below 150 minutes per week was taken as the sedentary life criterion. If the patient was exercising at least five days a week for more than 30 min/day, patient was noted as exercising regularly. Patients who were consuming 2-3 days a week around 30 g alcohol per day and were identified as alcohol consumers. Patients with a history of anginal symptoms, ECG variations and elevated cardiac enzyme levels indicating the presence of coronary artery disease, if the coronary angiography of the patient showed at least one lesion with more than 50 % stenosis, if the patient underwent percutaneous coronary intervention at any time or underwent coronary artery bypass surgery, the patient was then included in the CHD group.

After a 12-hour fasting period, total cholesterol, LDL-c, TG, HDL-c and hsCRP levels of the patients were measured. The patient was then given a breakfast as described in the oral lipid loading test protocol below and measurements were repeated four hours later. Breakfast was prepared by the

Nutrition and Dietetics Unit in the cafeteria of our hospital and served as a breakfast plate.

Since the biochemical markers measured in our study are highly affected by diet, patients were requested not to make any dietary changes during the study period. Patients were recommended to take their medicines at the same time of day. The patients were questioned whether they were using their drugs properly or not at the first month follow-up.

In oral fat load tests conducted by administering fat-enriched enteral solutions or meals with high calorie and high fat content, the fat content ranges from 31% to 80% [35-38]. In our study, breakfast was preferred for fat loading because it was easier to tolerate and provide. All patients were given an average breakfast consisting of 60% fat, 16.8% protein and 23.2% carbohydrate with a total energy content of 891 kcal.

Complete blood count and blood biochemistry (TG, total cholesterol, LDL-c, HDL-c, hsCRP, blood glucose, alanine aminotransferase (ALT), aspartate aminotransferase (AST), creatine kinase (CK), blood urea nitrogen (BUN), creatinine, sodium (Na+), potassium (K+) and thyroid stimulating hormone (TSH)) measurements were conducted on the admission day and one month after. TG, total cholesterol, LDL-c, HDL-c, blood glucose, AST, ALT, CK, BUN, creatinine, Na+ and K+ measurements were conducted by using a modular autoanalyzer (Roche Diagnostics GmbH, Germany), hsCRP measurements were conducted by using a CRP Ultra reagent Abbott® Architect C8000 Analyser (Sentinel Diagnostics, Italy), TSH measurements were conducted by using an Architect i2000 autoanalyzer (Abbott, Wiesbaden, Germany) and haematology measurements Abbott Cell-Dyne® 3700 System (Abbott Diagnostics, Santa Clara, USA)..

2.1. Statistical analyses

Shapiro-Wilk test was used to check the normal distribution of the continuous variables. The homogeneity of the variances was analysed by Levene test. Student's t-test was used to compare the gender differences in several variables. In case of the variables did not meet prerequisites of parametric tests, Mann-Whitney U test was used to compare the gender differences. The relation between the data were investigated by Pearson Chi-square, G-test and Fisher Exact test where applicable. Two-way repeated measures of analysis of variance by including sex factor was used to compare the pre- and post-treatment and fasting and postprandial values of the parameters by including sex factor. Before this analysis was performed, it was determined that the variables had a right skewed distribution, the logarithmic transformation was applied to the variables to provide the prerequisites for analysis of repeated measurements.

Statistical analysis results were expressed as n (%) for categorical variables and mean ± standard deviation (SD) and median for continuous variables. A p value lower than 0.05 was considered statistically significant. SPSS 16.0 statistical package program (Statistical Package for the Social Sciences, version 16.0, SSPS Inc., Chicago, IL, USA) was used to analyse the data set.

3. Results

This study included 51 patients (Table 1). The mean age of the patients was 54.3±11.6 and 26 of the patients were female (Table 1). Mean BMI of the patients were 28.1 ± 4.1 (mean body weight 77.4 ± 16.1 kg and mean height 165.8 ± 10.3 cm). Waist circumference was 108.4±9.4 cm and mean hip circumference was 108.9 ± 9.4 cm). A group of 12 patients (23.5 %) had CHD history and 5 out of them had MI, six of them had coronary artery bypass surgery and one patient percutaneous coronary intervention history. Forty patients (78.4 %) had metabolic syndrome. 19 patients were obese, and 36 patients had sedentary lifestyle (Table 1). 17 patients were smokers while 11 patients were exercising regularly. The results of basal laboratory examination for blood parameters and complete blood counts of patients are also summarized in Table 1.

The comparison between the genders with regards to the demographical and lifestyle characteristics, significant differences were found only in the CHD history and alcohol use and diet between the genders ($p<0.05$; Table 2). When the basal fasting and postprandial (after oral lipid load) lipid and hsCRP values were investigated it was found that TG and total cholesterol values were significantly higher ($p<0.001$, LDL-c and HDL-c were significantly lower ($p<0.01$ and $p<0.001$, respectively) in the patients after lipid load (under postprandial conditions), while hsCRP levels were found unaffected (Table 3). After oral lipid loading, patients received 10 mg/day rosuvastatin for one month, then patients fasting ALT, AST, CK and blood lipid profile, as well as the postprandial blood lipid profile after lipid load was investigated. There were no significant differences between the basal and post-treatment ALT (22.2±5.7 and 22.8±6.0, respectively), AST (24.1±9.2 and 24.7±7.1, respectively), and CK values (65.3±26.2 and 76.0±27.6, respectively). On the other hand, TG and total cholesterol levels were significantly

Table 1. *Demographical characteristics of the patients (n=51).*

	Female(n=26)	Male(n=25)	p-value
Age (years (mean ± SD)	55.2 ± 11.2	49.9 ± 12.1	0.588
Patient condition			
BMI (kg/m²)	27.9 ± 4.7	28.3 ± 3.4	0.758
Waist circumference (cm)	107.4±11.5	109.1±5.5	0.155
Metabolic syndrome, n (%)	19 (73.1 %)	21 (84.0 %)	0.499
CHD history, n (%)	2 (7.6 %)	10 (40 %)	**0.040***
Hypertension, n (%)	17 (65.4 %)	16 (64.0 %)	0.918
Obesity, n (%)	69 (34.6 %)	10 (40 %)	0.691
Lifestyle Sedentary lifestyle, n (%)	19 (73.1 %)	17 (68.0 %)	0.764
Smoking, n (%)	6 (23.1 %)	11 (44.0 %)	0.090
Alcohol use, n (%)	0	2 (8.0 %)	**0.034***
Exercise, n (%)	6 (23.1 %)	5 (20 %)	0.789
Diet, n (%)	7 (26.9 %)	1 (4.0)	**0.026***

Table 2. *Comparison between the female and male patients with regards to demographical characteristics *p<0.05*

Age (years (mean ± SD))	54.3 ± 11.6
Gender, n (%)	
Female	26 (50.9 %)
Male	25 (49.1 %)
Patient condition	
BMI (kg/m²)	28.1 ± 4.1
Waist circumference (cm)	108.4 ± 9.4
Metabolic syndrome, n (%)	40 (78.4 %)
CHD history, n (%)	12 (23.5 %)
Family history of CHD, n (%)	21 (41.2 %)
Hypertension, n (%)	33 (64.7 %)
Obesity, n (%)	19 (37.3 %)
Lifestyle	
Sedentary lifestyle, n (%)	36 (70.6 %)
Smoking, n (%)	17 (33.3 %)
Alcohol use, n (%)	3 (5.9 %)
Exercise	11 (21.6 %)
Laboratory parameter	
Fasting glucose (mg/dL)	93.9 ± 8.8
Sodium (mmol/L)	139.1 ± 2.5
Potassium (mmol/L)	4.2 ± 0.4
Haemoglobin (g/dL)	14.5 ± 1.3
Haematocrit (%)	42.7 ± 4.4
Leukocyte (10^3/mm³)	7,354 ± 1,620
Thrombocyte (10^3/mm³)	285,333 ± 51,690
AST (U/L)	22.2 ± 5.7
ALT (U/L)	24.1 ± 9.2
CK (U/L)	65.3±26.2
TSH (IU/mL)	2.1±1.0
BUN (mg/dL)	15.3±4.3
Creatinine (mg/dL)	0.8±0.2

ALT, Alanine aminotransferase; AST, Aspartate aminotransferase; BMI, body mass index; BUN, Blood urea nitrogen; CHD, coronary heart disease; CK, Creatine kinase; TSH, Thyroid stimulating hormone.

Table 3. *Basal fasting and postprandial (after lipid load) lipid and hsCRP levels (n=51).*

	Fasting	Postprandial	p value
TG (mg/dL)	191.0 ± 41.4	337.4 ± 117.1	**<0.001***
Total cholesterol (mg/dL)	212.6 ± 23.7	237.0 ± 28.1	**<0.001***
LDL-c (mg/dL)	133.8 ± 19.6	129.8 ± 20.5	**<0.01***
HDL-c (mg/dL)	41.5 ± 8.4	39.4 ± 8.6	**<0.001***
hsCRP (mg/L)	5.5 ± 5.1	5.7 ± 5.0	0.168

HDL-c, high-density lipoprotein-cholesterol; hsCRP, high-sensitivity C-reactive protein; LDL-c, low-density lipoprotein-cholesterol; TG, triglyceride.

Table 4. *Post-treatment fasting and postprandial (after lipid load) lipid and hsCRP levels (n=51).*

	Fasting	Postprandial	p value
TG (mg/dL)	152.1±50.6	258.0±95.9	**<0.001***
Total cholesterol (mg/dL)	154.9±22.0	172.9±24.4	**<0.001***
LDL-c (mg/dL)	80.4±16.9	77.0±16.0	**<0.001***
HDL-c (mg/dL)	43.6±9.7	41.9±9.0	**<0.001***
hsCRP (mg/L)	4.9±4.8	4.8±4.6	0.474

HDL-c, high-density lipoprotein-cholesterol; hsCRP, high-sensitivity C-reactive protein; LDL-c, low-density lipoprotein-cholesterol; TG, triglyceride.

higher at the post-treatment period after lipid load (p<0.001; Table 4), while LDL-c and HDL-c levels were significantly lower (p<0.001; Table 4). On the other hand, there were no significant differences between the fasting and postprandial hsCRP levels (p=0.474; Table 4). When the fasting lipid parameters and hsCRP values were compared at the baseline and post-treatment, TG, total cholesterol and LDL-c levels were found to be significantly lower (p<0.001; Table 5). On the other hand, fasting HDL-c levels were found higher and hsCRP was found lower at post-treatment period, but these differences were not statistically significant (p=0.068 and p=0.091, respectively; Table 5). On the other hand, postprandial TG, total cholesterol, LDL-c and hsCRP levels were significantly lower after one-month rosuvastatin treatment when compared with basal values(p<0.001 for TG, total cholesterol and LDL-c and p<0.05 for hsCRP;

Table 5). In addition, postprandial HDL-c levels were found to be higher after rosuvastatin treatment compared to baseline ($p<0.05$; Table 5).

The differences between the pre-treatment fasting and postprandial TG levels (191.0±41.4 mg/dL and 337.4±117.1 mg/dL, respectively) and post-treatment fasting and postprandial TG levels (152.1±50.6 mg/dL and 258.0±95.9 mg/dL, respectively) were compared with Wilcoxon test. The differences between the fasting and postprandial TG levels at the baseline and post-treatment period were found as 38.9±46.2 mg/dL and 79.4±96.8 mg/dL, respectively and the change in the decrease in TG levels (30.5±46.2 mg/dL) were found significant ($p<0.001$).

When the fasting and postprandial TG values of male and female subjects were compared at the baseline and after one-month rosuvastatin treatment, both fasting and postprandial TG levels were found to be decreased after rosuvastatin treatment ($p<0.001$; Table 6). On the other hand, there were no statistically significant differences in TG levels between the genders when the basal fasting ($p=0.47$), basal postprandial ($p=0.14$), post-treatment fasting ($p=0.57$) and post-treatment postprandial ($p=0.19$) levels were compared. In both males and females, the level of decrease in postprandial TG levels were higher than the decrease in fasting TG levels after one-month rosuvastatin administration ($p<0.001$). However, Wilcoxon test revealed that this decrease in the TG levels did not differ between the genders ($p=0.784$).

In the patients both with or without metabolic syndrome, TG levels were significantly higher after lipid load compared to fasting TG levels both at baseline and after one-month rosuvastatin treatment ($p<0.001$; Table 7). On the other hand, fasting TG levels were significantly lower after one-month rosuvastatin treatment in the patients with metabolic syndrome ($p<0.001$) while no difference was observed in the patients without metabolic syndrome ($p<0.112$; Table 7). Similarly, post-lower after rosuvastatin treatment in the patients with metabolic syndrome ($p<0.001$) but there was no significant effect of rosuvastatin level in postprandial TG levels patients without metabolic syndrome ($p<0.089$; Table 7). In addition basal fasting TG levels were significantly lower in the patients without metabolic syndrome compared to the patients with metabolic syndrome ($p<0.009$; Table 7), however, no significant differences were observed in basal postprandial, post-treatment fasting and post-treatment postprandial TG levels between the patients with metabolic syndrome and patients without metabolic syndrome (Table 7).

The analyses in the obese and non-obese patients revealed that the basal, as well as after one-month rosuvastatin treatment, postprandial TG levels were significantly higher than fasting levels in both patient groups ($p<0.001$; Table 8). On the other hand, fasting TG levels after rosuvastatin treatment were significantly lower than the baseline levels in both groups ($p\leq0.001$; Table 8). Similarly, postprandial TG levels after rosuvastatin treatment were significantly lower than the baseline levels ($p<0.01$; Table 8). However, there were no significant differences between the groups any of the parameters that were compared (Table 8).

Table 5. *Comparison of fasting and postprandial (after lipid load) lipid and hsCRP levels at the baseline and one-month rosuvastatin treatment (n=51; in the statistical analysis of postprandial measurements log-transformed values were used).*

	Fasting		
	Basal	**Post-treatment**	**p value**
TG (mg/dL)	191.0±41.4	152.1±50.6	**<0.001***
Total cholesterol (mg/dL)	212.6±23.7	154.9±22.0	**<0.001***
LDL-c (mg/dL)	133.8±19.6	80.4±16.9	**<0.001***
HDL-c (mg/dL)	41.5±8.4	43.6±9.7	0.068
hsCRP (mg/L)	5.5±5.1	4.9±4.8	0.091
	Postprandial		
	Basal	**Post-treatment**	**p value**
TG (mg/dL)	337.4±117.1	258.0±95.9	**<0.001***
Total cholesterol (mg/dL)	237.0±28.1	172.9±24.4	**<0.001***
LDL-c (mg/dL)	129.8±20.5	77.0±16.0	**<0.001***
HDL-c (mg/dL)	39.4±8.6	41.9±9.0	**<0.05***
hsCRP (mg/L)	5.7±5.0	4.8±4.6	**<0.05***

HDL-c, high-density lipoprotein-cholesterol; hsCRP, high-sensitivity C-reactive protein; LDL-c, low-density lipoprotein-cholesterol; TG, triglyceride.

4. Discussions

HTG is an independent risk factor for CHD [9]. TG levels are routinely measured under fasting conditions to obtain more stable TG levels and therefore to calculate LDL levels [14]. Nevertheless, it was recently suggested that fasting is not necessary for routine TG profiling [15]. In addition, previous studies indicated that postprandial TG levels are as important risk factor as fasting TG levels for CHD [39-41]. In our study, we investigated the effects of rosuvastatin, a statin that is used in the treatment of hyperlipidaemia, on fasting and postprandial TG and hsCRP levels. Rosuvastatin is known to decrease fasting TG levels between 17% and 25% [27]. Several other studies indicated significant reductions in fasting

Table 6. *Comparison of fasting and postprandial (after lipid load) TG levels at the baseline and one-month rosuvastatin treatment within the genders.*

	Basal		Post-treatment		^{a}p value	^{b}p value	^{c}p value	^{d}p value
	Fasting	Postprandial	Fasting	Postprandial				
Female (n=26)	186.8 ±36.5	313.8 ±88.5	148.5 ±46.1	240.7 ±88.0	**<0.001***	**<0.001***	**<0.001***	**<0.001***
Male (n=25)	195.3 ±46.3	362.0 ±138. 4	156.2 ±55.0	275.8 ±102. 2	**<0.001***	**<0.001***	**<0.001***	**<0.001***

*p<0.05

[a]p: Comparison of the basal fasting and postprandial TG levels within genders

[b]p: Comparison of the post-treatment fasting and postprandial TG levels within genders

[c]p: Comparison of the basal and post-treatment fasting TG levels within genders

[d]p: Comparison of the basal and post-treatment postprandial TG levels within genders

Table 7. *Comparison of fasting and postprandial (after lipid load) TG levels at the baseline and one-month rosuvastatin treatment within and between the patients with and without metabolic syndrome.*

	Basal		Post-treatment		^{a}p value	^{b}p value	^{c}p value	^{d}p value	^{e}p value	^{f}p value	^{g}p value	^{h}p value
	Fasting	Postprandial	Fasting	Postprandial								
α (n=40)	197.0±43.4	350.3±124.7	155.5±48.3	264.7±92.2	**<0.001***	**<0.001***	**<0.001***	**<0.001***	**0.009***	0.059	0.329	0.919
Ø (n=11)	169.3±23.3	290.3±69.2	139.1±58.7	234.2±109.7	**<0.001***	**0.003***	0.112	0.089				

α: patients with metabolic syndrome, Ø: patients without metabolic syndrome, *p<0.05

[a]p: Comparison of the basal fasting and postprandial TG levels within the groups

[b]p: Comparison of the post-treatment fasting and postprandial within the groups

[c]p: Comparison of the basal and post-treatment fasting TG levels within the groups

[d]p: Comparison of the basal and post-treatment postprandial TG levels within the groups

[e]p: Comparison of the basal fasting TG levels between the groups

[f]p: Comparison of the basal postprandial between the groups

[g]p: Comparison of the post-treatment fasting TG levels between the groups

[h]p: Comparison of the post-treatment postprandial TG levels between the groups

Table 8. *Comparison of fasting and postprandial (after lipid load) TG levels at the baseline and one-month rosuvastatin treatment within and between obese and non-obese patients.*

	Basal		Post-treatment		^{a}p value	^{b}p value	^{c}p value	^{d}p value	^{e}p value	^{f}p value	^{g}p value	^{h}p value
	Fasting	Postprandial	Fasting	Postprandial								
Obese (n=19)	197.0±43.7	325.3±130.7	160.6±37.3	264.7±92.2	**<0.001***	**<0.001***	**0.001***	**0.009***	0.721	0.623	0.231	0.424
Non-obese (n=32)	187.3±40.3	344.3±109.2	147.1±56.7	262.2±100.7	**<0.001***	**<0.001***	**<0.001***	**<0.001***				

*p<0.05

[a]p: Comparison of the basal fasting and postprandial TG levels within the groups

[b]p: Comparison of the post-treatment fasting and postprandial within the groups

[c]p: Comparison of the basal and post-treatment fasting TG levels within the groups

[d]p: Comparison of the basal and post-treatment postprandial TG levels within the groups

[e]p: Comparison of the basal fasting TG levels between the groups

[f]p: Comparison of the basal postprandial between the groups

[g]p: Comparison of the post-treatment fasting TG levels between the groups

[h]p: Comparison of the post-treatment postprandial TG levels between the groups

TG levels at different doses for different treatment periods [42,43]. In our study, 10 mg/day rosuvastatin treatment for one month resulted in a 20% decrease in fasting TG levels, similar to the results published previously. Atorvastatin, another statin, treatment led to significant reductions in the postprandial TG levels [30,44]. In our study, besides the decrease in postprandial TG level was significant, the decrease in postprandial TG value was more pronounced from the decrease in fasting TG level upon rosuvastatin treatment. This finding suggests that control of postprandial TG levels by rosuvastatin treatment, similar to the control of fasting TG levels, may be another aspect of the efficacy of rosuvastatin in the prevention of CHD.

In our study, when the hs-CRP levels were examined, the only significant change was seen between the baseline postprandial levels and postprandial levels after one-month rosuvastatin treatment. Several long-term (two to 33 months) studies revealed beneficial effects of rosuvastatin on decreasing hsCRP levels [27,42,45]. The fact that the significant difference appeared only at the levels of postprandial levels in our study may be related to the short length of the treatment period.

The frequency, occurrence, treatment process and outcomes of CHD show some differences between women and men. For example, CHD mortality and stroke risk are higher in women in the presence of DM, but the evaluation of women in studies is not as clear and detailed as men and besides cultural, behavioural, psychosocial and socioeconomic differences, gender-dependent factors and CHD outcomes in women are not as well explained as in men [46]. Lipoprotein risk factors that are important for CHD also differ in women. The risk prediction of HDL-c is stronger than that of men, oestrogen prevents the storage of LDL-c in arterial wall, and in postmenopausal women, TG is an independent risk factor (proatherogenic lipid profile) for CHD in women [47, 48]. In a 2-year study conducted revealed that BMI, HDL-c are most correlated risk factors with hsCRP for CHD for both genders and hsCRP levels were positively correlated with mean blood pressure and blood glucose in men while it was with TG levels in women [49]. Also, a recent meta-analysis revealed that statins have beneficial effects on both genders, they are more effective in improving lipid profile in women older than 70 years [50]. In our study, rosuvastatin treatment was found equally affecting TG levels in men and women.

The positive effects of statins on dyslipidaemia in the patients with metabolic syndrome was shown by various groups [51,52]. On the other hand, atherosclerosis was shown to progress in the obese patients although they receive statin treatment [53]. Another study suggested that the type of statin to be used should be chosen in obese patients with type 2 DM depending on their lipid profile and condition [54]. In our study, independent of condition of the patients with regards to metabolic syndrome, postprandial TG levels significantly higher than fasting TG levels both at baseline and after one-month rosuvastatin treatment. Similar results were obtained when obese patients were compared with non-obese patients. However, both fasting and postprandial TG levels were significantly lower after one-month rosuvastatin treatment compared to the baseline fasting and postprandial TG levels in the patients with metabolic syndrome but in the patients without metabolic syndrome. However, no significant differences in the TG levels between obese and non-obese patients were observed. These results suggest that one-month rosuvastatin treatment may improve TG levels in patients with metabolic syndrome. In our study, no side effects of rosuvastatin treatment were observed. In addition, liver function parameters were not significantly affected by rosuvastatin treatment. As treatment period was limited with one month, safety profile of short-term 10 mg/day rosuvastatin seems reliable.

In our study, we evaluated the effect of rosuvastatin treatment on laboratory parameters as the risk factors for CHD (Lipid profile and hsCRP), however, clinical endpoints were not determined. Nevertheless, the importance of postprandial lipid metabolism on the atherosclerotic pathogenesis has been implicated by several studies and postprandial TG levels may be more important indicators than fasting TG levels. Therefore, we believe that the significant decrease in the postprandial TG levels is clinically important. In order to investigate this clinically important effect, studies evaluating the clinical endpoints on larger cases are needed.

Author Statements:

- The authors declare that they have equal right on this paper.
- The authors declare that they have no known competing financial interests or personal relationships that could have appeared to influence the work reported in this paper
- The authors declare that they have nobody or no-company to acknowledge.

References

[1]. Shi A, Tao Z, Wei P, Zhao J. Epidemiological aspects of heart diseases. Experimental and

therapeutic medicine. 2016;12(3):1645-50. doi:10.3892/etm.2016.3541.

[2]. Johansen CT, Wang J, Lanktree MB, McIntyre AD, Ban MR, Martins RA et al. An increased burden of common and rare lipid-associated risk alleles contributes to the phenotypic spectrum of hypertriglyceridemia. Arteriosclerosis, thrombosis, and vascular biology. 2011;31(8):1916-26. doi:10.1161/ATVBAHA.111.226365.

[3]. Ariza M-J, Sánchez-Chaparro M-A, Barón F-J, Hornos A-M, Calvo-Bonacho E, Rioja J et al. Additive effects of LPL, APOA5 and APOE variant combinations on triglyceride levels and hypertriglyceridemia: results of the ICARIA genetic sub-study. BMC medical genetics. 2010;11:66-. doi:10.1186/1471-2350-11-66.

[4]. Berneis KK, Krauss RM. Metabolic origins and clinical significance of LDL heterogeneity. J Lipid Res. 2002;43(9):1363-79. doi:10.1194/jlr.r200004-jlr200.

[5]. Gordon DJ, Probstfield JL, Garrison RJ, Neaton JD, Castelli WP, Knoke JD et al. High-density lipoprotein cholesterol and cardiovascular disease. Four prospective American studies. Circulation. 1989;79(1):8-15. doi:10.1161/01.cir.79.1.8.

[6]. Hulley SB, Rosenman RH, Bawol RD, Brand RJ. Epidemiology as a guide to clinical decisions. The association between triglyceride and coronary heart disease. N Engl J Med. 1980;302(25):1383-9. doi:10.1056/nejm198006193022503.

[7]. Sarwar N, Danesh J, Eiriksdottir G, Sigurdsson G, Wareham N, Bingham S et al. Triglycerides and the risk of coronary heart disease: 10,158 incident cases among 262,525 participants in 29 Western prospective studies. Circulation. 2007;115(4):450-8. doi:10.1161/circulationaha.106.637793.

[8]. Grundy SM. Hypertriglyceridemia, atherogenic dyslipidemia, and the metabolic syndrome. Am J Cardiol. 1998;81(4a):18b-25b. doi:10.1016/s0002-9149(98)00033-2.

[9]. Han SH, Nicholls SJ, Sakuma I, Zhao D, Koh KK. Hypertriglyceridemia and Cardiovascular Diseases: Revisited. Korean circulation journal. 2016;46(2):135-44. doi:10.4070/kcj.2016.46.2.135.

[10]. National C. Third Report of the National Cholesterol Education Program (NCEP) Expert Panel on Detection, Evaluation, and Treatment of High Blood Cholesterol in Adults (Adult Treatment Panel III) final report. Circulation. 2002;106(25):3143-421.

[11]. Brunzell JD, Schrott HG. The interaction of familial and secondary causes of hypertriglyceridemia: role in pancreatitis. J Clin Lipidol. 2012;6(5):409-12. doi:10.1016/j.jacl.2012.06.005.

[12]. Chait A, Brunzell JD. Severe hypertriglyceridemia: role of familial and acquired disorders. Metabolism. 1983;32(3):209-14. doi:10.1016/0026-0495(83)90184-1.

[13]. Rygiel K. Hypertriglyceridemia - Common Causes, Prevention and Treatment Strategies. Current cardiology reviews. 2018;14(1):67-76. doi:10.2174/1573403X14666180123165542.

[14]. Berglund L, Brunzell JD, Goldberg AC, Goldberg IJ, Sacks F, Murad MH et al. Evaluation and treatment of hypertriglyceridemia: an Endocrine Society clinical practice guideline. The Journal of clinical endocrinology and metabolism. 2012;97(9):2969-89. doi:10.1210/jc.2011-3213.

[15]. Nordestgaard BG, Langsted A, Mora S, Kolovou G, Baum H, Bruckert E et al. Fasting is not routinely required for determination of a lipid profile: clinical and laboratory implications including flagging at desirable concentration cut-points-a joint consensus statement from the European Atherosclerosis Society and European Federation of Clinical Chemistry and Laboratory Medicine. European heart journal. 2016;37(25):1944-58. doi:10.1093/eurheartj/ehw152.

[16]. Driver SL, Martin SS, Gluckman TJ, Clary JM, Blumenthal RS, Stone NJ. Fasting or Nonfasting Lipid Measurements. Journal of the American College of Cardiology. 2016;67(10):1227. doi:10.1016/j.jacc.2015.12.047.

[17]. Langsted A, Freiberg Jacob J, Nordestgaard Børge G. Fasting and Nonfasting Lipid Levels. Circulation. 2008;118(20):2047-56. doi:10.1161/CIRCULATIONAHA.108.804146.

[18]. Masuda D, Yamashita S. Postprandial Hyperlipidemia and Remnant Lipoproteins. Journal of atherosclerosis and thrombosis. 2017;24(2):95-109. doi:10.5551/jat.RV16003.

[19]. Nordestgaard BG, Benn M, Schnohr P, Tybjærg-Hansen A. Nonfasting Triglycerides and Risk of Myocardial Infarction, Ischemic Heart Disease, and Death in Men and Women. JAMA. 2007;298(3):299-308. doi:10.1001/jama.298.3.299.

[20]. Bansal S, Buring JE, Rifai N, Mora S, Sacks FM, Ridker PM. Fasting compared with nonfasting triglycerides and risk of cardiovascular events in women. Jama. 2007;298(3):309-16. doi:10.1001/jama.298.3.309.

[21]. Egeland GM, Igland J, Sulo G, Nygard O, Ebbing M, Tell GS. Postprandial triglycerides predict incident acute myocardial infarction among those with favourable HDL-cholesterol: Cohort Norway. Eur J Prev Cardiol. 2015;22(7):872-81. doi:10.1177/2047487314535681.

[22]. Endo A, Kuroda M, Tsujita Y. ML-236A, ML-236B, and ML-236C, new inhibitors of cholesterogenesis produced by Penicillium citrinium. J Antibiot (Tokyo). 1976;29(12):1346-8. doi:10.7164/antibiotics.29.1346.

[23]. Taylor F, Huffman MD, Macedo AF, Moore TH, Burke M, Davey Smith G et al. Statins for the primary prevention of cardiovascular disease. Cochrane Database Syst Rev. 2013(1):Cd004816. doi:10.1002/14651858.CD004816.pub5.

[24]. Stancu C, Sima A. Statins: mechanism of action and effects. J Cell Mol Med. 2001;5(4):378-87. doi:10.1111/j.1582-4934.2001.tb00172.x.

[25]. Tripodi A, Pellegatta F, Chantarangkul V, Grigore L, Garlaschelli K, Baragetti A et al. Statins decrease thrombin generation in patients with

hypercholesterolemia. Eur J Intern Med. 2014;25(5):449-51. doi:10.1016/j.ejim.2014.03.016.

[26]. Cortese F, Gesualdo M, Cortese A, Carbonara S, Devito F, Zito A et al. Rosuvastatin: Beyond the cholesterol-lowering effect. Pharmacological Research. 2016;107:1-18. doi:https://doi.org/10.1016/j.phrs.2016.02.012.

[27]. Ridker PM, Danielson E, Fonseca FA, Genest J, Gotto AM, Jr., Kastelein JJ et al. Rosuvastatin to prevent vascular events in men and women with elevated C-reactive protein. N Engl J Med. 2008;359(21):2195-207. doi:10.1056/NEJMoa0807646.

[28]. Otokozawa S, Ai M, Van Himbergen T, Asztalos BF, Tanaka A, Stein EA et al. Effects of intensive atorvastatin and rosuvastatin treatment on apolipoprotein B-48 and remnant lipoprotein cholesterol levels. Atherosclerosis. 2009;205(1):197-201. doi:10.1016/j.atherosclerosis.2008.11.001.

[29]. Battula SB, Fitzsimons O, Moreno S, Owens D, Collins P, Johnson A et al. Postprandial apolipoprotein B48-and B100-containing lipoproteins in type 2 diabetes: do statins have a specific effect on triglyceride metabolism? Metabolism. 2000;49(8):1049-54. doi:10.1053/meta.2000.7744.

[30]. Parhofer KG, Laubach E, Barrett PH. Effect of atorvastatin on postprandial lipoprotein metabolism in hypertriglyceridemic patients. J Lipid Res. 2003;44(6):1192-8. doi:10.1194/jlr.M300011-JLR200.

[31]. Parhofer KG, Barrett PH, Schwandt P. Atorvastatin improves postprandial lipoprotein metabolism in normolipidemlic subjects. J Clin Endocrinol Metab. 2000;85(11):4224-30. doi:10.1210/jcem.85.11.6978.

[32]. Ng TW, Watts GF, Stuckey BG, Ching HL, Chan DC, Uchida Y et al. Does pravastatin increase chylomicron remnant catabolism in postmenopausal women with type 2 diabetes mellitus? Clin Endocrinol (Oxf). 2005;63(6):650-6. doi:10.1111/j.1365-2265.2005.02396.x.

[33]. Chan DC, Watts GF, Barrett PH, Martins IJ, James AP, Mamo JC et al. Effect of atorvastatin on chylomicron remnant metabolism in visceral obesity: a study employing a new stable isotope breath test. J Lipid Res. 2002;43(5):706-12.

[34]. Tonu S, Dewan Z, Akhter N, Banerjee S. A comparative study of atorvastatin and rosuvastatin on lipid lowering efficacy in hyperlipidemic patients. Bangabandhu Sheikh Mujib Medical University Journal. 2018;11(1):17-0. doi:10.3329/bsmmuj.v11i1.35244.

[35]. Hadjadj S, Paul JL, Meyer L, Durlach V, Verges B, Ziegler O et al. Delayed changes in postprandial lipid in young normolipidemic men after a nocturnal vitamin A oral fat load test. J Nutr. 1999;129(9):1649-55. doi:10.1093/jn/129.9.1649.

[36]. Karpe F, Bell M, Bjorkegren J, Hamsten A. Quantification of postprandial triglyceride-rich lipoproteins in healthy men by retinyl ester labeling and simultaneous measurement of apolipoproteins B-48 and B-100. Arterioscler Thromb Vasc Biol. 1995;15(2):199-207.

[37]. Guerci B, Paul JL, Hadjadj S, Durlach V, Verges B, Attia N et al. Analysis of the postprandial lipid metabolism: use of a 3-point test. Diabetes Metab. 2001;27(4 Pt 1):449-57.

[38]. Atar A, Atar I, Gülmez Ö, Ertan Ç, Özgül AS, Yücel M et al. Postprandial triglyceride levels in patients with or without metabolic syndrome and their relationship with coronary artery disease. Turk Kardiyoloji Dernegi Arsivi. 2007;35:482-8.

[39]. Meyer E, Westerveld HT, de Ruyter-Meijstek FC, van Greevenbroek MM, Rienks R, van Rijn HJ et al. Abnormal postprandial apolipoprotein B-48 and triglyceride responses in normolipidemic women with greater than 70% stenotic coronary artery disease: a case-control study. Atherosclerosis. 1996;124(2):221-35. doi:10.1016/0021-9150(96)05832-7.

[40]. Karpe F, Steiner G, Uffelman K, Olivecrona T, Hamsten A. Postprandial lipoproteins and progression of coronary atherosclerosis. Atherosclerosis. 1994;106(1):83-97. doi:10.1016/0021-9150(94)90085-x.

[41]. Boccalandro F, Farias J, Boccalandro C, Vaisman D. Frequency of postprandial lipemia after a first acute coronary event (unstable angina pectoris or non-ST-segment elevation acute myocardial infarction) and the effects of atenolol on the lipemia. Am J Cardiol. 2002;90(2):153-6. doi:10.1016/s0002-9149(02)02440-2.

[42]. Saito Y, Yamada N, Shirai K, Sasaki J, Ebihara Y, Yanase T et al. Effect of rosuvastatin 5-20mg on triglycerides and other lipid parameters in Japanese patients with hypertriglyceridemia. Atherosclerosis. 2007;194(2):505-11. doi:10.1016/j.atherosclerosis.2006.11.028.

[43]. Hunninghake DB, Stein EA, Bays HE, Rader DJ, Chitra RR, Simonson SG et al. Rosuvastatin improves the atherogenic and atheroprotective lipid profiles in patients with hypertriglyceridemia. Coron Artery Dis. 2004;15(2):115-23.

[44]. Schaefer EJ, McNamara JR, Tayler T, Daly JA, Gleason JA, Seman LJ et al. Effects of atorvastatin on fasting and postprandial lipoprotein subclasses in coronary heart disease patients versus control subjects. Am J Cardiol. 2002;90(7):689-96. doi:10.1016/s0002-9149(02)02591-2.

[45]. Wedel H, McMurray JJ, Lindberg M, Wikstrand J, Cleland JG, Cornel JH et al. Predictors of fatal and non-fatal outcomes in the Controlled Rosuvastatin Multinational Trial in Heart Failure (CORONA): incremental value of apolipoprotein A-1, high-sensitivity C-reactive peptide and N-terminal pro B-type natriuretic peptide. Eur J Heart Fail. 2009;11(3):281-91. doi:10.1093/eurjhf/hfn046.

[46]. Pilote L, Dasgupta K, Guru V, Humphries KH, McGrath J, Norris C et al. A comprehensive view

of sex-specific issues related to cardiovascular disease. Cmaj. 2007;176(6):S1-44. doi:10.1503/cmaj.051455.

[47]. Regitz-Zagrosek V, Lehmkuhl E, Mahmoodzadeh S. Gender aspects of the role of the metabolic syndrome as a risk factor for cardiovascular disease. Gend Med. 2007;4 Suppl B:S162-77.

[48]. LaRosa JC. Women, lipoproteins, and cardiovascular disease risk. Int J Fertil. 1992;37 Suppl 2:63-71.

[49]. Nasermoaddeli A, Sekine M, Kagamimori S. Gender differences in associations of C-reactive protein with atherosclerotic risk factors and psychosocial characteristics in Japanese civil servants. Psychosom Med. 2006;68(1):58-63. doi:10.1097/01.psy.0000195882.00407.05.

[50]. Karlson BW, Palmer MK, Nicholls SJ, Barter PJ, Lundman P. Effects of age, gender and statin dose on lipid levels: Results from the VOYAGER meta-analysis database. Atherosclerosis. 2017;265:54-9. doi:10.1016/j.atherosclerosis.2017.08.014.

[51]. Pyorala K, Ballantyne CM, Gumbiner B, Lee MW, Shah A, Davies MJ et al. Reduction of cardiovascular events by simvastatin in nondiabetic coronary heart disease patients with and without the metabolic syndrome: subgroup analyses of the Scandinavian Simvastatin Survival Study (4S). Diabetes Care. 2004;27(7):1735-40. doi:10.2337/diacare.27.7.1735.

[52]. Deedwania PC, Hunninghake DB, Bays HE, Jones PH, Cain VA, Blasetto JW. Effects of rosuvastatin, atorvastatin, simvastatin, and pravastatin on atherogenic dyslipidemia in patients with characteristics of the metabolic syndrome. Am J Cardiol. 2005;95(3):360-6. doi:10.1016/j.amjcard.2004.09.034.

[53]. Sandfort V, Lai S, Ahlman MA, Mallek M, Liu S, Sibley CT et al. Obesity Is Associated With Progression of Atherosclerosis During Statin Treatment. J Am Heart Assoc. 2016;5(7):e003621. doi:10.1161/JAHA.116.003621.

[54]. Sindhu S, Singh HK, Salman MT, Fatima J, Verma VK. Effects of atorvastatin and rosuvastatin on high-sensitivity C-reactive protein and lipid profile in obese type 2 diabetes mellitus patients. J Pharmacol Pharmacother. 2011;2(4):261-5. doi:10.4103/0976-500X.85954.

International Journal of Computational and Experimental Science and ENgineering (IJCESEN)
Vol. 7-No.3 (2021) pp. 156-163
http://dergipark.org.tr/en/pub/ijcesen

ISSN: 2149-9144

Research Article

The Prediction of Chiral Metamaterial Resonance using Convolutional Neural Networks and Conventional Machine Learning Algorithms

Aybike URAL YALÇIN[1], Zeynep Hilal KİLİMCİ[2,*]

[1]Doğuş University, Engineering Faculty, Department of Mechanical Engineering, 34775, İstanbul-Turkey
Email: aural@dogus.edu.tr **ORCID:** 0000-0002-3923-1821

[2]Kocaeli University, Technology Faculty, Department of Information Systems Engineering, 41001, Kocaeli-Turkey
* **Corresponding Author Email**: zeynep.kilimci@kocaeli.edu.tr **ORCID:** 0000-0003-1497-305X

Article Info:

DOI: 10.22399/ijcesen.973726
Received : 22 July 2021
Accepted : 29 November 2021

Keywords:

Chiral metamaterials
Convolutional neural network
Deep learning
Machine learning
Microwave resonance

Abstract:

Electromagnetic resonance is the most important distinguishing property of metamaterials to examine many unusual phenomena. The resonant response of metamaterials can depend many parameters such as geometry, incident wave polarization. The estimation and the design of the unit cells can be challenging for the required application. The research on resonant behavior can yield promising applications. We investigate the resonance frequency of the chiral resonator as a unit of chiral metamaterial employing both traditional machine learning algorithms and convolutional deep neural networks. To our knowledge, this is the very first attempt on chiral metamaterials in that comparing the impact of various machine learning algorithms and deep learning model. The effect of geometrical parameters of the chiral resonator on the resonance frequency is studied. For this purpose, convolutional neural networks, support vector machines, naive Bayes, decision trees, random forests are employed for classification of resonance frequency. Extensive experiments are performed by varying training set percentages, epoch sizes, and data sets. Experiment results demonstrate that the usage of convolutional neural networks is superior in terms of prediction performance of chiral metamaterial resonance compared to the other techniques with 58.29% of accuracy on dataset1, and 68.77% of accuracy on dataset2.

1. Introduction

The chirality refers to a structural property of an object that cannot be superimposed on its mirror image [1]. The existence of chirality in nature at macro and molecular scale lead to a wide variety of research. Despite the natural phenomenas [2], artificially made materials called metamaterials can exhibit chiral properties. Metamaterials are composed of periodically arranged resonant elements, unit cells, which show unnatural electromagnetic and optical properties, such as negative refraction, which are not seen in naturally occurring materials [3,4]. Various chiral resonators are used to build chiral metamaterials such as helical wires, chiral split ring resonators (SRR) [5], gammadions [4] or cross-wire [6] structures. The optical response of chiral metamaterials is studied also in terahertz regime [7-10]. Some designs are proposed to avoid bianisotropic effects [11-12]. Omega shaped particles are another building blocks of metamaterials for the realization of the negative index which is experimentally verified [13-14]. Transmission properties of metamaterials formed by omega shaped inclusions are investigated in [15]. It is shown that the periodic arrays can be employed in stop/pass band applications due to the magnetoelectric resonances. Another artificial chiral object is called a canonical spiral replacing a helix in order to simplify the electromagnetic analysis [16]. In [17], an analytical antenna model is used to analyze such chiral scatterers. The canonical spiral is designed for chiral metamaterials where independently the linear polarization of the incident wave can be radiated as a circularly polarized wave [18]. As a consequence of the design, a particular helicity is completely transparent for circular electromagnetic waves of the same helicity [18]. The canonical spirals are capable also in cloaking application [19].

In this work, we design a metamaterial structure given a desired chiral response or even to simply predict the trend in chiral response as the structure transforms. The electromagnetic response of canonical spiral shaped chiral resonators in the microwave regime will be examined by a proposed method based on both machine learning algorithms and deep learning methodology. The application of deep learning algorithms are rather popular in recent years in different research fields such as image processing, natural language processing, speech recognition, video processing, sentiment analysis, text classification, computer vision, pattern recognition, and machine translation. Furthermore, deep neural network models are also utilized in various research domains beyond computer science such as physics with various subfields like material science, chemistry, laser physics, particle physics, quantum mechanics, and microscopy [20-26]. Deep learning networks applied in many studies to the inverse engineering to reveal the metamaterials response in optics and acoustics [27-30]. For the purpose of eliminating disadvantages of conventional machine learning algorithms, deep learning methodology is preferred by the researches in many fields because of its superior performance. In other words, the main reason behind the choice of deep learning models by the researchers both better representation of features, predictions, and results when compared with traditional machine learning algorithms. Deep learning models are mostly employed to ensure automatic feature extraction procedure thereby training complex features with minimal external support to achieve meaningful representation of data through deep neural networks. Besides automatic feature extraction, deep learning methods are also used for the purpose of classification tasks in many fields. Due to both excellent performance of deep learning models in the state-of-the-art studies and the lack of implementation of deep learning models on optical chiral metamaterials subfield, we concentrate on Convolutional Neural Network (CNN) as deep learning model for the purpose of eliminating this deficiency in this study, in addition to machine learning algorithms.

In the present work, the resonance frequency of the chiral structure as a unit of chiral metamaterial is studied using both traditional machine learning algorithms and convolutional deep neural networks. The main objective of this study is the prediction of the resonance response of the canonical spiral through the proposed model. For this purpose, convolutional neural networks, support vector machines, naive Bayes, decision trees, random forests are used for frequency selective classification. The novelty of this study is to investigate the impact of the most popular deep learning method, CNN, which is not implemented yet on the chiral metamaterial design. To the best of our knowledge, this is the very first study on chiral metamaterials in that comparing the impact of various machine learning algorithms and deep learning model.

The paper is organized as follows: In section 2, machine learning algorithms and convolutional neural network employed in this study is introduced. In section 3, we describe the chiral resonator and the numerical model from which we gathered the data and the proposed framework. The section 4 discusses the results and then we conclude the paper.

2. Models

In this section, methods used in this work are briefly presented.

2.1. Naive Bayes Algorithm (NB)

Naive Bayes is a well-known and mostly employed classification model for both two-class (binary) and multi-class classification problems. The naive Bayes algorithm is based upon independency of features in the data set that is base of Bayes's theorem. It is easy to construct and not complex which makes it especially beneficial for huge data sets. In spite of its simpleness, the Naive Bayes algorithm works well and presents superior classification performances compared to more complicated classification models. There are different event models for NB algorithm such as Gaussian naive Bayes, Multinomial naïve Bayes, Bernoulli naive Bayes, etc. Gaussian NB model is the easiest way to forecast the distribution of the data set because it predicts just the standard deviation and the mean of training data set. In this work, we focus on the Gaussian naive Bayes method [31-36].

2.2. Support Vector Machine (SVM)

Support vector machine (SVM) is employed as a supervised learning method that is used for classification and regression problems. The main purpose of support vector machine method is to discover a hyperplane in an N-dimensional space that plainly categorizes the points of data set. However, support vector machine is responsible for finding a plane with the maximum space between data points of both categories among many potential hyperplanes for the purpose of dividing the two classes. This procedure is called margin maximization that facilitates the classification task for unseen instances with more confidence. Furthermore, SVM is also capable to implement

non-linear classification task in addition to linear classification which is called kernel trick, implicitly mapping their inputs into high-dimensional spaces. According to data set distribution, there are too many kernel tricks such as linear, polynomial, radial basis function, sigmoid when SVM is constructed. In this work, each version is implemented and polynomial is selected as the best [33-40].

2.3. Decision Tree (DT)

Decision tree method is one of the predicting models employed in machine learning. Decision trees are also popular machine learning algorithms in terms of their comprehensibility and simplicity. The main objective of decision trees is to construct a model that predicts a target value (class) based upon different inputs. A decision tree is evaluated as a predictive model with branches and leaves. Here, observations are the branches while target value of related observation is represented as leaves. In classification trees, class labels are demonstrated with leaves and association of the features are indicated as branches. In other words, a tree is constructed by dividing the source data set, composing the root node of the tree, into subsets (children). The dividing procedure is implemented with a set of splitting rules based upon features of classification. When this procedure is repeated for each derivate subset, it is called as recursion. Recursion is finished when target variable has same results at a node for each subset. This widely accepted approach for decision trees is known as top-down induction that signs the greedy algorithm. As a summary, decision trees ensure the consolidation of computational and mathematical methods to obtain the classification of the dedicated data set [33,41-43].

2.4. Random Forest (RF)

Random forest is based on a large number of decision trees that constructs a community decision system. Each decision tree in a community demonstrates the class forecast and final decision is determined by voting according to majority. Random forests are proposed in order to eliminate the over-fitting problems of decision trees. The basic idea behind of random forest is constructing the common decision of different models which exhibits more successful classification success compared to the only one classifier. Here, two main concepts are important. It is expected that each individual tree is constructed through low correlated models in a random forest and high classification success. The main reason behind of this expectation is to interfere individual errors of each tree from each other by reducing relation between models. In this work, the number of individual trees is set to 25 due to its superior performance compared to 10, 50, 75, and 100 of trees [34-35,44-46].

2.5. Convolution Neural Network (CNN)

Convolutional neural network is a type of deep neural networks, mostly applied especially in image processing field. CNNs exhibits notable classification results in natural language processing, financial time series, video processing and are also popular in these domains. The name this network model comes from the series of mathematical process named as convolution and is a type of customized linear operations. CNN is mainly constructed with input layer, multiple hidden layers, and output layer. Hidden layers of CNN are comprised from the sets of convolutional layers that rely on a convolution instead of matrix multiplication in at least one of their layers. CNN methodology includes a set of convolutional layers intertwined with pooling layers, followed up several fully connected layers. During this procedure, the most significant layer is the convolution layer that implement a filter of convolution to input in order to attain a feature map of input data. In order to get multiple features, multiple filters are carried out during training process and filters are capable to define the context of an investigated problem. After that, convolution process is implemented to acquire feature maps which indicates dependencies among features, local features of data set. Then, pooling layers that are intertwined with convolutional layers are acted to decrease the number of instances in each feature map and keep the most significant information about data. Through down sampling characteristic, the decrease in training time of the system and dimension reduction of data set are provided. There are several kinds of pooling layers such as max pooling, average pooling, global max pooling, global average pooling. In this work, maximum pooling is utilized which is generally also employed in literature studies. Actually, feature extraction is performed through convolution and pooling layers until this step. After, the output of pooling layers is converted nx1 dimensional vector in order to feed fully connected layers which is called flattening. Then, final decision of the system is determined by the help of fully connected layers. In CNN architecture like other deep neural networks, there are too many methods to avoid over-fitting challenge such as regularization models, early stopping criteria. In this study, we use dropout, L2 regularizator, and early stopping criteria for this purpose [33, 35, 47-55].

3. Proposed Framework

3.1. Data Preparation

In this part, data preparation is introduced. Figure 1 shows the schematic view of the canonical spiral which is composed of a torus with a gap $g = 0.9\ mm$ and two rods residing from edges of the gap in opposite directions perpendicular to the plane of the torus. The outer radius of torus is $r_{out} = 2\ mm$ and torus thickness $r = 0.8\ mm$; two legs are of length $l = 2\ mm$. The thickness of the torus is kept fixed, while the gap size, radius of the torus and the length of the legs is varying. In data gathering process, three gap sizes are used between $0.9\ mm$ and $1.1\ mm$. For each gap size, we are changing the length of the rods and the radius of the torus between $2\ mm$ and $3\ mm$ with a step size $0.1\ mm$.

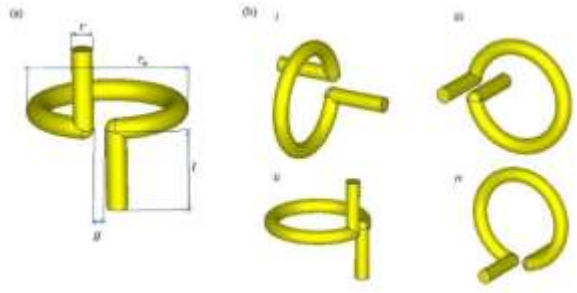

Figure 1. *The canonical spiral has gap g, length of the rods l, thickness r, and outer radius of the torus is r_0. Four orientations i-iv of the canonical spiral with respect to E, B field and the propagation direction of the incident plane wave.*

The structure is taken as perfect electric conductor (PEC). The embedding environment is taken as air. A plane wave travelling along +x-axis is incident on the structure where the electric field is linearly polarized along y-axis, and the magnetic field is along z-axis. The resonant frequency response of the canonical spiral is obtained analyzing the transmission (S_{21} dB) spectrum between $5-11\ GHz$. The four possible orientations of the canonical spiral with respect to the incident EM wave is examined and their resonance response is used in classification. The simulations are computed in CST Microwave studio software, which uses finite element methods, in frequency domain solver. The EM wave is excited defining ports and relevant boundary conditions

3.2. Model

In this work, we focus on the estimating resonance frequency of chiral metamaterial by employing both traditional machine learning models and a deep learning algorithm. For this purpose, naive Bayes (NB), support vector machine (SVMs), decision trees (DTs), random forests (RFs) are evaluated as machine learning algorithms and convolutional neural networks (CNNs) are appraised as a deep learning model in order to estimate of chiral metamaterial resonance. To demonstrate the efficiency of proposed design, we collect two data sets (dataset1, dataset2) that contain $1{,}210$ and $2{,}057$ instances, respectively. The number of features and class labels are the same for both data sets. Features evaluated in the training procedure are length of the rods, outer radius of torus, thickness of torus, gap, orientation in millimeters. Resonance frequency is located as class label in giga hertz. The main objective of our study is assigning resonance frequency of unseen/unlabeled instances in the data set by training model through machine learning algorithms and a deep learning model. In order to prepare data set for training procedure, there are some adaptations by converting categorical values into numerical ones such as orientation attribute. Moreover, class label is scaled per 0.05 precision starting from 0 to 1 corresponding to canonical spiral designs with a resonance frequency classes $5-11\ GHz$ with a stepsize 0.05. After that, the data set is randomly splitted into training and test sets by varying training set size as $80, 50, 30, 10$. The remainings are carried out as test set percentages. To achieve a reliable prediction, the holdout process is recurred 10 times and an overall accuracy is calculated by taking averages of each iteration. In the tables, the following abbreviations are employed. Ts: Training set size, NB: Naive Bayes algorithm, SVM: Support vector machine, DT: Decision tree, RF: Random Forest algorithm, CNN: Convolutional neural network. The best classification results are exhibited in boldface in the tables. Furthermore, accuracy is appraised as an evaluation metric. In Figure 2, the proposed framework is presented.

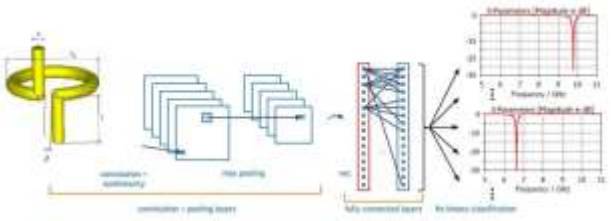

Figure 2. *The canonical spiral geometrical parameters and its orientation given as input to the convolution plus pooling layers, as output we get the resonance frequency which corresponds to a dip in the transmission spectrum.*

4. Experiment Results

Firstly, the effect of conventional machine learning algorithms is investigated on frequency prediction of chiral metamaterials. Then, convolutional neural networks are evaluated in order to observe the impact a deep learning model on this classification task. Table 1 and Table 3 demonstrates the classification accuracies of machine learning models and deep learning model on both data sets in terms of training set percentages. First of all, it is clearly observed in Table 1 and Table 3 that the usage of ts80 boosts the classification accuracy of each model. The poorest classification performance is exhibited at ts10 because the data set allocated for training is very small. As the training set percentage increases, classification accuracy of the system is enhanced as expected. For this reason, the setting of training set percentage to 80 is an effective way when system performance is considered.

In Table 1, the resonance frequency classification results of each algorithm are presented on dataset1 by varying training set sizes. When the average results are considered, the best classification accuracy is achieved with 51.76% of accuracy at ts80. It is followed by 50.07%, 48.74%, 43.48% of accuracies at ts50, ts30, and ts10, respectively. At ts80, CNN as a deep learning model outperforms all traditional machine learning algorithms by reaching 58.29% of accuracy level. This means that CNN exhibits an outstanding classification performance when both conventional machine learning models and mean classification success of the system are considered. The classification performance of each model is ordered at ts80 as CNN, RF, SVM, NB, DT with 58.29%, 54.45%, 54.22%, 53.70%, 38.15% of accuracies, respectively. This indicates that CNN has shown approximately an increase of at least 4% in classification performance compared to the best conventional machine learning classifier RF. Considering the poorest classification performance of the machine learning algorithm DT, CNN displays nearly a maximum 10% increase in classification success. If a deep learning algorithm was not included in the proposed system, the random forest method as a machine learning model would be the ideal method for this resonance frequency classification task. In Table 2, all evaluation metrics are demonstrated in order to observe the success of classifiers. In Table 3, the resonance frequency classification accuracies of each method are exhibited on dataset2 by changing training set percentages. We observe the significant improvement when data set is extended by gathering more instances in classification accuracies of CNN model. While the best classification algorithm presents 58.29% of accuracy on dataset1, CNN performs 68.77% of accuracy at the same training set size. success for CNN is arisen from the extended version Approximately, 10% enhancement in classification of data set when the same experimental settings are taken into account. The similar classification performance order is observed on dataset2 as CNN> RF> SVM> NB> DT at ts80. On dataset2 at ts80, a minimum of 13% enhancement and a maximum of 22% improvement is observed when the classification performances of RF and DT are considered, respectively. As a result of Table 1 and Table 3 on both data sets, CNN as a deep learning algorithm performs superior classification performance while DT as a machine learning algorithm performs the poorest resonance frequency classification success. In Table 4, all evaluation metrics are indicated to observe the performance of classifiers.

Table 1. *Classification accuracies of each model on dataset1 in terms of training set percentages*

Models	**Training Set Percentages (ts)**			
	ts80	***ts50***	***ts30***	***ts10***
CNN	58.29	56.05	55.12	49.50
SVM	54.22	53.85	52.46	47.17
DecTree	38.15	36.56	35.09	29.00
NavieBayes	53.70	50.11	49.20	44.82
Random Forest	54.45	53.78	51.84	46.90
Average	51.76	50.07	48.74	43.48

Table 2. *The results of evaluation metrics on dataset1 at ts80.*

Models	**Evaluation Metrics**			
	Accuracy	***F-measure***	***Precision***	***Sensitivity***
CNN	58.29	65.44	62.13	68.75
SVM	54.22	60.85	57.02	65.80
DecTree	38.15	33.67	30.33	38.24
NavieBayes	53.70	59.38	57.25	63.72
Random Forest	54.45	61.74	61.16	60.98
Average	51.76	56.22	53.58	59.50

Table 3. *Classification accuracies of each model on dataset2 in terms of training set percentages*

Models	**Training Set Percentages (ts)**			
	ts80	***ts50***	***ts30***	***ts10***
CNN	68.77	66.10	61.53	55.40
SVM	54.91	54.05	47.64	39.00
DecTree	46.42	45.11	38.88	32.56
NavieBayes	52.20	50.32	45.09	37.91
Random Forest	55.84	54.72	49.36	42.55
Average	55.63	54.06	48.50	41.48

Table 4. *The results of evaluation metrics on dataset2 at ts80.*

Models	Evaluation Metrics			
	Accuracy	***F-measure***	***Precision***	***Sensitivity***
CNN	68.77	76.51	73.04	80.59
SVM	54.91	59.27	56.75	64.82
DecTree	46.42	40.05	38.27	47.33
NavieBayes	52.20	57.78	55.15	65.10
Random Forest	55.84	61.42	60.09	69.71
Average	55.63	59.01	56.66	65.51

Figure 3 demonstrates training-validation loss and training-validation accuracy values of the best model CNN at ts80 in terms of epoch sizes on dataset2. As the number of epoch size increases, both training loss and test loss vary up to a certain epoch value which is 80 in this study.

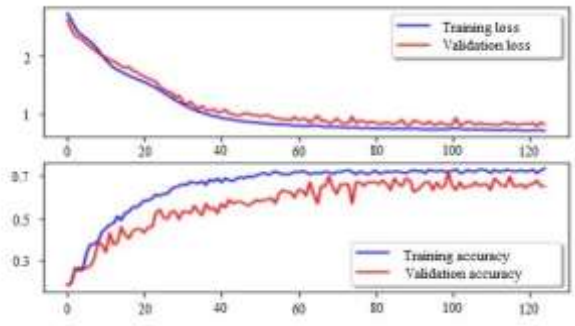

Figure 3. *Training-validation loss and training-validation accuracy results of CNN model at ts80 in terms of epoch size on dataset2.*

The training procedure can be stopped after this stage as no changes are observed in the subsequent increases in the number of attempts. Moreover, over-fitting problem is handled employing early stopping criterion, dropout function, and L2 regularization as seen in Figure 1. This means the proposed model is trained with CNN method on dataset2 without any over-fitting challenge.

5. Conclusion and Discussion

In this work, we concentrate on the estimation of chiral metamaterial resonance by comparing the classification performance of both conventional machine learning models and convolutional neural networks as deep learning model. For this purpose, convolutional neural networks, support vector machines, naive Bayes, decision trees, random forests are employed for the classification of resonance frequency. Comprehensive experiments are carried out by varying training set percentages, epoch sizes, and data sets. Experiment results demonstrate that the usage of CNN as a deep learning model exhibits superior classification success in resonance frequency compared to the traditional machine learning algorithms. Depending on the application, the resonant structure can be designed by its geometrical parameters and relative positioning in the electromagnetic field. In future, we plan to investigate the impact of various deep learning algorithms on frequency of chiral metamaterial resonance and relative importance of design parameters on the resonance frequency.

Author Statements:

- The authors declare that they have equal right on this paper.
- The authors declare that they have no known competing financial interests or personal relationships that could have appeared to influence the work reported in this paper
- The authors declare that they have nobody or no-company to acknowledge.

References

[1] Lord Kelvin, in Baltimore Lectures on Molecular Dynamics and the Wave Theory of Light, Clay and Sons: London, 1904, p. 449.

[2] Barron, Laurence D. Molecular light scattering and optical activity. Cambridge University Press,2004.

[3] Smith, D. R., Padilla, W. J., Vier, D. C., Nemat-Nasser, S. C., Schultz, S. "Composite medium with simultaneously negative permeability and permittivity." Physical review letters 84.18 (2000), 4184.

[4] Zhao, R., Zhang, L., Zhou, J., Koschny, T., Soukoulis, C. M. "Conjugated gammadion chiral metamaterial with uniaxial optical activity and negative refractive index." Physical Review B, 83.3 (2011): 035105.

[5] Wang, B., Zhou, J., Koschny, T., Soukoulis, C. M. "Nonplanar chiral metamaterials with negative index." Applied Physics Letters 94.15 (2009): 151112.

[6] Zhou, J., Dong, J., Wang, B., Koschny, T., Kafesaki, M., Soukoulis, C. M. "Negative refractive index due to chirality." Physical Review B 79.12 (2009): 121104.

[7] Kenanakis, G., Zhao, R., Stavrinidis, A., Konstantinidis, G., Katsarakis, N., Kafesaki, M., Economou, E. N. "Flexible chiral metamaterials in the terahertz regime: a comparative study of various designs." Optical Materials Express 2.12 (2012): 1702-1712.

[8] Zhang, S., Park, Y. S., Li, J., Lu, X., Zhang, W., Zhang, X. "Negative refractive index in chiral metamaterials." Physical review letters 102.2 (2009): 023901.

[9] Kuwata-Gonokami, M., Saito, N., Ino, Y., Kauranen, M., Je_movs, K., Vallius, T., Svirko, Y. "Giant optical activity in quasi-two-dimensional planar nanostructures." Physical review letters 95.22 (2005): 227401.

[10] Dong, J., Zhou, J., Koschny, T., Soukoulis, C. "Bi-layer cross chiral structure with strong optical activity and negative refractive index." Optics Express 17.16 (2009): 14172-14179.

[11] Marqus, R., Medina, F., Ra_i-El-Idrissi, R. "Role of bianisotropy in negative permeability and left-handed metamaterials." Physical Review B 65.14 (2002): 144440.

[12] Marqus, R., Mesa, F., Martel, J., Medina, F. "Comparative analysis of edge-and broadside-coupled split ring resonators for metamaterial design-theory and experiments." IEEE Transactions on antennas and propagation 51.10 (2003): 2572-2581.

[13] Huangfu, J., Ran, L., Chen, H., Zhang, X. M., Chen, K., Grzegorczyk, T. M., Kong, J. A. "Experimental con_rmation of negative refractive index of a metamaterial composed of –like metallic patterns." Applied Physics Letters 84.9 (2004): 1537-1539.

[14] Ran, L., Huangfu, J. T., Chen, H. S., Li, Y., Zhang, X., Chen, K., Kong, J. A. "Microwave solid- state left-handed material with a broad bandwidth and an ultralow loss." Physical Review B , 70.7 (2004): 073102.

[15] Aydin, K., Li, Z., Hudlika, M., Tretyakov, S. A., Ozbay, E. "Transmission characteristics of bianisotropic metamaterials based on omega shaped metallic inclusions." New Journal of Physics, 9.9 (2007): 326.

[16] Jaggard, D. L., Mickelson, A. R., Papas, C. H. "On electromagnetic waves in chiral media." Applied physics 18.2 (1979): 211-216.

[17] Tretyakov, S. A., Mariotte, F., Simovski, C. R., Kharina, T. G., Heliot, J. P. "Analytical antenna model for chiral scatterers: Comparison with numerical and experimental data." IEEE Transactions on Antennas and Propagation 44.7 (1996): 1006-1014.

[18] Saenz, E., Semchenko, I., Khakhomov, S., Guven, K., Gonzalo, R., Ozbay, E., Tretyakov, S. "Modeling of spirals with equal dielectric, magnetic, and chiral susceptibilities." Electromagnetics 28.7 (2008): 476-493.

[19] Guven, K., Saenz, E., Gonzalo, R., Ozbay, E., Tretyakov, S. "Electromagnetic cloaking with canonical spiral inclusions." New Journal of Physics 10.11 (2008): 115037.

[20] I. Malkiel, M. Mrejen, A. Nagler, U. Arieli, L. Wolf and H. Suchowski, "Deep learning for the design of nano-photonic structures," 2018 IEEE International Conference on Computational Photography (ICCP), Pittsburgh, PA, 2018, pp. 1-14, doi: 10.1109/ICCPHOT.2018.8368462.

[21] Kiarashinejad, Yashar, et al. "Deep learning reveals underlying physics of lightmatter interactions in nanophotonic devices." Advanced Theory and Simulations 2.9 (2019): 1900088.

[22] Ma, Wei, Feng Cheng, and Yongmin Liu. "Deep-learning-enabled on-demand design of chiral metamaterials." ACS nano 12.6 (2018): 6326-6334.

[23] Yao, Kan, Rohit Unni, and Yuebing Zheng. "Intelligent nanophotonics: merging photonics and artifcial intelligence at the nanoscale." Nanophotonics 8.3 (2019): 339-366.

[24] Peurifoy, John, et al. "Nanophotonic particle simulation and inverse design using arti_cial neural networks." Science advances 4.6 (2018).

[25] Malkiel, Itzik, et al. "Plasmonic nanostructure design and characterization via deep learning." Light: Science Applications 7.1 (2018): 1-8.

[26] Ma, W., Cheng, F., Xu, Y., Wen, Q., Liu, Y. (2019). Probabilistic Representation and Inverse Design of Metamaterials Based on a Deep Generative Model with SemiSupervised Learning Strategy. Advanced Materials, 31(35), 1901111.

[27] Ahmed, Waqas W., et al. "Deterministic and probabilistic deep learning models for inverse design of broadband acoustic cloak." Physical Review Research 3.1 (2021): 013142.

[28] Huang, Wei, et al. "Inverse engineering of electromagnetically induced transparency in terahertz metamaterial via deep learning." Journal of Physics D: Applied Physics 54.13 (2021): 135102.

[29] Tao, Zilong, et al. "Optical circular dichroism engineering in chiral metamaterials utilizing a deep learning network." Optics Letters 45.6 (2020): 1403-1406.

[30] Lininger, Andrew, Michael Hinczewski, and Giuseppe Strangi. "General Inverse Design of Thin-Film Metamaterials with Convolutional Neural Networks." arXiv preprint arXiv:2104.01952 (2021).

[31] McCallum, A., Nigam, K." A comparison of event models for naive bayes text classification." In AAAI-98 workshop on learning for text categorization (Vol. 752, No. 1, pp. 41-48),1998.

[32] Manning, C., Schutze, H. "Foundations of statistical natural language processing." MIT press,1999.

[33] Kilimci, Z. H., Gven, A., Uysal, M., Akyokus, S." Mood detection from physical and neurophysical data using deep learning models." Complexity, 2019.

[34] Kilimci, Z. H., Omurca, S. I." Extended feature spaces based classifier ensembles for sentiment analysis of short texts." Information Technology and Control, 47(3), 457-470, 2018.

[35] Kilimci, Z. H., Akyokus, S." Deep learning-and word embedding-based heterogeneous classifier ensembles for text classification." Complexity, 2018.

[36] Kilimci, Z. H., Ganiz, M. C. "Evaluation of classification models for language processing." In 2015 International Symposium on Innovations in Intelligent SysTems and Applications (INISTA) (pp. 1-8). IEEE, 2015.

[37] Joachims T. "Text Categorization with Support Vector Machines: Learning with Many Relevant Features." In: 10th European Conference on Machine Learning; 1998; Chemnitz, Germany: pp.137-142.

[38] Burges CJC." A Tutorial on Support Vector Machines for Pattern Recognition." In: 3rd International Conference on Knowledge Discovery and Data Mining; 1998; New York, USA: pp. 121-167.

[39] Yang Y, Liu X. "A Re-examination of Text Categorization Methods." In: 22nd Annual nternational ACM SIGIR Conference on Research and Development in Information Retrieval; 1999; Berkeley, CA, USA: pp. 42-49.

[40] Kilimci, Z. H., Akyuz, A. O., Uysal, M., Akyokus, S., Uysal, M. O., Atak Bulbul, B., Ekmis, M. A." An improved demand forecasting model using deep learning approach and proposed decision integration strategy for supply chain." Complexity, 2019.

[41] Quinlan, J. R. (1986)."Induction of decision trees. Machine learning." 1(1), 81-106.

[42] Kilimci, Z. H., Akyokus, S. (2019, July). "The analysis of text categorization represented with word embeddings using homogeneous classifiers." In 2019 IEEE International Symposium on Innovations in Intelligent SysTems and Applications (INISTA) (pp. 1-6). IEEE.

[43] Kilimci, Z. H., Omurca, S. I. (2017, August). "A Comparison of Extended Space Forests for Classifier Ensembles on Short Turkish Texts." In International Academic Conference on Engineering, IT and Artificial Intelligence (pp. 96-104).

[44] L. Breiman, "Random forests." Machine Learning, vol. 45, no. 1, pp. 532, 2001.

[45] Kilimci, Z. H., Akyokus, S., Omurca, S. I. (2016, August). "The effectiveness of homogenous ensemble classifiers for Turkish and English texts." In 2016 International Symposium on Innovations in Intelligent SysTems and Applications (INISTA) (pp. 1-7). IEEE.

[46] Kilimci, Z. H., Akyokus, S., Omurca, S. . (2017, July). "The evaluation of heterogeneous classifier ensembles for Turkish texts." In 2017 IEEE International Conference on Innovations in Intelligent SysTems and Applications (INISTA) (pp. 307-311). IEEE.

[47] Y. Lecun, L. Bottou, Y. Bengio, and P. Ha_ner, "Gradientbased learning applied to document recognition." Proceedings of the IEEE, vol. 86, no. 11, pp. 22782324, 1998.

[48] J. Schmidhuber, "Deep learning in neural networks: an overview." Neural Networks, vol. 61, pp. 85117, 2015.

[49] Y. LeCun, Y. Bengio, and G. Hinton, "Deep learning." Nature, vol. 521, no. 7553, pp. 436444, 2015.

[50] Tanberk, S., Kilimci, Z. H., Tkel, D. B., Uysal, M., Akyoku, S. "A Hybrid Deep Model Using Deep Learning and Dense Optical Flow Approaches for Human Activity Recognition." IEEE Access, 8, 19799-19809, 2020.

[51] Kilimci, Z. H., Akyokus, S." The evaluation of word embedding models and deep learning algorithms for Turkish text classification." In 2019 4th International Conference on Computer Science and Engineering (UBMK) (pp. 548-553). IEEE.

[52] Kilimci, Z. H. "Sentiment Analysis Based Direction Prediction in Bitcoin using Deep Learning Algorithms and Word Embedding Models." International Journal of Intelligent Systems and Applications in Engineering, 8(2), 60-65, 2020.

[53] Kilimci, Z. H. "Borsa tahmini için Derin Topluluk Modelleri (DTM) ile finansal duygu analizi." Journal of the Faculty of Engineering Architecture of Gazi University, 35(2), 635-650, 2020.

[54] Cevik, F., Kilimci, Z. H."The evaluation of Parkinson's disease with sentiment analysis using deep learning methods and word embedding models." Pamukkale University Journal of Engineering Sciences, 27(2), 151-161, 2021.

[55] Othan, D., Kilimci, Z. H., Uysal, M." Financial Sentiment Analysis for Predicting Direction of Stocks using Bidirectional Encoder Representations from Transformers (BERT) and Deep Learning Models." In Proc. Int. Conf. Innov. Intell. Technol., vol. 2019, pp. 30-35, 2019.